egt

EUROPEAN SCIENCE FOUNDATION E·S·F

A CONTINENT REVEALED

The European Geotraverse

Atlas of compiled data

Edited by Roy Freeman
and Stephan Mueller

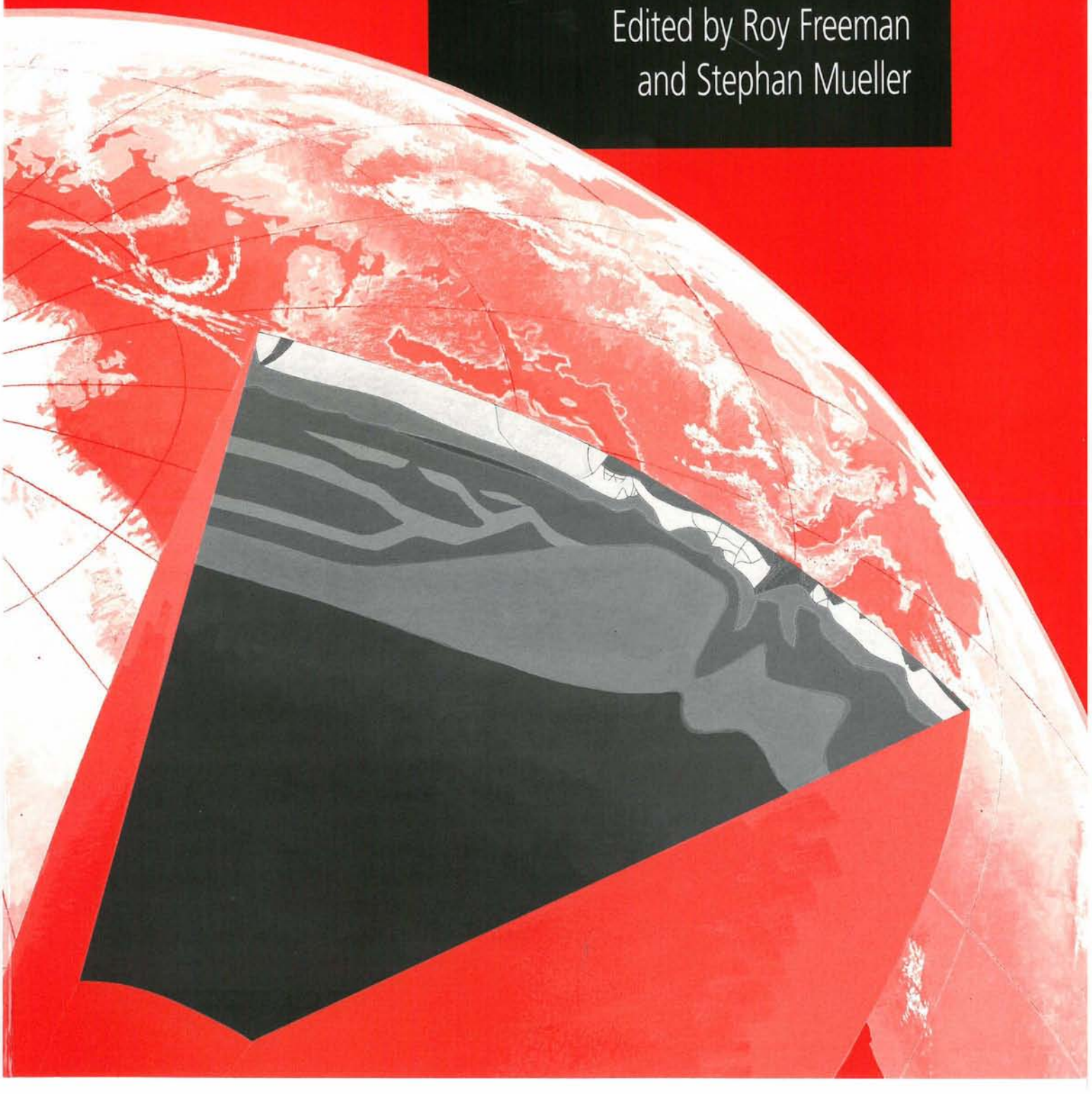

A CONTINENT REVEALED

The European Geotraverse

Atlas of Compiled Data

Edited by
ROY FREEMAN AND STEPHAN MUELLER,
ETH Zurich

ILLUSTRATIONS BY SUE BUTTON

Coordinators of individual compilations: J. Ansorge A. Berthelsen V.Cêrmák P. Giese E. Gubler V. Haak A. Hahn S.-E. Hjelt E. Klingelé D. Lelgemann N. Pavoni L. J. Pesonen

CAMBRIDGE
UNIVERSITY PRESS

Published by the Press Syndicate of the University of Cambridge
The Pitt Building, Trumpington Street, Cambridge CB2 1RP
40 West 20th Street, New York, NY 10011-4211, USA
10 Stamford Road, Oakleigh, Victoria 3166, Australia

First published 1992

Printed in Great Britain at the University Press, Cambridge

A catalogue record for this book is available from the British Library

Library of Congress cataloguing in publication data available

ISBN 0 521 42948 X paperback
ISBN 0 521 41923 9 boxed set, including this booklet

Contents

Maps

1 **Tectonics**
North sheet: *A. Berthelsen*
South sheet: *P. Burollet, G.V. Dal Piaz, W. Franke and R. Trümpy*

2 **Moho depth**
North sheet: *P. Giese and H. Buness*
South sheet: *P. Giese and H. Buness*

3 **Historical seismicity**
North sheet: *T. Ahjos and M. Uski*
South sheet: *G. Leydecker*

4 **Instrumental seismicity** (1975-1989)
North sheet: *T. Ahjos and M. Uski*
South sheet: *N. Pavoni, H. Langer and P. Suhadolc*

5 **Focal mechanisms**
North sheet: *S. Gregersen*
South sheet: *N. Pavoni, H. Langer and P. Suhadolc*

6 **Recent vertical crustal movement**
North sheet: *J. Kakkuri*
South sheet: *E. Gubler, S. Arca and K. Zippelt*

7 **Geoid undulations**
North sheet: *D. Lelgemann and H. Kuckuck*
South sheet: *D. Lelgemann and H. Kuckuck*

8 **Horizontal gravity disturbance components**
North sheet: *D. Lelgemann and H. Kuckuck*
South sheet: *D. Lelgemann and H. Kuckuck*

9 **Bouguer gravity anomalies**
North sheet: *E. Klingelé, B. Lahmeyer and R. Freeman*
South sheet: *E. Klingelé, B. Lahmeyer and R. Freeman*

10 **Magnetic anomalies**
North sheet: *T. Wonik and A. Hahn*
South sheet *T. Wonik, A. Galdéano, A. Hahn and P. Mouge*

11 **Magnetovariational and magnetotelluric results (Northern Europe)**
S.-E. Hjelt, T. Korja and K. Koivukoski

12 **Low-resistivity anomalies (Central Europe)**
A. Berktold and E. Ritter

13 **Heat-flow density**
North sheet: *N. Balling*
South sheet: *V. Cêrmák, B Della Vedova, F. Lucazeau, V. Pasquale, G. Pellis, R. Schulz and M. Verdoya*

14 **Drift history of Fennoscandia**
S. Å Elming, M. Leino, L. J. Pesonen, A. N. Khramov, G. Bylund, S. Mertanen, A. F. Krasnova, and M. Terho

Authors

Ahjos T., Institute of Seismology, University of Helsinki, Et. Hesperiankatu 4, SF–00100 Helsinki
Ansorge, J., Institut für Geophysik, ETH-Hönggerberg, CH–8093 Zürich
Arca, S., Istituto di Geologia, Univeristà di Firenze, Firenze
Bahr, K., Institut für Meteorologie und Geophysik, Johann Wolfgang Goethe Universität, Feldbergstrasse 47, D–6000 Frankfurt a. M.–1
Balling, N., Geophysical Laboratory, Department of Geology, University of Århus, DK–8200 Århus N
Berktold, A., Institut für Allgemeine und Angewandte Geophysik, Theresienstrasse 41/4, D–8000 München 2
Berthelsen, A., Institut for almen Geologi, Øster Voldgade 10, DK–1350 København
Brink, H. J., BEB Erdöl und Erdgas Gmbh, Riethorst 12, Postfach 51 03 60 D–W–3000 Hannover 51
Buness, H., Institut für Geophysik, Freie Universität Berlin, Rheinbabenallee 49, D–1000 Berlin 33
Burollet, P., CIFEG, 1344, Parc de Cassan, F–92590 L'Isle Adam
Bylund, G., Department of geology, University of Lund, S–22362 Lund
Cêrmák, V., Geophysical Institute, Czechoslovak Academy of Sciences, Bocní II. cp. 1401, CS–141 31 Praha 4 Sporilov
Della Vedova, B., Istituto di Miniere e Geofisica Applicata, Università degli Studi, Piazzale Europa, 1, I–34127 Trieste
Elming, S.–Å., Department of applied geophysics, Luleå University of Technology, S–95187 Luleå
Freeman, R., Institut für Geophysik, ETH-Hönggerberg, CH–8093 Zürich
Galdéano, A., Institut de Physique du Globe, 4, place Jussieu, Paris, F–75005
Giese, P., Institut für Geophysikalische Wissenschaften, Freie Universität Berlin, Rheinbabenallee 49, D–1000 Berlin 33
Gregersen, S., Geodætisk Institut, Seismik afdeling, Gamlehave allé 22, DK–2920 Charlottenlund
Gubler, E., Bundesamt für Landestopographie, Abt. Geodäsie, Seftigenstr. 264, CH–3084 Wabern
Haak, V., Institut für Meteorologie und Geophysik, Johann Wolfgang Goethe Universität, Feldbergstrasse 47, D–6000 Frankfurt a. M.–1
Hahn, A., Niedersächsisches Landesamt für Bodenforschung, Postfach 51 01 53, D–3000 Hannover 51
Hjelt, S.–E., Department of Geophysics, University of Oulu, SF–90570 Oulu
Jödicke, H., Institut für Geophysik, Correnstrasse 24, D–4400 Münster
Junge, A., Institut für Geophysik, Herzberger Landstrasse 180, D–3400 Göttingen
Kakkuri, J., Institute of Geodesy, University of Helsinki, Et. Hesperiankatu 4, SF–00100 Helsinki
Khramov, A., N. Neftianoi Institute, VNIGRI Liteiny 39, 191104 St. Peterburg
Klingelé, E., Institut für Geophysik, ETH–Hönggerberg, CH–8093 Zürich
Knödel, K., Bundesanstalt für Geowissenschaften und Rohstoffe, Stilleweg, D–W–3000 Hannover 51
Krasnova, A. F., Institute of Precambrian Geology and Geochronology, nab. Makarova 2, 199034 St. Peterburg
Lahmeyer, B., BEB Erdöl und Erdgas Gmbh, Postfach 51 03 60 D–W–3000 Hannover 51
Langer, H., Institut für Geophysik, Universität Stuttgart, Richard–Wagner–Strasse 44, D–7000 Stuttgart–1
Leino, M., Department of Geophysics, Geological Survey of Finland, 02150 Espoo
Losecke, W., Bundesanstalt für Geowissenschaften und Rohstoffe, Stilleweg, D–3000 Hannover 51
Lucazeau, F., Centre Géologique et Géophysique, Université de Montpellier, Place Eugène Battaillon, F–34095 Montpellier Cedex 2
Mertanen, S., Department of geophysics, Geological Survey of Finland, 02150 Espoo
Mouge, P., Bureau de Recherches Géologiques et Minières, F–45060 Orleans
Mueller, St., Institut für Geophysik, ETH-Hönggerberg, CH–8093 Zürich
Pasquale V., Dipartimente della Scienza della Terra, Università di Genova, Viale Benedetto XV, 5, I-16132 Genova
Pavoni, N., Institut für Geophysik, ETH-Hönggerberg, CH–8093 Zürich
Pellis, G., Istituto di Miniere e Geofisica Applicata, Università degli Studi, Piazzale Europa, 1, I–34127 Trieste
Pesonen, L. J., Department of Geophysics, Geological Survey of Finland, Betonimiehenkuja 4, SF–02150 Espoo
Ritter, E., Adolf–Schmidt–Observatorium, Lindenstr.7, D–O–Niemegk
Schulz, R., Niedersächsisches Landesamt für Bodenforschung, Postfach 51 01 53, D–3000 Hannover 51
Suhadolc, P., Istituto di Geodesia e Geofisica, Universitá degli Studi, Via dell'Università, 7, I–34127 Trieste
Terho,M., Department of geophysics, Geological Survey of Finland, 02150 Espoo
Uski, M., Institute of Seismology, University of Helsinki, Et. Hesperiankatu 4, SF–00100 Helsinki
Verdoya, M., Dipartimento della Scienza de la Terra, Università di Genova, I–161432 Genova
Volbers, R., Institut für Geophysik, Correnssstr. 24, D–4400 Münster
Winter, H., Institut für Meteorologie und Geophysik, Johann Wolfgang Goethe Universität, Feldbergstrasse 47, D–6000 Frankfurt a. M.-1
Wonik, T., Niedersächsisches Landesamt für Bodenforschung, Postfach 51 01 53, D–3000 Hannover 51
Zippelt, K., Geodätisches Institut, Universität Stuttgart, Keplerstrasse 44, D–7000 Stuttgart–1

1 Introduction

R. FREEMAN AND ST. MUELLER

The aim of the accompanying text, maps, and CD-ROM is to provide a data basis for interpreting long-wavelength features (λ>500 km) along the length of the European Geotraverse (EGT). The EGT transect is roughly 250 km wide and centred along the main EGT seismic refraction lines and runs a length of *ca.* 4600 km from the North Cape of Norway to central Tunisia. All maps are on the same scale (1: 2.5 million) and projection (Lambert conic conformal), identical to the International Tectonic Map of Europe (IGC-CGMW-SCTMW 1973). By producing maps of the same scale and projection, we hope to encourage an integrated approach to interpretation.

Essential to using the EGT data is a knowledge of their origin, accuracy, and range of applicability. Most raw data in the Earth sciences are not actually 'raw', but are inherently modified by characteristics of their measuring devices and the application for which they were originally collected. In addition, many data have, in some way or another, undergone implicit 'corrections' to make them comparable to other data. We have tried to supply information on these factors in the following explanatory texts. In addition, on the reverse side of many of the maps we have plotted indications of data quality and/or density of distribution. When viewing the front side of the map with backlighting, one can thus gain crucial information regarding the spatial distribution of the data.

The EGT compilation is the result of nearly ten years of labour, mostly involving tedious hours of detailed collection and correction ranging from pulling drill strings to typing lists of numbers into computer terminals. With some compilations we were not able to reach the goal of compiling high-quality data sets in uniform standard and quality and had to settle for what, in the end, was available. (For instance, we often had to combine original data with data digitized from maps). In some cases (e.g. lithosphere thickness) we deemed the available data insufficient to produce a map. Geochronological and petrological data, although included in the EGT Joint Programme and vital to any integrated interpretation, were only partially compiled due to lack of funding and time. Other European individuals and groups are involved in such compilations and we hope that they will be published soon. The palaeomagnetic catalogues by the EGT compilers M. Westphal (Institut de Physique du Globe, Strasbourg) and L. J. Pesonen (Geological Survey of Finland, Espoo) have already been published and are being continuously updated. They have not been included here.

We see the EGT compilations as a beginning, an initial attempt that must be improved and extended by future workers. We do not claim to have made the best possible choice of

formats, parameters, or indeed, even of kinds of data compiled. (After compiling the Bouguer gravity anomalies many interpreters voiced preference for free air gravity data instead). Uniform standards among fourteen European countries is a worthy goal, but one that is as difficult to realise as any political or social union. In several cases, universal formats are not agreed upon and we had to choose those most suiting our needs. In addition, uniform standards often mean less accuracy. Data compiled on a local or national scale tend to have smaller error bars and are better suited to more detailed, smaller-wavelength analyses. Global or international scale compilations have less precision but more accurate long-wavelength quality. In most cases we opted for the long-wavelength case to conform to the EGT goal of investigating the nature of Europe's lithosphere across a wide variety of crustal types.

Many active researchers may use the maps to gain an overall picture of the data and to compare large-scale features, but go directly to the CD-ROM for the actual data. We have therefore included on the CD-ROM as many of the original data sets as possible, although the completeness of the data sets varies. (Due to the nature of the data, not all compilations, e.g. Moho depths, are available on the CD-ROM). We often had to edit and generalise the data and decide on one from many alternatives for the 'best' type of display. These choices severely limit the purposes to which the maps can actually be put to use. For example, the primary purpose of the seismicity maps is to give a graphic impression of the geographic distribution of seismicity and are not to be used for spatial or temporal statistics.

The scale of the maps also determined the choice of allowable error in data precision and positioning. Not correcting for different datum shifts of national reference ellipsoids can give horizontal positioning errors up to 150m for the same location originally determined with an accuracy of better than 3m by very precise national surveys. This error being obviously negligible on the scale of 1:2.5 million, we did not correct for datum shifts. However, those using data off the CD-ROM for small-scale work should know the origin and accuracy of each type of data. In spite of these reservations, we hope that this data set encourages you, the reader, to dig into 'real' Earth data.

The European Geotraverse project, in calling upon help from top specialists in many fields, has often profited by compilation projects running simultaneously within the international Earth science community. Many of the EGT compilations include data from such existing projects and we gratefully acknowledge those responsible for allowing us to use these data. We also thank the large number of people, not listed as co-authors of the following chapters, who contributed their time and energy and we would like to mention a few among them: M. Baumann, D. Blundell, S. Button, F. Delany, M. Fratta, P. Fricker, D. A. Galson, M. Huch, M. Marker, I. Marson, C. Morelli, N. Okaya, the ETH Computing Centre, and the European Science Foundation and its Member Organizations. In particular we are deeply grateful to J. Ansorge for his tireless support, unselfish help, and excellent advice; to E. Kissling and E. Klingelé for contributing their programming skills, experience, and critical knowledge of data quality; and especially to B. Niedermann of Aerni-Leuch AG, Berne, for bringing a rare combination of technical command and artistic sense to bear in the thankless task of displaying foreign and complex data on a map. This is a cumbersome, seemingly endless, back-and-forth process between printers, editors, and compilers. As all those involved know only too well, there is no end to possible improvements to the last plot after it is finished, errors that mysteriously appear on the 'final' version, lost data that surface once everything else is carefully drafted onto film, artifacts that insist on appearing in print, disk crashes, plotter quirks, and other manifestations of the spirit in matter. Without the help of those mentioned above and numerous other colleagues this collection of data would never have become an Atlas.

2 Tectonics

A. BERTHELSEN, P. BUROLLET, G.V. DAL PIAZ, W. FRANKE AND R. TRÜMPY

Atlas Map 1 shows the major tectonic divisions and structures along the EGT transect. The north sheet encompasses the Baltic Shield and adjacent off-shield (platform) regions. To the south, in northern Germany, it overlaps with the northernmost part of the south sheet. The south sheet covers the geologically youngest part of the EGT and in its southernmost part reaches the African plate. The north and south sheets and their respective legends reflect not only the different geology and tectonics of the regions they comprise but also the distinct styles of the authors who compiled them.

To understand some of the tectonic features along the EGT, it is imperative to look laterally. To this end we have placed a sketch map and accompanying explanatory text drawn up by A. Berthelsen at the bottom of the legend for the north sheet and on the reverse side of the legend for the south sheet.

NORTH SHEET (A. BERTHELSEN)

Principles behind the compilation: Baltic Shield

The continental crust of the Baltic Shield acquired its 'sialic' composition and obtained its most important structural imprints during successive Archaean and Proterozoic episodes of crustal accretion and orogenic activity (3.5–0.9 Ga). This crust is now directly exposed at the surface, and to arrive at a tectonic division that describes its crustal evolution in a clear but simple way, main emphasis was placed on portraying the *orogenic* structures: their trend, style, age, and method of formation.

In general, rocks and structures that were formed under *cratonic* conditions (with cooled and stiffened crust) appear to have influenced the gross crustal structure considerably less. For this reason, cratonic features are only portrayed if they record major tectonic events, or if they serve to constrain the timing of preceding orogenies.

This selective presentation was chosen to highlight large-scale structures that possibly control the bulk physical parameters in different parts of the crust, so that results from geological, seismic and/or potential field surveys can be compared and, possibly, correlated.

The orogenic framework. Available geological, structural, petrological, geochemical, isotope-geological and geochronological information were taken into consideration; however, to prevent important crustal features from being blurred by an overload of details,

much of this data background has not been directly documented on the Tectonics Map. Geochronological data, and geochemical-isotopic discrimination between rocks originating from mantle-derived and/or crustal-derived magmas formed an essential tool in distinguishing between tectonic palaeo-environments (see legend).

Regionally-developed fold patterns in low- to high-grade supracrustals, gneisses, migmatites, and deformed plutonics are illustrated by structural trend lines. They provide information about the deformational regimes that prevailed when orogeny was ongoing. Together with lithology contrasts and geophysical anomalies, they serve to outline the actual boundaries between tectonic domains and terranes.

In places, low-angle to moderately dipping shear zones outline major tectonic boundaries developed towards the close of the orogenic evolution when ductile conditions still prevailed. Their mylonitic/banded structure attest to the intense shear and strain accumulation, suggestive of long-range tectonic transport/thrusting. Although outlined by conventional thrust/detachment symbols, they may be several hundred metres wide.

Individual plutonic bodies that form part of orogenically deformed terranes are generally not outlined (by contacts), and no particular colour scheme was used to indicate whether they are of mafic, intermediate, or acidic composition. In general, the occurrence of massive plutonic bodies may be inferred by local absence of structural trend lines in the basement.

But the map shows a number of minor post-kinematic granite massifs that were emplaced shortly after cessation of orogenic or major strike-slip deformation. They comprise the distinct age groups (*ca.* 1.9, 1.45, and 0.9 Ga), which all appear to have been emplaced during transition from orogenic to cratonic conditions.

Depicted cratonic features. Represented are also the most important igneous massifs and central intrusions that were emplaced in wholesale cratonised crust. They comprise 1.65–1.5 Ga old intrusions of the Rapakivi-gabbro-anorthosite kindred, and 300–275 Ma old plutonic and subvolcanic rocks of the alkaline province of the Oslo region. The 1.65–1.5 Ga Rapakivi intrusions occur in a NW–SE trending belt on both sides of the Bothnian Bay and on the Åland islands. The same trend is outlined by the *ca.* 1.3–0.6 Ga old Jotnian and Vendian graben structures beneath the Bothnian Bay.

Faults with prominent offsets of basement, aeromagnetic trends, or cover strata were selected first for presentation. Then, other parallel faults were added to make age-specific fault systems more visible (e.g. the *ca.* 0.8 Ga old Vättern graben system of southern Sweden). However, most of the intended consistency is lost when faults traced by detailed subsurface mapping of the southern off-Shield region's cover sequences were added. Their distribution and trend document the influence of Phanerozoic tectonics. Deep fault zones that primarily affect the basement are shown with a special signature.

Basement features not shown. Due to lack of consistent data and for technical reasons, dyke swarms, sills and other mafic intrusions of Late Archaean, Proterozoic, or Phanerozoic age, are not shown in the map, even though they form important time markers. Neither are the Scandinavian Caledonides treated since they are not crossed by the FENNOLORA seismic profile.

Southern off-shield region: the link to the south

The change in geology from the shield to the southern off-shield region necessitated a change in the method of presentation. To incorporate both the record contained in the thick and extensive post-orogenic cover sequences and that of the buried basement, several guidelines were followed and are outlined below.

(1) In the southern off-shield region, onshore areas have been coloured according to the

orogenic *age* of the underlying basement (either Precambrian, Caledonian, or Variscan). It would have been desirable to show also the total thickness of the sedimentary layer by contouring the depth to top crystalline basement. But for this purpose, data are still much too scarce. Instead, depths to base Zechstein were contoured. They show the minimum thickness of the 'sedimentary layer'.

(2) Different colour schemes are used to show depth to base Zechstein in offshore and onshore areas.

(3) In offshore areas depth intervals between 2000 and 4000, 4000 and 6000, and in excess of 6000 metres are coloured in different shades of light blue, most intense where deepest. Onshore, the same depth intervals are indicated by changing intensities of the colour for the basement's orogenic age. In this way, the buried Caledonian and Variscan deformation fronts and fold belts stand out clearly and the map links up with that of the central and southern EGT Segments.

SOUTH SHEET (P. BUROLLET, D. V. DAL PIAZ, W. FRANKE AND R. TRÜMPY)

Four geologists compiled the south sheet and we have retained differences in style since the geology and tectonics is itself distinct. For example, fold trends are displayed in Tunisia, but not elsewhere on the map, because they provide valuable information on the characteristics of Tunisian tectonics that would otherwise not be evident. We have in general followed similar principles used for previous maps and therefore there is no need to elaborate them here.

REFERENCES

Many different sources were consulted and used during compilation, which in some areas on the north sheet was started on the scale of 1:50 000 or 1:250 000. Besides general reference to papers cited in Chapters 2 and 6 of the EGT Book (Blundell *et al.* 1992), a list of specific maps and publications used in drawing up the Tectonics Map is given on the reverse side of each legend.

ACKNOWLEDGEMENTS

We would like to express our particular gratitude to M. Marker, for his assistance in the compilation north of 69°N, R. Madsen for his excellent draftsmanship in preparing the black line plans of the north sheet and legends to both sheets, F. Delany for her comments and corrections to the maps, H.-M. Herrmann for his cartography in preparation of the plates, and especially to B. Niedermann for his technical skill in translating geologists' colour coding into printers' colour coding and for coordinating the final production.

(Editors' acknowledgment: we thank A. Berthelsen for his instrumental work in preparing the legends and colour codes for both the north and south sheets.)

3 Seismic refraction and reflection data

J. ANSORGE

Any hypothesis on the evolution and present tectonic style of the lithosphere requires information about its structure and composition. The distribution of seismic velocities with depth are the most important parameters from which to derive such information. Seismic refraction and wide-angle surveys are best suited to provide the necessary data. All refraction and wide-angle results acquired within the EGT project have been collected in a series of eight Open File Reports available separately. These data were crucial sources for deriving the seismic structure of the lithosphere under the EGT as described in Chapter 3 of the book (Blundell *et al.* 1992). The reports contain technical and logistic information together with seismograms plotted as record sections. The data (paper plots and digital media) are preserved so that they can and should be used in further studies beyond the immediate scope of the EGT. In addition, all the data are available on magnetic tape from the individual compilation groups (addresses given below) and are not on the CD-ROM. Many of the EGT refraction and wide-angle reflection experiments were accompanied by normal incidence reflection surveys mostly as parts of special national programs. Major references are given below to facilitate access.

REFRACTION AND WIDE-ANGLE REFLECTION SURVEYS

Along the EGT six major seismic refraction and wide-angle reflection experiments were carried out through close international cooperation of all the countries and institutions involved in EGT. Locations of the regions covered are shown in Fig. 3.1 and the projects are listed below with capital letters identifying the respective region on the figure.

(1)	(P)	1985	POLAR Profile
(2)	(F)	1979	Fennoscandian Long-Range Project (FENNOLORA)
(3)	(E)	1984	EGT Northern Segment - Southern Part (EUGENO-S)
(4)	(C)	1986	EGT Central Segment (EUGEMI)
	(A)	1986	Central Alps, Po-Plain, Northern Apennines (EGT-S86)
(5)	(A)	1983	EGT Western Alps, Northern Apennines (EGT-S83)
	(S)	1983	EGT Southern Segment, N. Apennines to Sardinia Channel (EGT-S83)
(6)	(S)	1985	EGT Southern Segment, Sardinia-Sardinia Channel (EGT-S85)
	(S)	1985	EGT Southern Segment, Tunisia and Pelagian Sea (EGT-S85)

The large amount of data collected with these seismic wide-angle reflection and refraction experiments prohibits including them in this Atlas. Instead, all the data were compiled separately for each experimental survey or region listed above at various geophysical institutions. These groups or individuals have painstakingly compiled the large amount of seismic refraction data, which were obtained originally in a large variety of formats. The final result is a series of eight Open File Reports consisting mostly of two parts containing all necessary information and parameters for further independent use of the data and seismogramme montages. In most cases there will be no need to resort to the original field tapes or reports. The reports are edited as a publication of the institution that is responsible for the compilation and can be cited as such in the literature. These same institutions will provide copies of the Open File Reports and/or the digital data upon request at the nominal costs for reproduction. Full references for the compilations and addresses are given below.

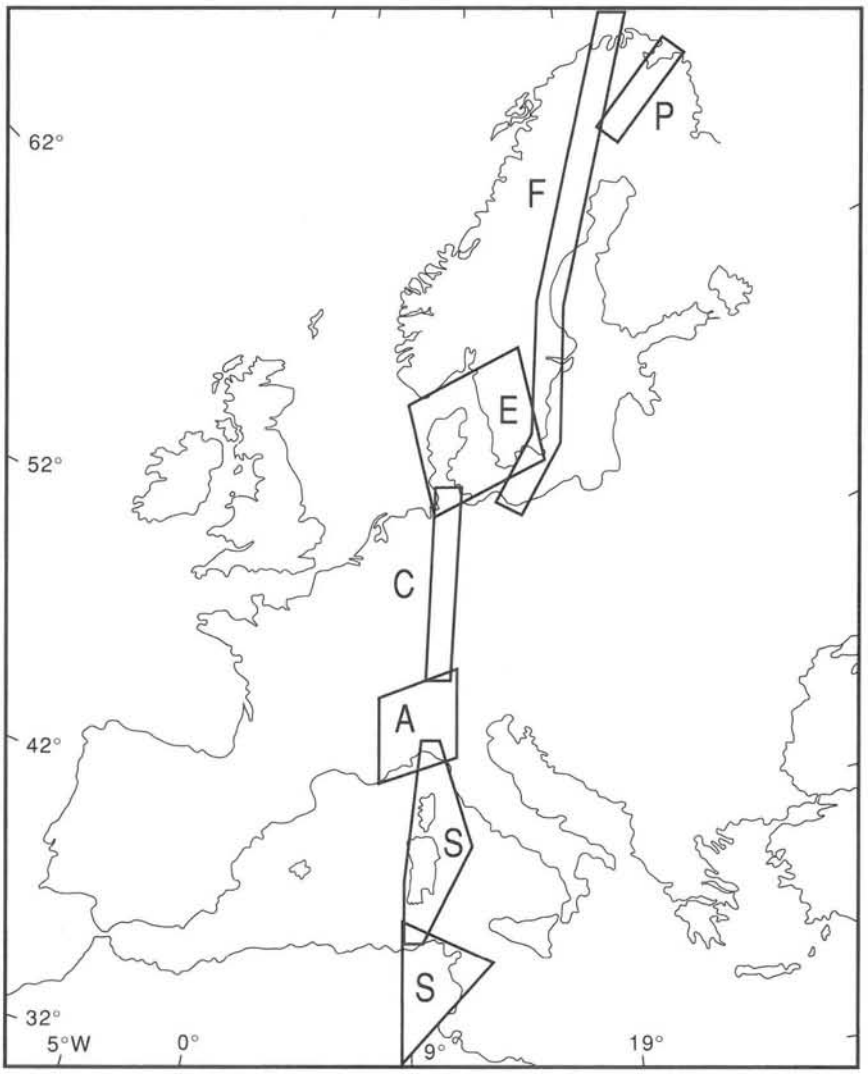

Fig. 3.1: Location of regions covered by the 8 Open File Reports with compilations of seismic refraction and wide-angle reflection data. P: POLAR Profile; F: Fennoscandian Long-Range Project (FENNOLORA); E: EGT Northern Segment-Southern Part (EUGENO-S); C: EGT Central Segment (EUGEMI); A: Central Alps, Po-Plain, Northern Apennines (EGT-S86) and EGT Western Alps, Northern Apennines (EGT-S83); S: EGT Southern Segment, Northern Apennines-Sardinia Channel (EGT-S83 and EGT-S85) and EGT Southern Segment, Tunisia and Pelagian Sea (EGT-S85).

The collections serve several purposes and their form was chosen accordingly. The data were compiled to give quick and easy access to all interested persons involved in the interpretation of the EGT data. This is achieved by the choice of a common format for paper plots and associated experimental and technical information in addition to the digital format of data on magnetic tape. Common digital formats are valid for each subset of data that covers a certain tectonic or geographic region. Not all the information contained in the data has been fully interpreted.

Each report contains the seismic refraction data collected on land from borehole shots or at sea by ocean-bottom seismographs from offshore explosions. Most of the reports include also references for older data collected in the same area prior to the EGT Project. The A3 size and the scale of the plots were chosen such that the sections can be used directly for a crude identification of phases and can be rescaled on a photocopy machine. The compilations include the following technical data for shots and recordings:

(1) Tables with shot parameters: coordinates, elevation, special borehole or quarry shots, depth of boreholes, depth of shots in water, water depth, charge size, single or dispersed charges, dates and shot times, and a location map.
(2) For each seismic profile the following information.
   (a) A listing of recording stations with coordinates, elevation, the recorded shots, distance from shotpoint, azimuth from shotpoint.
   (b) Three record sections, one each for the vertical (Z), radial (R), and transverse (T) components.
      - Amplitudes are normalised so that the main phases stand out clearly.
      - Reduction velocities are 6.0 kms^{-1} for Z, and 3.46 kms^{-1} for R and T. For profiles longer than 500 km the reduction velocity is 8.0 kms^{-1} for Z, and 4.62 kms^{-1} for R and T.
      - A fixed ratio of travel time versus distance scale of 1 s corresponding to 5 km for normal crustal profiles, or 1 s corresponding to 10 km for long-range profiles longer than 500 km. Because of the higher station density on the marine profiles in the Mediterranean Sea 1 s corresponds to 4 km.
      - The time scale of radial and transverse components is reduced by a factor of 1.732 such that these phases can be compared directly with the P-waves.
      - Filter settings are chosen such that only the main high and low frequency noise is cut out.

LIST OF REPORTS INCLUDING ADDRESSES FOR THE REQUEST OF REPORTS AND DIGITAL DATA:

(1) Luosto, U. and Lindblom, P. (1990).
Seismic Refraction Data of the EGT Polar Profile. Institute of Seismology, University of Helsinki (Finland), Report S-23, 19p., 18 plates.
Address: U. Luosto, Institute of Seismology, University of Helsinki, Et. Hesperiankatu 4, SF-00100 Helsinki 10, Finland.

(2) Hauser, F., Prodehl, C. and Schimmel, M. (1990).
A Compilation of Data from the Fennolora Seismic Refraction Experiment 1979. Geophysical Institute, University of Karlsruhe (Federal Republic of Germany), Open File Report, 6p., 1 table, 114 plates.

Address: C. Prodehl, Geophysical Institute, University of Karlsruhe, Hertzstrasse 16, D-7500 Karlsruhe, Federal Republic of Germany.

(3) Gregersen, S., Flüh, E.R., Moeller, C. and Hirschleber, H. (1987).
Seismic Data of the EUGENO-S Project. Department of Seismology of the Danish Geodetic Institute Charlottenlund (Denmark), 42p., 60 plates with vertical components only.
Address: S. Gregersen, KMS Geodetic-Seismic Division, Office of Seismology, Rentemestervej 8, DK-2400 Copenhagen NV, Denmark.

(4) Aichroth, B., Ye, S., Feddersen, J., Maistrello, M. and Pedone, R. (1990).
A Compilation of Data from the 1986 European Geotraverse Experiment (Main Line) from Genova to Kiel. Geophysical Institute, University of Karlsruhe (Federal Republic of Germany), Open File Report 90-1, Part I, 115p. including tables ; Part II, 89 plates.
Address: C. Prodehl, Geophysical Institute, University of Karlsruhe, Hertzstrasse 16, D-7500 Karlsruhe, Federal Republic of Germany.

(5) Buness, H. (1990).
A Compilation of Data from the 1983 European Geotraverse Experiment from the Ligurian Sea to the Southern Alps. Institute of Geophysics, Free University of Berlin (Federal Republic of Germany), 75p. including tables and 45 plates.
Address: P. Giese, Institut fuer Geophysikalische Wissenschaften, Free University of Berlin, Rheinbabenallee 49, D-1000 Berlin 33, Federal Republic of Germany.

(6) Maistrello, M., Scarascia, S., Ye, S. and Hirn, A. (1991).
EGT 1986 Central Segment - Compilation of seismic data (additional profiles and fans) in Northern Apennines, Po Plain, Western, and Southern Alps. CNR Istituto per la Geofisica della Litosfera, Milano (Italy), Open File Report. 26p., 56 plates.
Address: M. Maistrello, Istituto per la Geofisica della Litosfera, C.N.R., Via Bassini 15, I-20133 Milano, Italy.

(7) Egger, A. (1990).
A Comprehensive Compilation of Seismic Refraction Data along the Southern Segment of the European Geotraverse from the Northern Apennines to the Sardinia Channel (1979-1985). Institute of Geophysics, ETH Zürich (Switzerland), Open File Report, Part I, 108p. including tables; Part II, 202 plates.
Address: J. Ansorge, Institute of Geophysics, ETH-Hoenggerberg, CH-8093 Zürich, Switzerland.

(8) Maistrello, M., Scarascia, S., Corsi, A., Egger, A. and Thouvenot, F. (1990).
EGT 1985: Compilation of Data from Seismic Refraction Experiments in Tunisia and the Pelagian Sea. CNR Istituto per la Geofisica della Litosfera, Milano (Italy), Part I, 115p., Part II, 79 plates.
Address: M. Maistrello, Istituto per la Geofisica della Litosfera, C.N.R., Via Bassini 15, I-20133 Milano, Italy.

NORMAL INCIDENCE REFLECTION SURVEYS

Normal incidence seismic reflection techniques provide the best resolution of the deep structure. EGT has been able to take advantage of the work of a number of deep seismic reflection programmes, particularly BIRPS (UK), CROP (Italy), DEKORP (Germany), ECORS (France) and NFP 20 (Switzerland). Several surveys of these national programmes are related to the EGT and were carried out in close cooperation with the EGT, although the normal incidence reflection survey is far from a continuous coverage of the EGT. Some special reflection profiling programmes which are directly related to the EGT are:

- A special reflection line coincides with the central section of the POLAR Profile (Behrens *et al.* 1989).
- The BABEL project runs parallel to the FENNOLORA profile and to the southeastern EUGENO-S profiles in the Gulf of Bothnia and Baltic Sea (BABEL Working Group 1990).
- Several reflection surveys are part of and supplement the EUGENO-S (Behrens *et al.* 1986; EUGENO-S Working Group, 1988; Green *et al.* 1988; Bialas *et al.* 1990; Dahl-Jensen *et al.* 1991)
- DEKORP-2N and DEKORP-2S profiles cross the refraction profile EUGEMI of the EGT Central Segment obliquely (DEKORP Research Group, 1985; Franke *et al.* 1990; Wever *et al.* 1990) For a complete set of DEKORP data see Meissner and Bortfeld (1990).
- The NFP 20 Eastern and Southern Traverses including a CROP segment across the central and southern Alps are paralleling the EGT-S86 within a couple 10 km (Valasek *et al.* 1991).
- The ECORS-CROP traverse across the Western Alps helped to map a three-dimensional picture of the different crustal units in the complicated transition from the Eurasian plate to the western Mediterranean sea (Roure *et al.* 1990; Tardy *et al.* 1990).

ACKNOWLEDGEMENTS

The compilation of the tremendous amount of seismic refraction and wide-angle reflection data would not have been possible without the dedication of H. Buness (Berlin), R. Pedone (Genova), F. Thouvenot (Grenoble), H. Hirschleber (Hamburg), P. Lindblom, U. Luosto (Helsinki), B. Aichroth, J. Feddersen, F. Hauser, C. Prodehl, M. Schimmel (Karlsruhe), E. Flüh (Kiel), S. Gregersen, C. Möller (København), A. Hirn (Paris), A. Corsi, M. Maistrello, S. Scarascia (Milano) and A. Egger, S. Ye (Zürich).

4 Moho depth

P. GIESE AND H. BUNESS

The crust/mantle boundary, i.e. the Mohorovicic, or simply Moho, discontinuity represents the major petrological boundary between the continental crust and upper mantle. Referring to wave velocity the Moho discontinuity is defined as that horizon where the compressional (P-) wave velocity increases rapidly or discontinuously to a value between 7.6 and 8.3 kms^{-1}. In the absence of an identifiable rapid increase in velocity the Moho discontinuity is taken to be the level at which the compressional velocity exceeds 7.6 kms^{-1}.

The Moho discontinuity is generally detected by deep seismic sounding (i.e. seismic refraction) studies, in particular by wide-angle arrivals from the Moho discontinuity, the so-named P_MP phase, the wave reflected at that interface or quasi-reflected in a strong gradient zone in the transition between the lower crust and uppermost mantle. In the case of older profiles the depth of the Moho discontinuity has been determined by means of (1) the P_MP phase at the critical distance range, (2) by the P_n phase, the head, or weakly penetrating, wave from the upper mantle by the disappearance of near vertical reflections at the base of the lower crust.

The compilation and construction of Moho depths (Atlas Map 2) are based on all three methods. In addition in areas with only widely spaced seismic profiles Bouguer gravity anomaly maps have been used for the interpolation the Moho contour lines. The accuracy of depth determination is in general ±5%.

The construction of the EGT Moho-contour map is based mainly on regional maps elaborated for the northern segment by Luosto (1991), for the central segment by Giese and for the southern segment by Buness. The adjustment between the sectional maps were performed by the authors of this chapter. Highlighted in red are areas where Moho depth is supported by seismic data. The regional maps used in the compilation are indicated on the reverse side of the map with a code identifying the source. All profiles used by the authors to draw the contours are also shown on the backside of the map.

NORTHERN SEGMENT

The northern part of the Moho map is based on the map published by Luosto (1991) who compiled the interpretations of a large number of seismic profiles observed in northern Europe. The FENNOLORA profile was the backbone for the deep seismic sounding studies on the northern segment of EGT. The field work was already done in 1979 (e.g. Guggisberg

1986; Prodehl and Kaminski 1984, Olsen and Lund 1986, Clowes *et al.* 1987). These investigations have been completed by the profiles of the EUGENO-S Project in 1984 (Eugeno-S Working Group 1988) and the POLAR Profile in 1985 (Luosto *et al.* 1989). The Blue Road profile (Lund 1979) crossed the FENNOLORA profile in northern Sweden. Another profile crossing the Caledonides was the Transcandinavian Seismic profile in southern Norway (Kanestrom and Haugland 1971). The North Sea–southern Norway profile (Cassell *et al.* 1983) and the Lofoten Profiles (Goldschmidt-Rokita *et al.* 1988) give information about crustal structure in the transition from the continental to oceanic structure. The most important seismic refraction profiles in Finland other than the Polar profile are the Sveka profile 1981 (Grad and Luosto 1987) and the Baltic profile in 1982 (Luosto *et al.* 1990) in Central and SE Finland.

For the transition between the Baltic Shield and central Europe a Moho contour map has recently been elaborated by Thybo *et al.* (1990).

To calculate contours for Moho depth, values were collected from the refraction profiles cited above. Readings were made at 50–100 km intervals depending on stability of structure along the profiles and isolines were calculated by a computer program using quite strong smoothing. Contours were drawn at 2 km depth interval.

CENTRAL SEGMENT

Moho depth in central Europe is based on a very large amount of seismic reflection and refraction data that have been measured and compiled over the last 35 years. This activity is documented in a huge number of publications and internal reports describing the data and discussing the results obtained. In this contribution only the main references have been cited; these may be used as further data sources.

The first data compilation of DSS data in central Europe was published by the German Research Group for Explosion Seismology (1964). A comprehensive data collection comprising all record sections recorded up to 1972 is found in the monograph 'Explosion Seismology in Central Europe' (Giese *et al.* 1976). Mostaanpour (1984) compiled typical crustal parameters for the whole western European area.

The activities in seismic crustal studies increased remarkably in the Eighties, focussing mainly on regional problems. We will only cite those regional studies used as data base for the compilation of the Moho depth map.

Data for northern Germany are taken from Bachmann and Grosse (1989). For the central part of Europe, in particular the Rhenish Massif, the publications by Mooney and Prodehl(1978), Meissner *et al.* (1980) and Mechie *et al.* (1983) are valuable; for the 'South German Triangle', Zeis *et al.* (1990); for southwest Germany, Gajewski *et al.* (1987); for the Swabian Jura, Bartelsen *et al.* (1982) and Gajewski and Prodehl (1985); and for the Black Forest, Gajewski and Prodehl (1987). In eastern Germany the results of seismic refraction studies have been reported by Bormann *et al.* (1987, 1989). The results of the deep seismic sounding studies along the central segment of the EGT are presented by Aichroth and Prodehl (1990), Aichroth *et al.* (1992), EUGEMI (1990), and Prodehl and Giese (1990).

Since mid-1983 a deep seismic reflection program for the investigation of the Earth's crust in the Federal Republic of Germany (DEKORP) has been carried out using modern seismic methods. The following deep seismic reflection profiles carried out up to the end of 1989 provide detailed data for the construction of the Moho map in central Europe: DEKORP 2 South: Bortfeld *et al.* (1985), DEKORP Research Group (1985); DEKORP 2 North: Franke *et al.* (1990); DEKORP 1A, 1B, 1C: DEKORP Research Group *et al.* (1991); DEKORP 9 North: Wenzel *et al.* (1991).

In addition, special profiles and networks were surveyed in close cooperation with the Continental Deep Drilling Program of the Federal Republic of Germany (KTB) in order to obtain a detailed picture of crustal structure at the potential drilling sites Black Forest (Luschen *et al.* 1987,1989) and Upper Palatinate (Schmoll *et al.* 1989, Bortfeld *et al.* 1988, DEKORP Research Group 1988, Gebrande *et al.* 1989).

From the profiles recorded before 1980 we have calculated Moho depth values based mainly on the critically reflected P_MP-wave thus giving only one value along the seismic line. Profiles observed since 1980 have been interpreted by ray-tracing techniques, which provide more-or-less continuous depth information along the corresponding line. In regions with poor seismic coverage the Moho contours have been completed using the Bouguer gravity map of central Europe published by Grosse *et al.* (1990). Finally, the contour lines of the depth of the Moho discontinuity have been constructed by hand interpolation (Giese 1990).

SOUTHERN SEGMENT

In the Alpine region of the EGT there have been nearly continuous seismic research studies since 1956. Several compilations of the early profiles are available (e.g. Closs *et al.* 1963, Angenheister *et al.* 1972, Giese and Prodehl 1976). In the 1970s two long-range profiles were carried out along strike of the Alps, the Alpine longitudinal profile 1975 (Alpine Explosion Seismology Group 1976, Miller *et al.* 1982, Yan and Mechie 1989) and the Southern Alps profile 1977 (Italian Explosion Seismology Group 1978, 1981, Deichmann *et al.* 1986).

Data from a large-scale refraction experiment done in 1974 in the area of the northern Ligurian Sea, the northern Apennines, Tuscany, and Corsica are presented by Morelli *et al.* (1977). Two years earlier measurements in Sicily were carried out (Morelli *et al.* 1975). Results from numerous seismic reflection and also a few refraction profiles in the central Tyrrhenian and the northern Ligurian Sea, some of it reaching deep crustal levels, are available (Finetti *et al.* 1973, Le Douran *et al.* 1984). A profile through Sardinia was observed in 1979 (Scarascia 1980).

Within the frame of the EGT three large experiments were carried out in 1983, 1985, and 1986. The first comprised the area between the Sardinia channel and the southern Alps, including several lines through the western Alps (Banda *et al.* 1985, Egger *et al.* 1988, Ginzburg *et al.* 1985, Thouvenot *et al.* 1985). The second continued the EGT to the south, from the Sardinia channel to central Tunisia (Research Group for Lithospheric Studies in Tunisia 1990, 1992). The last one connected the southern to the central segment of the EGT with profiles recorded in the northern Apennines, the Po plain, and in the southern and central Alps (Ye and Ansorge 1990, Buness and Giese 1990, Nadir 1988, Scarascia and Maistrello 1990).

In the southern segment several published maps were included in the construction of the EGT Moho map. In the area south of the Sardinia channel a map of Moho contours from the Research Group for Lithospheric Studies in Tunisia (1990, 1992) was used. Northwards, from the Sardinia channel to the Ligurian Sea, results from Egger (1992) were used. Some values in the Tyrrhenian Sea were taken from Steinmetz *et al.* (1983); most of the information for the Tyrrhenian Sea and west of the Corso–Sardian block were taken from Nicolich (1987). In the northern Apennines and Tuscany a map published by Wigger (1984) was used as basis, in the Po plain and the surrounding Alpine arc, the one by Giese *et al.* (1991). The last two maps have been modified to a minor degree to account for the latest results of the interpretation of the EGT refraction measurements. As in the central segment most of the newer profiles in the southern segment (i.e. those measured after about 1975) were checked by raytracing. Also in the southern segment contour lines were drawn by hand.

5 Seismicity and focal mechanisms

N. PAVONI, T. AHJOS, R. FREEMAN, S. GREGERSEN, H. LANGER, G. LEYDECKER, PH. ROTH, P. SUHADOLC AND M. USKI

The following text is a short explanation of the Atlas maps on seismicity and focal mechanisms. Historical seismicity (AD 1000/1375–1983) is presented on Map 3. Instrumental seismicity (1975–89) is displayed on Map 4. A selection of well-defined fault-plane solutions are reproduced on Map 5. Most of the source files, station and reference lists, and all the plot files are on the CD-ROM. In this explanatory note we give the main references and discuss criteria of data selection and representation.

The main goal of compiling and representing seismicity data was to identify and delineate in a general way the seismically and tectonically active regions within the EGT, i.e. those with relatively high seismic energy release. Although constantly being improved, the uncertainty in epicentre location precludes use of the EGT seismicity data to reveal or outline single, tectonically active features such as seismoactive faults. The detection of distinct seismoactive tectonic features requires the installation and operation, over an extended time period, of local seismic networks specifically designed for microearthquake observation. In addition, lack of seismic activity does not necessarily indicate absence of tectonic movement. Aseismic creep may also be operative (e.g. possibly in the North Sea). Future GPS surveys, laser ranging, and VLBI networks may be able to quantify aseismic tectonic movements and are thus an important companion to seismicity studies.

HISTORICAL SEISMICITY (MAP 3)

Display

As on all the EGT seismicity maps, we divided the EGT transect into 0.5° x 0.5° rectangles (0.25° x 0.25° for instrumental seismicity) with intensity of red shading increasing as the number of epicentres per unit area (400 km^2) located within each rectangle (see legends on maps for details). The position of the rectangles used for counting events was offset from the geographic coordinate net since many historical events were located on the degree or half degree. In addition, all earthquakes with intensity or magnitude above a certain minimum (i.e. $I_0 \geq 7.5$ for Fennoscandia) are plotted as black circles with origin at the epicentre and radii proportional to intensity or magnitude. The idea behind this choice of presentation was threefold: (1) accuracy of location generally does not warrant epicentral positioning more precise than *ca.* 50 km (25 km for instrumental location since 1975), (2) areas with high seismicity plot so dense that differentiation is impossible, and (3) displaying

energy release instead of number of earthquakes would only compound the uncertainties inherent in intensity or magnitude and location determinations with the additional inaccuracies introduced by the energy calculation.

North sheet

Data for this map were taken from the catalogue of Ahjos and Uski (1992) supplemented by three events from Van Gils and Leydecker (1991). Ahjos and Uski (1992) discuss all aspects of data collection and quality and the reader is referred to that publication for more details. Their data set is included on the EGT CD-ROM.

Period. 1375–1984.

Date and origin time. The origin time is given in Gregorian calendar and Greenwich mean time. For many historical earthquakes the only time information available was the year or month of the earthquake's occurrence. In the listing on the CD-ROM uncertain dating is identified with a question mark in the column after the origin time (the same column is used for additional one-letter information about the nature of the event). Uncertainty of the origin time was roughly evaluated by a one-letter symbol according to Båth's (1956) determination. For the oldest earthquakes the symbol may be missing, which indicates that an estimation of the uncertainty was not possible. Since the 1960s, the origin time has been derived from instrumental recording.

Accuracy of location. In Fennoscandia the historical epicentres are given to an accuracy of one decimal, but at best the location precision is within 0.2° (*ca.* 20 km), in most cases only 0.5–1.0° (*ca.* 50–100 km), and sometimes it is even worse. In the listing uncertainties are expressed by Båth's (1956) symbols.

Number of events, minimum intensity. For the map all events with intensities $I_0 \geq$ V were counted. In the catalogue historical intensities are given in the 12-part MSK-scale or MM-scale. Observed intensities vary between II and VIII, the uncertainty being half to one unit. In this interval, the MSK- and the MM-intensities are comparable to each other.

Focal depths. There is no discrimination of focal depths on the map although estimates derived from isoseismal areas and maximum intensity values are given in the listing.

Completeness. Assuming internal homogeneity between the different regional magnitude scales, Ahjos and Uski (1992) estimate their catalogue to be complete for events with intensity-equivalent magnitude ≥ 4.5 since the 1880s, 4.0–4.4 since the 1940s and 3.5–3.9 since the 1970s.

Sources of data. The historical data is compiled from national and regional catalogues, separate studies and reports, macroseismic observations collected from old documents, church manuals, newspapers, and folklore. The present compilation was based on a catalogue of earthquakes in the Fennoscandian area from 1375–1983 compiled by Ahjos and Korhonen (1984) in cooperation with H. Bungum (NORSAR) and R. Wahlström (Seismological Department, Uppsala University). Ahjos and Uski (1992) provide complete references.

Contamination with explosions and aseismic events. Considering the various uncertainties in the collection of macroseismic information, it is very likely that some events of aseismic origin are also included in the historical dataset.

South sheet

The earthquakes represented on the south sheet are selected from the catalogue of European earthquakes (BC 479–AD 1983) compiled and published by Van Gils and Leydecker (1991) augmented for the region Sardinia channel–Tunisia by data (AD 856–1985) from USGS/NEIC Global Hypocentre Data Base version 1.0 (USGS/NEIC 1991).

Van Gils and Leydecker collected all available source catalogues and eliminated duplications and questionable events. After merging data from the NEIC compilation, duplicate events were again checked and eliminated. The source catalogues are available on magnetic tape and CD-ROM respectively from G. Leydecker, Bundesanstalt für Geowissenschaften und Rohstoffe (BGR), Hannnover; and the USGS, Denver, Colorado, and are *not* included on the EGT CD-ROM.

Period. 1000–1983.

Accuracy of location. One to several tens of kilometres.

Number of events, minimum intensity. Red-shaded rectangles according to number of epicentres; minimum intensity counted: $I_0 \geq 5.0$ (intensities in the 1992 version of the Van Gils and Leydecker catalogue are listed with decimal points in Arabic, not Roman, numerals). In addition, earthquakes with $I_0 \geq 7.5$ are plotted as circles with origin at the epicentre and radii proportional to intensity.

Focal depths. Not discriminated on the map, some estimates are given in the listing; see discussion about accuracy and use of focal depths for instrumental data .

Completeness and data sources. See Van Gils and Leydecker (1991) for discussion.

INSTRUMENTAL SEISMICITY (MAP 4)

General description

Period. 1975–89. The main reason to select this rather short period is the general improvement in quality of most networks since 1975. Earthquake location in Europe had then reached a level where completeness of national catalogues was comparable.

Accuracy of location. The accuracy of epicentre location depends strongly on the procedure, velocity model, number of seismic phases, and geographic distribution of the stations used in the calculation. The maximum accuracy of epicentre location within a dense, modern, well-equipped regular network is ±1 km (Ahjos and Uski 1992); in most cases the error is much larger. The accuracy of location of earthquakes in Europe before 1970 was, by comparison, very poor.

Number of events, minimum magnitude. As for the historical seismicity, instrumental seismicity is displayed as shaded red rectangles with intensity of red proportional to number of epicentres per unit area (400 km^2). The minimum magnitude for the counting procedure was $M_L = 2.5$. In addition, events with $M_L \geq 5.0$ are plotted as circles centred on the epicentre with radii proportional to magnitude. Instrumental magnitudes are based on Richter's classical local magnitude scale M_L. For Fennoscandia, magnitude has been computed from amplitude and period measurements (Båth *et al.* 1976; Panasenko 1977, 1979; Wahlström and Ahjos 1982), and seismic moment (Slunga 1982) or signal coda duration (Wahlström and Ahjos 1982) calibrated to accord with the corresponding M_L-formula used by the seismic agency. In cases where several magnitudes for the same event were available, we preferred national solutions and magnitudes based on amplitude and period. Standard deviation of individual station magnitudes is about 0.2 units.

For the south sheet, seven international, national, and regional catalogues were merged and double entries deleted by selecting those events recorded by the geographically closest network to the event. In most cases this amounted to choosing the event from the country in which the earthquake occurred. (Anyone wishing to get a feeling for the actual accuracy of epicentral location is encouraged to make this exercise.) All events $M_L \geq 2.5$ were counted, there has been no elimination of fore- and aftershocks.

Focal depths. Focal depths are not distinguished. Like epicentre location, instrumental depth is also dependent on the location procedure, velocity model, number of seismic phases used in the calculation, and station distribution. Reliable depth estimates can be obtained only for events inside a dense seismic network with station-to-epicentre distance not exceeding twice the depth. Comparing entries for the same event from different files on the CD-ROM for the Alpine region shows that focal depth estimates can vary as much as from 0 to 100 km. Given this situation, differentiating focal depths on the map would not be very meaningful. Deichmann and Baer (1990) and Eva *et al.* (1990) plot depth distributions in the Alpine region and discuss uncertainties involved in extracting such information from the data files. Due to the absence of error estimates, we advise extreme caution when considering focal depths listed on the CD-ROM.

Station distribution. Accuracy of epicentral location depends on the number and geographical distribution of seismological stations relative to the earthquake hypocentres. In order to give some idea of this distribution, we have plotted on the backside of the map locations of all seismological stations that were active during more than 10 years during the period 1975–1989 and whose coordinates were available to us. This is certainly a small portion of the actual number of stations used in locating the majority of earthquakes in the catalogues. The available station lists with station names or codes and coordinates are listed on the CD-ROM.

Contamination with explosions and aseismic events. Although great care has been taken to filter out man-made events some explosions may still exist in the data.

Source catalogues:

Fennoscandia. We have again used the Ahjos and Uski (1992) catalogue for the north sheet. The input data are provided by the seismic agencies in Bergen, Oslo, Uppsala, Copenhagen, Apatity and Helsinki. For complete references see Ahjos and Uski (1992).

Germany. The present data catalogue essentially represents the data compiled by Leydecker (1986) and Leydecker (1992, pers. comm.). The geographical boundaries are given by the meridians 6°E and 12°E and the latitudes 48°N and 55°N. An additional square between 11° and 12°E respectively 47° and 48°N has been added to this file. Data from the German Democratic Republic are included. The compilation procedure of the national German catalogue undergoes several stages of checking by the different local contributors and the BGR. This is necessary in order to guarantee a high degree of reliability of the data and has been applied to the data through 1988. To make the time period compatible with the rest of the map, the data for 1989 were included; however, they have not undergone the rigorous checking procedure and a few double or man-made events may be included.

Switzerland. The Swiss catalogue on the CD-ROM covers the period 1975–90 recorded and located by the Swiss Seismological Service (ETH Zürich). Plotted are events with magnitudes $M_L \geq 2.5$ from 1975–89. Deichmann and Baer (1990) show a map for all events 1975–90 and discuss location accuracy and selection criteria.

Western Alps. Two regional catalogues have been used to supplement the data for the area of the Western Alps kindly supplied by C. Eva (Istituto di Geofisica, Università di Genova) and J. Fréchet, L. Jenatton, and F. Thouvenot (LGIT-IRIGM, Grenoble). Both of these catalogues in turn contain events registered by other groups. Eva *et al.* (1990) discuss some details of accuracy and selection. Thouvenot *et al.* (1990) describe the Sismalp network used at Grenoble.

Italy. The listing of earthquakes in Italy has been prepared by merging the CNR PFG (Progetto Finalizzato Geodinamico, Postpischl 1985) and the published ING (Istituto Nazionale di Geofisica) catalogues. Comparison with other catalogues, accuracy of

location, and selection criteria are discussed by Suhadolc (1990). Supplementary data has been added to cover events with $2.5 \leq M_L < 3.0$ and events within the region 11°–12°E. These have not undergone any selection criteria and should be accorded less accuracy.

Mediterranean area. Since station coverage here is poor, relatively few events have been recorded in the Mediterranean area even though we know that there is active seismicity in this region. The EMSC catalogue prepared under the direction of J. Bonnin (Centre Sismologique Europe-Mediterranéen, Strasbourg) contains some events in the Mediterranean region in the period 1975–1986. This catalogue (listed on the CD-ROM) has been carefully prepared under relatively strict selection criteria and therefore the data are accorded a high degree of confidence. A description of the catalogue and selection criteria is given by Legros and Bonnin (1990). Additional data up to 1985 from the USGS/NEIC Data Base (USGS/NEIC 1991) were included after deleting double entries. However, coverage for magnitudes $M_L < 4$ is certainly not complete in this region.

Seismicity files on the CD-ROM.

The EGT CD-ROM contains the edited files used to create the maps ('plot files') and several of the original unedited source catalogues. Each file contains a header with reference and format information. A typical file contains the event time (year, month, day, hour, minute, second), geographic location (latitude, longitude), focal depth (if determined), magnitude (and alternative magnitude determinations), source catalogue identifier, location parameters if available (rms, gap, number of readings, etc.) and a catalogue code.

FOCAL MECHANISMS (MAP 5)

Display

Map 5 shows focal mechanism diagrams plotted in equal area (Schmidt) lower hemisphere projection with compressional quadrants in black and the P-axis as dots. The definition of the strike angle follows the one adopted by Aki and Richards (1980). Diagrams are plotted at the site of the epicentre of the earthquake where possible. All solutions available to us and listed on the file on the CD-ROM are indicated by a cross (on the backside). We have generally plotted only those solutions with highest quality ('A') as indicated by the compilers on their source files, regardless of magnitude. In Fennoscandia very few of the solutions had any quality designations and we plotted those solutions from earthquakes having magnitude $M_L \geq 2.5$. In Italy some solutions are also plotted where no quality was given but were judged reliable due to the magnitude of the earthquake ($M_L \geq 6$). These are indicated by quality code 'M' (for 'magnitude selection') on the reverse side of the maps. In some areas where several good quality ('B') solutions but no 'A' solution are given, we have selected a single solution judged to be typical (quality code 'BT', for 'B typical'). For the solutions plotted we have also given the magnitude of earthquake and, for reference to the listing, the number of the event/solution.

Data sources

Fennoscandia. Of the 246 focal mechanism solutions from Fennoscandia only a small number are made in the usual way by dividing the focal sphere into compressional and dilatational quadrants (Bungum *et al.* 1979, Bungum and Fyn 1980, Havskov and Bungum 1987, Assinovskaya 1986, Kim *et al.* 1988, 1989). A large number of focal mechanism solutions have been made by Slunga (1981a, 1981b, 1982, 1985, 1989a, 1989b), Slunga *et al.* (1984), and Slunga and Ahjos (1986) by fitting first-motion directions and spectral

amplitudes for vertical components of P- and S-waves. Scattering by local seismograph-to-ground couplings and possible interference of P-waves, which have travelled different routes to the seismograph station are not eliminated in this method. In a first-order attempt to select from these the more reliable solutions, we have plotted on the map only those solutions from events with $M_L \geq 2.5$. In addition we have included 18 solutions by Arvidsson (Arvidsson 1991, Arvidsson and Kulhanek, submitted) calculated from earthquakes with $M_L \geq 3$ by using P-wave first motions and synthetic waveform modeling.

Germany. 110 fault plane solutions have been compiled, most of them taken from publications (e.g. Ahorner and Schneider 1974, Kunze 1982, Bonjer *et al.* 1984). Each solution has an identifying number (ID) referring to the earthquake event listed in an accompanying seismicity file. Events without an ID are too small to be listed in the seismicity file. The area considered is constrained by 48°–55°N and 6°–12°E with an additional square defined by 47°–48°N and 11°–12°E. All given solutions are derived from P-wave first motions. No explicit magnitude threshold was used because recording quality of recent minor earthquakes may be better than for older larger ones. In other cases only fault-plane solutions from small earthquakes are available. Most of the events had magnitudes $M_L \geq 3$. Good quality fault-plane solutions are indicated with an 'A' or 'B'; 'C' stands for composite solutions, 'D' indicates very poor resolution. Solutions without any qualifying character belong to earthquake clusters represented by typical solutions.

Switzerland. 97 solutions from Switzerland are included on the listing with references to original authors. Where available, quality factors are also given but they have slightly different meanings from the German set mentioned above: 'A' denotes a high-quality uniquely determined solution (to within 0.5°); 'B' denotes a good solution (other solutions within 10° are possible); 'C' solutions are less certain, the focal depth is uncertain or number of stations is limited although the P- and T-axes are relatively certain; 'D' solutions are relatively uncertain; 'E' solutions are very uncertain. More detailed information is contained in Jimenez-Garcia and Pavoni (1984), Pavoni (1987, 1990), Pavoni and Roth (1990), and Deichmann (1987, 1990).

Italy, Sardinia, Tunisia. 213 fault-plane solutions for earthquakes in the Italy–Western Mediterranean region have been compiled by critically assembling information contained in several data sets (e.g. McKenzie 1972; Gasparini *et al.* 1985; Anderson and Jackson 1987). This set includes additional solutions from earthquakes in the Western Alps provided by C. Eva (Eva 1989) and a selection of well-constrained solutions from Suhadolc (1990), which also contains a discussion of parameters and general aspects of compilation.

Focal mechanism files on the CD-ROM

On the CD-ROM are listed three files: (1) selected data as plotted on the map, (2) all solutions available to us regardless of quality, and (3) a composite reference list. In contrast to the seismicity listings, file (2) contains all solutions available to us put into a standard format. The listed data set has been homogenised as far as possible by applying a consistent convention (explained in the header) to express the various fault-plane parameters.

ACKNOWLEDGMENTS

We are very grateful to all those who let us use and list their data, in particular C. Eva, J. Fréchet, L. Jenatton and F. Thouvenot. The idea to represent seismicity not conventionally as one circle per event but as map elements shaded proportional to number of events within each element originated in discussions with E. Kissling and D. Mayer-Rosa; we thank them for their generous advice on the compilations.

6 Recent vertical crustal movement

E. GUBLER, S. ARCA, J. KAKKURI, AND K. ZIPPELT

The geodetic contribution to the EGT data compilations consists of the collection of gravity, geoid and recent crustal movement (RCM) data. The primary task of the RCM compilation was to collect and transform the available data into a common and suitable form, e.g. into a map in the EGT standard scale and projection and a database. The actual data were provided in 5 parts. Several problems had to be dealt with: (1) coordinate transformations (national geodetic nets), (2) relationship between different surveys (only the Swiss and German contribution contain bench marks which are indeed common), and (3) different reference systems (the Fennoscandian data refer to mean sea level whereas the others refer to local reference bench marks). In the following we will deal mostly with points (2) and (3), the first point being a routine procedure (a FORTRAN routine for the transformation of geographic coordinates to the 'EGT' Lambert conical conform projection is provided on the CD-ROM).

RECENT CRUSTAL MOVEMENT DATA

In the future, space techniques will provide extremely valuable information on the behaviour of the Earth's crust. Already today relative motions of a few VLBI (Very Long Baseline Interferometry) and SLR (Satellite Laser Ranging) stations are known (Reigber *et al.* 1989, Campbell *et al.* 1989). Many measurements have been made with these techniques as well as with GPS (Global Positioning System). Within a few years, remeasurements will be able to give a more detailed picture. Since these data were not ready in time for the EGT data compilation, the present compilation was restricted to terrestrial techniques.

For large-scale investigations of RCM, up to now mainly national geodetic surveys have been used. These are higher-order triangulation networks and higher-order levelling networks that have been remeasured in a large enough time interval and with sufficient accuracy. In most cases, however, the existing triangulation networks are either not accurate enough to determine horizontal displacements or no remeasurements exist. So far significant results have been reported for limited areas only (e.g. Reilly and Gubler 1990). The EGT compilation was therefore restricted to the vertical component of RCM, levelling being at least one order of magnitude more accurate than triangulation .

It is the coordinator's task to collect the data from the countries concerned and to transform them into a common and suitable form. In principle the same is being attempted by the IAG-

Subcommissions on Recent Crustal Movements. Maps of vertical RCM are available only for a few areas. While the Nordic Subcommission was able to compile a map for Fennoscandia (Kakkuri 1985, 1986), the European Subcommission is far from reaching that goal (Augath 1986). Therefore, it was necessary to seek an intermediate solution. Data from the different countries were collected and are shown side by side.

Atlas Map 6 shows vertical uplift in contour lines of equal uplift rates. The reverse side of the south sheet shows the data in the form of scale bars with their origin at the site of measurement. We had hoped to show the standard deviations (2σ) for all data sets, however, this information was only available for the Swiss and German data. Where available it is plotted flanking the main bars. The CD-ROM contains four files (Fennoscandia, Germany North, Germany South, Switzerland, and Italy) with coordinates, velocities and, for the Swiss and German data sets, the rms errors of the bench marks used for this data compilation. Coordinates of the reference bench marks are also listed.

RCM DATA AVAILABLE ON THIS PROFILE

Fennoscandia

Fennoscandia has a long tradition in determining RCM and probably has among the largest velocities along the EGT profile (up to 10 mm/year). Denmark, Finland, Norway and Sweden work together in the Nordic Subcommission on Recent Crustal Movements. The data were provided by JK in the form of a map in the scale 1:2 million showing contour lines of equal uplift rates. It was compiled from a combination of tide gauge records from all four countries (data on reverse side of map and as listing on the CD-ROM) and the repeated levelling data from Denmark, Finland and Sweden (this data only available to us as contour lines) and covers the Fennoscandia and the northeastern part of Denmark. Further information may be found in Kakkuri (1985, 1986) and Ekman (1989). Deviations to the general picture given by the contour lines reach 0.6 mm/year where known.

Since our source map was not in Lambert conic conformal projection, the contours had to be digitized and replotted. At the same time we digitized locations of tide gauge recordings and bench marks where they were indicated on the map.

Federal Republic of Germany

The German contribution was compiled by KZ and H. Mälzer. It consists of two parts: a northern one identical to the so-called North Sea Coast Levelling Network (NKN) and a southern one containing the precise levellings of Bavaria, Baden-Württemberg, Rheinland-Pfalz, Saarland, parts of Hessen, Nordrhein-Westfalen and Niedersachsen. The northern and the southern parts have the southernmost levelling lines of the NKN in common, including the fundamental bench mark Wallenhorst, but so far they have not been treated in a common adjustment. The northern part consists of about 180 points and the height changes are provided by the Geodetic Institute of the Hannover University (Leonhard 1988). The levelling data of the southern part are summarised using data from different recent investigations (Mälzer 1979, Zippelt 1988, Mälzer 1990). These data consist of two and in some cases three and more levellings and were introduced in an adjustment procedure to determine time-dependent height changes. The model and the applied strategy is described by Zippelt (1988). More than 1200 height changes were estimated in the adjustment. The data of the northern and southern parts are listed as two files containing coordinates, vertical velocities and their standard deviation (1σ).

Switzerland

The Swiss contribution consists of an analysis of the first-order levelling of Switzerland. The first measurement was carried out between 1905 and 1927. The second was completed in 1991. The rms errors computed from the adjustment of the two levellings are 1.4 and 0.8 mm$\sqrt{D}$km respectively. These levellings allow the determination of significant relative movements between the Swiss Plateau on the one side and the Alps on the other side. Since no accurate connection could be computed to coastal areas, only relative movements have been determined so far. These relative movements exceed their standard deviation by a factor of four and therefore can be regarded as highly significant. The procedure used for this investigation is described in detail in Gubler *et al.* (1984). Preliminary results and geophysical interpretation are given in Gubler *et al.* (1981) and in Geiger *et al.* (1986).

The data were available in the form of a file containing coordinates, vertical velocities and their standard deviation of some 170 bench marks covering the whole country.

Italy

Arca and Beretta (1985) published the first results of vertical RCM studies for northern Italy in the form of contour lines on a map on the scale of approximately 1:1 million. In addition, SA provided the coordinates and the vertical velocities of some 310 bench marks. The data cover the area between the Swiss border and the Ligurian Sea and from Cuneo to Venezia. Instead of transforming the map into the desired projection, we plotted a new map using the digital data. Contouring in several areas, notably at the Adriatic coast, was difficult due to data originating from single widely spaced and spatially diverging profiles. Therefore we masked off regions where contours were supported by very few data points. The bench marks are plotted (without standard deviations since none were available) on the back side of the map. Therefore data extending beyond our contours can be easily read off the map.

THE PROBLEM OF THE REFERENCE

Reference surfaces

In order to compute vertical velocities of bench marks, one has to define a suitable reference. Potential users of the EGT data compilation naturally seek 'absolute' velocities, whatever that means. From a geodetic point of view, 'absolute' could mean 'relative to mean sea level' or 'relative to the geoid' or even better, 'relative to the Earth's centre of gravity'.

However, mean sea level shows a secular rise of the order of magnitude of 1–2 mm/year (Warrick and Oerlemans 1990) with respect to the geoid but it is not certain that this rise is the same all along the European coastline. At the moment no one can produce more accurate figures. In the future, geodetic measurements should be able to answer this question (Carter *et al.* 1989), but it will take many years until significant results can be expected.

To make the problem even more complex, each uplift of the crust provokes a change in the geoid. Sjöberg (1982 and 1983) estimated the change of the geoid induced by the uplift process. He found that an uplift of 9 mm of the crust provoked an uplift of 0.7 mm of the geoid, e.g. somewhat less than 10% of the uplift of the crust. To compute 'absolute' velocities, meaning relative to the Earth's centre of gravity, observed vertical movements, eustatic rise, and uplift of the geoid must be summed up.

References used

In many countries it has not yet been possible to refer the RCM data to mean sea level. Therefore, these countries refer their results to more or less arbitrarily-chosen bench marks regarded as stable, which means that every contribution to this data compilation has its own reference.

The Fennoscandian part refers to mean sea level as defined by tide gauges all around the Fennoscandia (Kakkuri 1985). No corrections have been applied for either the eustatic rise of mean sea level or the change in the geoid produced by the uplift. These two effects could add some 2 mm/year to the provided uplift rates.

The contribution of northern Germany refers to the fundamental bench mark Wallenhorst near Osnabrück. According to Augath (pers. comm.) this reference shows no significant movement with respect to the Dutch reference N.A.P. The latter subsides with respect to mean sea level by 1.0–1.5 mm/year (Lorenz 1991), which could be caused by the eustatic rise of mean sea level.

The contribution of southern Germany refers to four fundamental bench marks Wallenhorst (Niedersachsen), Wahlenau (Rheinland-Pfalz), Freudenstadt (Baden-Württemberg) and Schernfeld (Bavaria). Statistical tests have shown that no significant relative motion can be found among them and no significant relative movement can be found between the fundamental bench marks of the northern and southern parts either (Mälzer 1979). This may be caused by the fact that these investigations are not very sensitive to long wavelength signals in RCM. To reduce these influences, the reference points are not used as fixed points but their assumed stability is introduced in the adjustment as uncorrelated information with a standard deviation of 0.1 mm/year.

The Swiss contribution refers to an arbitrarily chosen group of bench marks near Aarburg on the southern border of the Jura mountains, which seems to be representative of the flatter areas of Switzerland.

The Italian contribution refers to a bench mark in Genoa. From tide gauge records this bench mark has a vertical velocity of -1.2 mm/year (Salvioni 1957), which would correspond to the eustatic rise of mean sea level of the same amount. Therefore, the bench mark at Genoa would actually not have moved, or in other words, would show an 'absolute' vertical velocity of 0.

It was impossible to properly join the different parts in the given amount of time (until the end of 1991). To connection the Fennoscandian and the German data, for instance, was not possible since no velocities were available for common bench marks and the Fennoscandian map does not reach German territory. Only an indirect and uncertain connection is given by mean sea level (see above). Therefore we decided to plot the uplift rates independently and to separate the contours form the different data sets by a grey strip running around the borders of Switzerland. Anyone who would like to analyse the RCM data or compare them to other data should be aware that the results of the different parts may not be combined directly.

HOW TO COMPARE OR COMBINE THE DIFFERENT CONTRIBUTIONS

Despite the above warning we can attempt some tentative comparisons. For instance, the two German blocks have been tested and no significant relative movement could be found between the reference bench marks of the northern and the southern block (Mälzer 1979). We can therefore say that the two German blocks have a common reference to within the accuracy of the levellings concerned. A rough estimate of the relative uncertainty yields 0.5 mm/year.

The connection between Germany and Switzerland is well established with eight common bench marks along the border (Mälzer 1988). By comparing the velocities of these bench marks in the two computations, a rough estimate for the relative motion of the references may be computed. The Swiss reference bench marks seem to subside 0.4 mm/year with respect to the German reference but the standard deviation is of the same order of magnitude. Therefore, no significant relative motion can be proved between the German and the Swiss reference.

For comparing the relative motion of the references between Switzerland and Italy, there is only one supposedly common bench mark in Iselle at the southern end of the Simplon railway tunnel that could be used. A comparison of its velocities in the Swiss and the Italian computations yields an uplift rate of 1.3 mm/year for the Swiss reference with respect to the Italian reference in Genoa. This is more than two times the standard deviation of the two computations. Therefore, the Swiss reference bench marks at Aarburg seem to rise significantly with a velocity of 1.3 mm/year with respect to the Italian reference in Genoa.

OUTLOOK

We stress that the estimates mentioned here are very preliminary. More realistic estimates can only be expected from the map of recent vertical crustal movements of western Europe which is underway (Augath 1986). In the meantime, the EGT compilation will be useful for making comparisons with other geodetic, geophysical, or geological information. It will take even more time to get realistic 'absolute' vertical movements and it is up to the geodetic community to provide the 'absolute' velocities of the reference bench marks.

7 Geoid undulations and horizontal gravity disturbance components

D. LELGEMANN AND H. KUCKUCK

Atlas Map 7 presents contours of quasi-geoidal undulations ζ according to the definition of Molodensky (see, e.g. Vaníček and Krakiwsky 1986). These undulations describe the disturbing potential **T** of the Earth's gravity field at the Earth's surface

$$\mathbf{T}_P \equiv \gamma_P \bullet \zeta_P \equiv G \bullet \zeta_P$$

where $\boldsymbol{P}$ are positions at the Earth's surface, γ_P is the normal gravity at $\boldsymbol{P}$ and $G = 978.8$ gal is a mean gravity value.

The gravity disturbing vector is defined as

$$\delta\mathbf{g} = \begin{vmatrix} \partial\mathbf{T}/\partial y^1 \\ \partial\mathbf{T}/\partial y^2 \\ \partial\mathbf{T}/\partial y^3 \end{vmatrix} = \begin{vmatrix} -G\xi \\ -G\eta \\ -\delta g \end{vmatrix}$$

where $(y^1\ y^2\ y^3)$ is the local astronomical basis at **P**, y^3 the local vertical direction, y^1 the local north direction, y^2 the local east direction. ξ and η are the north–south and the east–west component of the deflection of the vertical. The gravity disturbance δg is related to the free air anomaly Δg_F at the Earth's surface by

$$\Delta g_F = \delta g - 2G/R \bullet \zeta$$

where R = 6 371 km, the mean Earth radius. The absolute value of the horizontal components of the gravity disturbance vector (δg_H) is given by

$$\delta g_H = G\,(\,\xi^2 + \eta^2\,)^{1/2}.$$

The values are derived from $\mathbf{T}_P$ by numerical differentiation and plotted in the isoline map of the horizontal gravity disturbance components (Atlas Map 8). The direction of the horizontal part of the gravity disturbance vector is orthogonal to the isolines of the quasi-geoidal undulations and is therefore best visualised on the geoid map. We have therefore plotted only the geoid undulations and the value of the horizontal component of the gravity disturbance vector.

GEOID COMPUTATION

The computation of a combined European astro-gravimetric geoid has been carried out in a cooperative project by the Institut für Erdmessung of the University Hannover (IfEH) and the Institut für Angewandte Geodäsie in Frankfurt a. M. (IfAG). It has been performed within the framework of the IAG Special Study Group 5.50 'Etude du Géoide en Europe Central et Meridionale'. The compilation was only possible due to the immense effort by

various geodetic institutions in collecting the data. Details of data collection, the quality of the data and the computation process are published in Brennecke *et al.* (1983).

A set of about 67 000 mean free air gravity anomalies of block size 6' x 10' have been collected for the European area at the IfEH. They have been combined with a global data set of about 12 000 mean free air gravity anomalies of block size 1° x 1° and a set of satellite-derived spherical harmonic coefficients of degree and order 20. As computation method we applied a least-squares spectral combination using integral formulas. The resulting disturbing potential is referred to the Geodetic Reference System 1980 with a=6 378 137 m and f=1/298.25722 (Moritz 1980). It has been computed in a 12' x 20' geographic grid.

The results for the EGT suffer from a very large data gap in Sweden, where only 1° x 1° mean values were available at the time, and a gap in the region of Austria. At the IfAG additional information in the form of about 7 000 components of the deflection of the vertical has been used to check and refine the part with wavelength longer then 2°. Since the deflection data are very sparse, the medium wavelengths ($12' < \lambda < 2°$) could only be computed from the gravity data available.

The combined solution shows deviations from a pure gravimetric solution between $\Delta\zeta = \pm 1$ m for wavelength longer than 2°.

Using GPS-observations and levelling data the disturbing potential T at the Earth's surface can be derived also from another, completely different, set of observational data. The results of a GPS-traverse from south Germany through Norway has shown that the long wavelength features of the European geoid are correct to within the error margin given above (Torge *et al.* 1989).

FURTHER DEVELOPMENT

There is fast progress in improving the computation of regional geoids because a precise knowledge of the geoid is necessary to derive heights above sea level from GPS-results. Since compiling the data for the EGT new and more precise geoid determinations have been performed for Germany, Switzerland, Austria, and Scandinavia and are in progress for southern Europe (Denker 1989, Tscherning and Forsberg 1986). These new determinations show much smaller discrepancies between different data sets such as gravity anomalies and deflection. A new European geoid computation is expected to be carried out in the middle of the 1990s.

8 Bouguer gravity anomalies

E. KLINGELÉ, B. LAHMEYER AND R. FREEMAN

Atlas Map 9 shows the Bouguer gravity anomalies along the EGT. These were produced by compiling all available Bouguer gravity data and, where possible, applying a standard density of 2.67 Mgm^{-3} for the topographic correction. The data points used to create the contours are printed on the reverse side so that an analyst using a light table can quickly identify artifacts produced by uneven data distribution. These data points and values are listed on the CD-ROM. The scale and accuracy of this compilation limits interpretation to large-scale regional elements only. The Bouguer gravity data have an accuracy of ± 2.5 mGal (1 mGal = $10^{-5}ms^{-2}$) with exception of a few small areas near the Caledonides where the accuracy is ± 5 mGal.

DATA AND BOUGUER REDUCTION

The available gravity data along the EGT have heterogeneous origins. To make them comparable all data have been shifted, where necessary, to the International Gravity Standardization Net 1971 (IGSN71) and recompiled with the 1967 Gravity Formula for the normal gravity. The 1967 formula was chosen because most gravity maps are published in this system and a more modern system would not have improved the results. In addition, this procedure is standard at the Bureau Gravimetrique International (BGI) in Toulouse, the major source of our data compilations. Most data sets are reduced for the topographic effect from the stations to a distance of 167 km using a density of 2.67 Mgm^{-3}. (This correction was adopted as our 'standard topographic correction' and will be referred to as such in the following text). In some areas, however, the Bouguer gravity was not available in the form of data points. In this case we had to digitize Bouguer gravity anomaly contour maps at a scale of 1: 1 million (or larger). The slight error incurred by assuming similar Bouguer gravity corrections when the original position is unknown (i.e. as when digitizing contours) is negligible at the scale of 1:2.5 million. A region-by-region summary of the data handling follows.

Northern Fennoscandia

The Bouguer data were digitized from the 1:1 million map 'Gravity Anomaly of Northern Fennoscandia' of the Nordkalott Project (Geodetic Institutes and Geological Surveys of Finland, Norway and Sweden 1986), which includes the standard topographic

correction as we have defined it in the preceding paragraph.

Sweden/Denmark

The data from Sweden (below 66° latitude) and Denmark were taken from the data files of the BGI, Andersen and Engsager (1977) and Andersen (1978). Most of these data are not topographically reduced. This is not a problem in the flat area of Denmark but the topographic effect of the Caledonides cannot be neglected in Sweden. The regional effect of the topographic masses was compiled for distances from 15 km to 167 km from the stations using the topographic 5' x 5' grid TUG87 (H. Sünkel, pers. comm.). It was not possible to calculate the local near-station topographic effect because no fine topographic grid was available. Therefore a few gravity values in the Caledonides may have an inaccuracy of about ± 5 mGal (in one extreme case ± 8 mGal), but these local errors will not disturb the content of the regional information.

Bothnian Bay

We were not able to acquire any accurate data from the Bothnian Bay. On the other hand, some data from Finland were available from BGI files. These latter were used to support the interpolation and to draw the contours extending into the Bothnian Bay from Sweden. These contours were, however, masked out on the coastline due to the aforementioned lack of data from the Bothnian Bay.

North Sea

Data for the North Sea were supplied on magnetic tape by J. Makris (University of Hamburg). The sources of these data are unknown to us, some are from Andersen and Engsager (1977) and Andersen (1978). Close observation of the location of these points (see reverse side of the north sheet) clearly shows that some are original ship track measurements whereas others are digitized contours. Most, but not all of data on the tape are identical to those in BGI files (at the time we requested them).

France/Benelux

The data in France were also taken from BGI data files. They have not been topographically corrected because no fine topographic grid was available and the data are only used at the border of the central segment to support the interpolation. The mountains in this area are comparable to the Harz Mountains in Germany, where the topographic reduction rarely exceeds 5 mGal.

FRG

We digitized the contours from a 1:1 000 000 version (kindly supplied by S. Plaumann) of the 'Bouguer Gravity Anomalies for the Federal Republic of Germany' that included the standard topographic reduction (Plaumann 1987).

Ex-GDR

The data in the ex-GDR were digitized from the 1:200 000 maps compiled in the 1930s by A. Schleusener (Closs and Hahn 1957). These data were calculated with variable density for the topographic reduction. An error in the density of 0.1 Mgm^{-3} for a station at a height of 100 m would cause an error in the Bouger anomaly of about 0.4 mGal. Since the region is flat and has low elevation (usually < 50 m) the inaccuracy due to the densities differing from the standard density is negligible for our purposes.

Austria

Original data from western Austria were taken from a diskette kindly sent to us by G. Wallach (later published in Posch and Wallach (1989).

Switzerland

For Switzerland we used the original data of the Gravity Map of Switzerland (Klingelé and Olivier 1979, 1980).

Italy

We digitized the data from northern Italy from the 'Gravimetric Map of Italy' (compiled by Ballerin *et al.* 1972) to which the standard topographic reduction had been applied. The original sources for the data can be found in that reference.

Mediterranean Sea

For the Mediterranean Sea we used data from a tape supplied by J. Makris and assumed they had the standard topographic reduction applied. The source of the data in the region of the EGT strip is Ballerin *et al.* (1972) (see also Morelli 1975).

Corsica

Corsican gravity data were digitized from the map of Bayer and Lesquer (1976). These data were already topographically reduced with the standard density of 2.67 Mgm^{-3} (Bayer and Lesquer 1977).

Sardinia

The data from Sardinia (Trudu 1962) were reduced with variable density. In this case we had access to the orginal data and the corrections. We recompiled them with the standard density for the Bouguer plate. Only for a few stations does the topographic reduction calculated with variable density exceed 5 mGal (maximum value less then 7 mGal). Therefore inaccuracies due to calculating with a density differing from 2.67 Mgm^{-3} amount only to some tenths of a mGal and can therefore be neglected.

Tunisia

The data for Tunisia, digitized from the 1: 1 million map compiled by Midassi (1974) for an M.Sc. thesis, are not corrected for topography. According to Midassi the error does not exceed ± 1 mGal. We note that there is some topography in northern Tunisia that, if not properly taken into account, could introduce larger inaccuracies. It was not possible to trace the corrections for this region and we simply report the error limits stated in the reference.

DATA STANDARDISATION AND RECOMPILATION

The coordinates of the available data as listed in the compilations or as digitized from the maps were first transformed to Lambert conic conformal projection. We made no special transformation for offset in datum between local (i.e. national or international) ellipsoids. Test calculations comparing French, Swiss, and German nets (Graf 1988) show that neglect of special transformations results in differences usually less than 100 m.

First, plots of all data were made to check and remove errors in the data files. We then compiled the basic grids with a grid spacing of 7.5 km x 7.5 km. The programme used for interpolation was an implementation of an algorithm after Briggs (1974) and Swain (1975) written by G. Weber (Institut für Geodesie und Photogrammetrie, TU Berlin). It is fast in

comparison to other algorithms and produces reliable results.

Second, these basic grids were then refined to a grid spacing of 2.5 km x 2.5 km by spline interpolation and plotted with the programme ISOVAG (E. Klingelé 1976). The original compilation comprised 7 maps including 4 approximately 250 km-wide segments (POLAR, FENNOLORA, central segment, and southern segment) and 3 regions of greater width in areas of special interest (EUGENO, Alps-Apennines, and Tunisia). For the final printing the seven compilations were combined into two strips for Atlas Map 9: the northern segment data making up the north sheet and the combined central and southern segments data making up the south sheet. The isoline spacing is 10 mGal. In regions where the horizontal gradient of the Bouguer gravity is relatively small, dashed isolines with a spacing of 5 mGal have been added to show more details.

USE OF THE BOUGUER GRAVITY ANOMALIES

The purpose of this compilation is to provide interpreters with a coherent and standardised data set. The data of the Bouguer gravity compilation can primarily be used to compare density distributions derived from seismic models of crustal structure (see for example, Klingelé *et al.* 1990). Combined with aeromagnetic data, the gravity data provides even a tighter constraint on acceptable crustal structures. The long-wavelength anomalies reflect density heterogeneities in the mantle, a crucial topic in crustal-scale geodynamic modelling. A further use will be to help calibrate satellite gravity data. One example of use of the data is given by Lee and Green (1990) who produced grey-scale shaded relief maps by regridding the EGT data set.

On the CD-ROM the EGT data set is represented by three files (north, central, south) containing the geographic location (latitude, longitude), the Bouguer anomaly (in mGal), and, where available, the height (in m) of the points plotted on the reverse side of the map.

ACKNOWLEDGEMENTS

Thanks to all those who helped us get as close as possible to the original data. J. Makris kindly supplied us with a magnetic tape containing data from the North Sea and the Mediterranean, S. Plaumann sent us an unpublished sheet of his Bouguer data, G. Wallach gave us a pre-publication version of the data from western Austria. E. Kissling critically reviewed the text and made many constructive remarks.

9 Magnetic anomalies

T. WONIK, A. GALDÉANO, A. HAHN AND P. MOUGE

During the 1983 General Assembly in Hamburg the International Association of Geomagnetism and Aeronomy (IAGA) established a working group chaired by A. Hahn, Hannover (vice chairman, A. Galdéano, Paris) charged with producing a map of geomagnetic anomalies for Europe. In collaboration with the coordinators of the EGT this working group also took over the task of producing a map showing geomagnetic anomalies for the EGT. The Hannover group has worked on the northern and central segments, and the Paris group on the southern segment.

The aim of this compilation is an anomaly map that can be used as a basis for interpreting broad anomalies with wavelengths up to 2000–3000 km. Such interpretations should yield information about the distribution of magnetised material within the Earth's crust as deep as material of that kind is present and give anomalies recognisable at the surface. The respective depth range is usually unknown or very uncertain. Depths that can be approximately resolved in magnetic interpretation are the Curie-isotherm of magnetite, the Moho, and in some circumstances even depths down to 70 km. However, wavelengths of the broadest discernible anomalies are much greater than this depth range. Anomalies of geological interest might be relatively small and it is important to keep the anomalies comparable over more than 1000 km within an error of ± 10 nT (Hahn 1986). The following guidelines were therefore used as a basis for our compilation. First, the anomalies should have the shape as if they were measured at the same altitude (3000 m above m.s.l.) and the same time (1980.0). Second, the anomalies should be residuals after subtracting an appropriate common reference field (DGRF 1980) from the total field.

DATA

Atlas Map 10 displays the resulting contours of aeromagnetic anomalies along the EGT strip. The source surveys are shown on the reverse side with pattern indicating the distribution and density of stations. In addition, each sheet has a table giving data parameters and a reference list for the sources. These data sets result from surveys which were not only carried out at different flight altitudes and epochs, but in some cases had also used different coordinate systems, profile spacing, instruments, and types of processing. Moreover the data were available in a variety of forms. Surveys (11) and (24) (see reverse of map sheets) were made available as punch cards. Lists or publications had to be used for surveys (6), (12), (14), (15), (16), (22), and (23). Surveys (5), (7), (8), and (17) were

available as maps which had to be digitized. All other survey results were copied on magnetic tapes or diskettes, but they all differed from one another in the tape format used.

For surveys measured on the ground or surveys carried out at constant ground clearance, information about topographic elevations were necessary. For surveys (6), (12), (14)–(16), (18)–(21), (22), and (23) no information about the elevation was given. A mean height for each survey was estimated using data given by Schleusener (1959) (in Table 1 these mean values are set in parenthesis). Additionally, mean topographic heights for the Finnish survey (3) were given by Mikkola (1983). A data set comprising the heights of Norway (1) and parts of Sweden (2) in a 1 km grid was purchased from the Norwegian Mapping Authority.

The Finnish Meteorological Institute (C. Sucksdorff and H. Nevanlinna) put data for the Gulf of Finland at our disposal. Since these data were included in the data set of Finland (3) by J. Korhonen, they do not appear in the table.

In compiling the data for the southern sheet we noted that, in addition to the previously-mentioned sources of heterogeneity, reference field approximations for regions south of the Alps differ strongly from one survey to another. Moreover, a regional model adopted for some territories has shown strong gradients inconsistent with surrounding panels. We had to use polynomial correction surfaces based on residuals measured on overlappings. In order to constrain the better reference levels, these correction surfaces were estimated from the widest panels; the smallest, such as the Alpine arc coverages, were then constrained by this framework. More information on the surveys, compilations, and their interpretation are given for the Italian region by Arisi Rota and Fichera (1987), for the western Alps by Mouge and Galdéano (1991), for Sardinia and surroundings by AGIP (1979) and Cassano *et al.* (1979), for southwestern France and the western Mediterranean by Le Mouël (1970), Le Borgne *et al.* (1971, 1972), Bayer *et al.* (1973), and Galdéano and Rossignol (1977a, 1977b).

DATA PROCESSING

Figure 9.1 shows the calculation steps necessary to achieve the above-mentioned aims using, as an example, anomaly values from the southern part of the German airborne survey at 1500 m above m.s.l. and referred to 1967.5.

Step 1: Values of total intensity are obtained by adding the 'old' reference field used for producing the anomaly map to the anomaly values of the map.

Step 2: To be sure of the reliability of these total intensity values we compared them with the results from ground measurements made at repeat stations for observing secular variation (*SV*) (G. Schulz, pers. comm.; M. Beblo, pers. comm.; Voppel and Wienert 1974, Fischer *et al.* 1979). For this we selected data from ground stations in magnetically quiet areas and transformed them to the same epoch and altitude referred to by the airborne data. In some areas the comparison revealed differences that were most probably due to deficiencies in processing the airborne survey data. Therefore, we added a correction term to these total intensity data.

In these comparisons, as well as in those between adjacent, overlapping airborne survey data, a linear function with slope of -21.5 $nTkm^{-1}$ was assumed for the relationship between total intensity and altitude. *SV* was estimated using records of the nearest observatories (Golovkov *et al.* 1983). The result is very satisfactory as in most cases differences of less than 10 nT between the individual surveys were found. These comparisons make it possible to reconcile the results of adjacent surveys. The use of a network of ground repeat stations

covering the entire area of all the airborne surveys involved guarantees that the agreement of adjacent surveys is not restricted to the small area of overlap but will be valid for the entire survey area.

Step 3: To transform the F_{cor} values corrected in this way to the epoch 1980.0 and the altitude 3000 m above m.s.l., a representation of *SV* (e.g. 1967.5 to 1980.0 in Figure 9.1) in the area under consideration is necessary. This was accomplished by calculating a quadratic polynomial for all of Europe using observatory data combined with results from repeat station measurements. This step yielded absolute values at 1500 m and for 1980.0.

Step 4: The Definitive Geomagnetic Reference Field 'DGRF 1980', altitude 1500 m, epoch 1980.0 (IAGA Division I Working Group 1, 1986) is subtracted.

Step 5: The residual values (anomalies) are continued upward to 3000 m using a programme published by Gibert and Galdéano (1985). This programme requires data in a regular grid. Irregularly spaced data sets were gridded with the GINTP1 subroutine (using the local fit method) from the UNIRAS software package. The appropriate grid interval is dependent on the data distribution. In the present case a 2.2 km grid (in Gauss-Krüger-coordinates) was used. The spatial distribution of the input data is shown on the reverse side of the colour plates. This step had to be modified for areas where measurements were carried out at constant ground clearance, as was the case in most parts of Norway (1), Finland (3), and Sweden north of 66°N (2). For this purpose we used a programme described by Cordell and Grauch (1985).

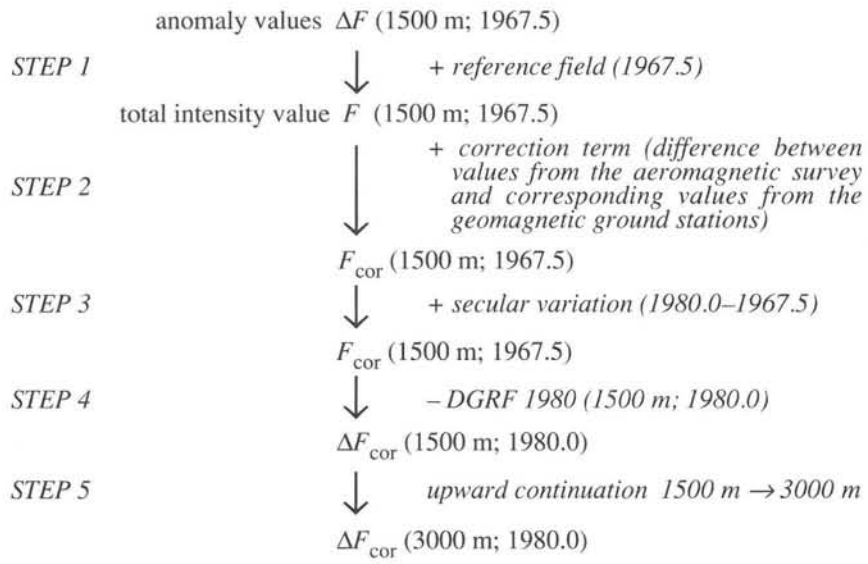

Figure 9.1 Procedure for converting anomaly values to a common altitude of 3000 m and epoch 1980.0

MAP PRODUCTION

The map was produced with the standard EGT parameters (scale: 1:2.5 million, projection: Lambert conic conform). Before transforming the coordinates of the data sets, gridded in their original coordinate systems, to this projection, they had to be transformed to geographic coordinates. This was done with the help of Grossmann (1964) for Gauss-Krüger or UTM coordinates and Bolliger (1967) for the Swiss rectangular kilometric coordinates.

A further use of the UNIRAS interpolation subroutine GINTP1 yielded a data set in a 5 km grid. This data set is on the CD-ROM accompanying the EGT Atlas. Note that this data set extends outside the area plotted on the map sheets.

Contouring and shading was done with the UNIRAS subroutines GCRN2V and GCRN2S. For the north sheet contour line spacing is 50 nT, for the south sheet it is 20nT.

PRECISION AND SOURCES OF ERROR

The resulting ΔF_{cor} values (3000 m; 1980.0) of the anomalies processed in this way meet the requirement that the values of two adjoining surveys differ by less than 10 nT in the overlapping area. In the case of the German and French surveys the mean difference is only 1–2 nT. This is important because this involves the boundary between the compilations of the two compilation teams.

The relative precision strongly depends on the gradients observed in the study regions. Moreover, important distortions on the IGRF coefficients occur, due to the poor distribution of observatories for some areas, and the resulting poor description of the secular variation and its rate of change. For these reasons, specific treatments have been necessary for the southern segment (Mouge and Galdéano 1991).

Along the northern and western margins of the compilations for northern and central Europe, errors increase but they do not exceed 20 nT. This decrease in precision occurs for the following reasons:

- Only rather widely-spaced ground measurements were available for the Netherlands (14), Belgium (16), and Czechoslovakia (22), (23) (see reverse side of the maps).
- Calculation of the secular variation between 1945.0 and 1980.0 for the Dutch data (14) was a problem because only a few observatories existed at that time.
- The airborne data for Denmark in 1963 (7) and (8) was obtained with a fluxgate magnetometer. At that time this instrument measured only relative values and showed large drift. Fortunately, results from a ground survey of Denmark (6), covering the entire onshore area are available. This data set has been used to adjust the aeromagnetic data.
- A correction term (Figure 9.1; Step 2) cannot be calculated for Scandinavia because this processing step provides reliable results only in cases where the anomalies in the area under consideration are relatively smooth.
- The low-level survey of Sweden has not yet been completed. Therefore, data measured on profiles 35 km apart had to be used for central and northern Sweden and the Gulf of Bothnia (4) (see reverse side of maps).

  The 1 km grid data set for the area of the former German Democratic Republic (ex-GDR) (13) were continued upward by 3000 m before being handed over to us. These data were based on aeromagnetic surveys in the southern GDR (profile spacing: 0.25 km; altitude: 100 m above ground) and on ground measurements (average spacing: 0.5 km) in the northern part of the ex-GDR. The field values were observed at different epochs.

With the help of survey (12), data set (13) could be adjusted with respect to the general level [no topographic elevations are provided with survey (13)]. The final amplitudes of the local anomalies are too small because they are continued to an altitude greater than 3000 m by an amount depending on the topographic elevation. Especially in the southern half of the country this cannot be neglected (the highest top reaches more than 1000 m above m.s.l.), so the error of the amplitude of small anomalies may be up to ± 25 nT.

ACKNOWLEDGEMENTS

We thank all those who made data available to us, especially those who are referenced in the tables. Thanks also to R. Freeman for his help in producing the maps.

10 Magnetovariational and magnetotelluric results (Northern Europe)

S.-E. HJELT

This chapter introduces Atlas Maps 11 and 12 dealing with electromagnetic data. In contrast other methods discussed in this booklet, electromagnetic data and methods are generally less well-known. Therefore, in this chapter I give a comprehensive introduction to the methodology and add some discussion of the results for the northern data.

Electromagnetic methods are used to obtain the lateral as well as the vertical distribution of the conductivity σ (or its reciprocal, resistivity ρ) within the Earth. The conductivity depends on the mineralogical composition, number of fractures in the bedrock, content and nature of pore fluids and the temperature of the bedrock.

Measurements should, if possible, start with areal mapping. Anomalous conducting structures and (regional) average values of conductivity are then studied in more detail along selected profiles or at selected sites. To determine the electrical properties of the deep crust and the upper mantle, the source energy from temporal variations of the ionospheric and magnetospheric current systems are used for periods above some tenths of a second. For shorter periods (audio magnetotellurics (AMT) cover the audio range: 1–0.0001 s) lightning discharges in the atmosphere produce the source field. Occasionally also (man-made) controlled sources are available to study the upper parts of the crust (Velikhov *et al.* 1987).

METHODS

In *geomagnetic depth sounding* (GDS) – also called the magnetovariational (MV) technique – the time variation of all three spatial components of the magnetic field is registered simultaneously at several sites. Preferably arrays of magnetometers are used, but profile measurements are also commonly employed.

In *magnetotellurics* (MT) the horizontal components of both the Earth's electric and magnetic field are recorded. In the *telluric method* (TT) only variations of the electric field are studied. A simultaneously recording reference station is often applied to reduce noise in MT and to provide a reference in TT profiling. The electrical equivalent to magnetometer array studies is called the EMAP technique.

The components of the Earth's electromagnetic field consist of two parts:

1. The primary (inducing) field and its time variations caused by changes in the source region.
2. The secondary field created by the currents induced in the Earth. This part depends on the conductivity distribution in the crust and upper mantle.

The secondary part can be further divided into its 'normal' and 'anomalous' parts. The 'normal' part contains the effects of a general increase of conductivity with depth following the increase in temperature. The 'anomalous' part then is thought to describe the contributions of all other, most notably tectono-geological variations in the Earth's conductivity (Berdichevsky and Zhdanov 1984).

The induced fields and the currents associated with them are distributed within the Earth and its structures according to the basic laws of electromagnetism: induction and conduction. The *inductive currents* give the main response, which varies with period (frequency), conductivity and size of the conducting structures. The induced currents redistribute themselves *conductively* and charges are accumulated at boundaries of changes in conductivity within the bedrock. The secondary fields of these charges are independent of the period. Their influence was originally called the galvanic effect (e.g. Berdichevsky and Dmitriev 1976), but has been renamed to 'static shift' to describe its effect on the sounding curves. The techniques of separating and modelling the different parts of the field vary from method to method and are the key points in translating EM responses to Earth structures.

DATA PROCESSING

The recorded time variation of the geoelectromagnetic field is in most techniques divided into harmonic components. The correlations between the spatial field components are computed and monitored for quality control purposes. Also the qualitative characteristics, e.g. the dimensionality of the Earth conductivity models can be studied from these properties.

The data are first developed into *transfer functions*, which basically are proportional to the quotients between the various components of the electric and magnetic field. For the magnetometer array studies *induction arrows* , the quotients between vertical and horizontal magnetic field components, are widely used. They are a useful graphical device, since they are constructed to point towards better conducting regions (actually, towards currents induced within these regions). If the Earth contains a well-conducting structure, the induced currents are more-or-less concentrated on the surfaces and the edges of the conductors. The change of direction or pattern of the arrows at various periods can be used to identify long, linear conductivity structures and boundaries of regional changes in conductivity within the crust (for example, see Atlas Map 12).

The induction arrow (vector) is a complex quantity at each period and the variation between the in-phase (real) and quadrature (imaginary) parts contains also information on the conductivity of the medium surrounding the conductor(s). There are several alternative techniques to process electromagnetic data. For example, when the *horizontal spatial gradient* (HSG) technique is applied to magnetometer array data the regional average of conductivity versus depth is obtained.

For MT the transfer functions are normally processed further into impedances and presented as *apparent resistivity*, ρ_a and its *phase*. The apparent resistivity has several useful properties: for a homogeneous Earth it is equivalent to true resistivity. For a layered Earth its asymptotic properties give approximate estimates for the best determined parameters, depth to conductive surfaces and the conductance (thickness x conductivity) of a conducting layer. Since induction of EM sources develops also horizontally, 2-D and 3-D structures can only in rare cases be modelled reliably by layer (1-D) models.

MODELS, MODEL PARAMETERS AND SOME LIMITATIONS

The processed MT sounding curves (= apparent resistivity as a function of period) are directionally dependent, both on source field direction and on the geological strike. They are transformed into Earth structures by modelling. The data-based sounding curves are compared with respective curves calculated for the model. The model parameters are changed until a satisfactory fit is obtained. Today comparison of phases of the measured and modelled fields is considered more reliable than interpretation based on apparent resistivity curves only.

If layering can be assumed (either from geological considerations or from the properties of the impedance functions), virtually any 1-D inversion technique gives a reliable conductivity model, provided all other assumptions are kept similar. For a layered Earth the best determined parameters are depth to conductive surfaces and conductance (thickness x conductivity) of a conducting layer. If a layered sequence contains a less-conducting layer below a better-conducting one, this boundary is in most cases not well resolved. The difficulty to separately model the thickness and the conductivity of a layer is called electrical or S-equivalence. If the thickness of a layer increases sufficiently, the S-equivalence limitation gradually disappears.

For laterally varying geoelectric properties of the Earth various components of apparent resistivity behave differently as a function of the period of the inducing field. 2-D or 3-D structural models have to be used, since 1-D models become misleading in that they can contain false layers etc. The depth to conductors and their conductance are still the best determined parameters, although their exact definition for 2-D and 3-D models can be difficult. For the EGT northern segment MT data care has been taken to select only such profiles where it has been reasonable to construct 2-D models. Mainly finite element modelling techniques have been used to obtain 2-D electrical cross-sections of the Earth's crust.

The controlling factor of EM methods is the depth of penetration $\delta = \sqrt{[T/(\pi \mu \sigma)]}$, where T = period, μ = magnetic permeability ($4\pi 10^{-7}$ Vs/Am) and σ =conductivity of the medium. The EM field is dissipative and any component of the field decreases exponentially with distance r as exp ($-r/d$). Thus information is obtained from greater depths, when either the period is great and/or the medium is resistive. Good conductors close to the surface are the major obstacles in EM deep soundings.

Screening caused by conductive overburden is considered for simplicity for a layered model. The conductance of the overburden has to be much smaller than the conductance of any deeper layer one wishes to be resolved by EM techniques. On the northern segment the Quaternary overburden itself is thin (at most a few tens of metres in thickness) consisting of Quaternary material with much lower total conductance than sedimentary basins. However, the topmost part of the crystalline bedrock has turned out to be geoelectrically very complicated. The upper bedrock forms a laterally varying conductive 'overburden' layer, which complicates the estimation of deeper structures. Conductive (e.g. graphitic) veins, fractures etc. are abundant in the upper parts of the crust. Resistivities of minerals already vary considerably, over several orders of magnitude. When in addition, fluids in pore spaces, partial melting, temperature, texture of minerals and many other factors affect and change the *in situ* resistivities of geological material, then interpretation of electromagnetic data requires a high degree of sophistication.

A rather uniform, resistive region in a granitic terrain with horizontal dimensions of about 200 km would be needed to obtain a completely distortionless conductivity distribu-

tion of the lower crust and to penetrate into the upper mantle. In the EUGENO-S region, the thicker conducting sediments form an electrically screening layer. The influence of conductivity variations on the surface parts of the bedrock can be minimised by averaging techniques, by additional short-period measurements, inclusion of the phase of apparent resistivity into interpretation, and by integrating information from other geophysical methods or borehole data.

Several conducting layers one above the other may be difficult to recognise from EM sounding data, if the layers are very close to each other. Depending, as most things in EMS, in a complicated manner on period, measuring configuration and especially on the geoelectrical structures and resistivities in the vicinity of the measuring site, no generally applicable rule can be given for the resolution of EM methods. It is only safe to say that a conductance increasing towards depth is easier to resolve than a decreasing conductivity. Complementary information from other geophysical methods is the best way to improve resolution as has been demonstrated for the POLAR profile of the northern segment by combining EM and seismic models (Korja *et al.* 1989).

For interpretation of GDS and MT data the primary field is assumed to be a plane wave. In the northernmost parts of the northern segment the condition may be violated, since the measuring sites are close to the horizontal projection of the inducing ionospheric currents. The slope of the decreasing asymptote of apparent resistivity sounding curves for plane wave conditions is a function of the depth to a conducting layer (curve at point X_2 in Fig. 10.1). Close to the source (sounding curve at point X_1 in Fig.10.1), the asymptote depends only on the vertical distance to the ionospheric source currents (Vanyan 1967). This limits the longest usable period and thus also the deepest depth to be reached by MTS. In the geologic environment of the EGT/POLAR region, only periods below a few 100 s may be used (Osipova *et al.* 1989, Korja *et al.* 1989), thus limiting the depth of mapping into the first 10 km of the crust.

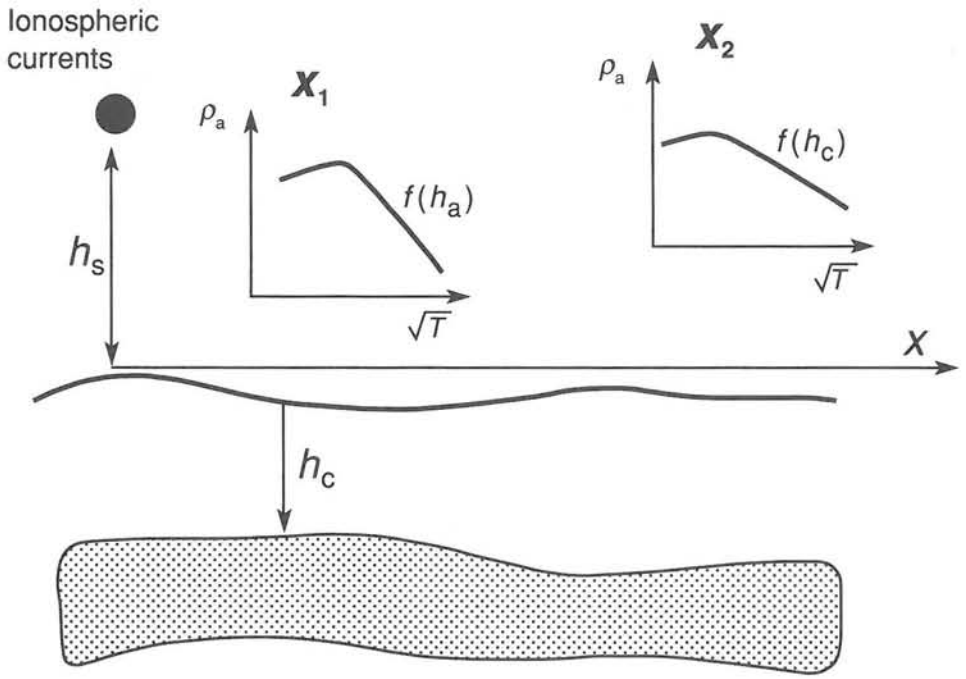

Figure 10.1 On the source field problem of interpreting MTS data at the northernmost part of the northern segment.

GEOLOGICAL INTERPRETATION OF CONDUCTIVITY MODELS

Electrical conductivity (and its reciprocal, resistivity) of Earth materials varies over an extremely large range. The complicated dependence on various properties of geological material in different parts of the crust and upper mantle makes the transformation of the conductivity models into a tectono-geological model far from unique. Combined use of all geophysical and geological information is therefore vital in understanding geoelectric models.

In many areas conductors with large horizontally extent in the middle and lower crust have been identified by deep EMS studies. This is the case for the Northern Segment region, too, although no uniform layer has been identified beneath the whole Baltic (Fennoscandian) Shield. The two most common explanations for the origin of these conductive structures are: saline fluids and graphite. A thorough discussion on questions related to the conductivity of continental crust and which are of significance also for EGT studies, have recently been published (Haak and Hutton 1986, Korja 1990).

At asthenospheric depths conductive layers are thought to be caused by partial melting of rock material. The possibilities of detecting such a layer in the northern segment region (on the Baltic Shield) are very small. In the northernmost parts of the Northern Segment source field problems do not allow information from greater depths to be obtained by EMS techniques. In other parts of the Baltic Shield, the conductance of the asthenosphere needs to be higher than 1000 S in order to be detectable.

DATA SETS

Extensive electromagnetic crustal and upper mantle investigations have been performed on the Baltic Shield during the 1980s. The geoelectromagnetic information on the northern segment (for this compilation more-or-less equivalent to the Baltic Shield) consists of magnetometer array (MV) and magnetotelluric profiling (MTP) data. The array data cover Finland approximately between latitudes 60 and 66.5°N and have provided so far a general horizontal distribution of electrical conductivity (resistivity) in the southern and central parts of Finland. The corresponding area of central Sweden has also been covered by arrays, but the processing and analysis of the data has just recently started (Olafsdottir *et al.* 1991).

At least six detailed MT profiles have so far been measured, processed and modelled for the northern segment. The SVEKA MT profile is only partly inside the full northern segment window, but it has been included in order to emphasise the lateral variability and differences among the geoelectric cross sections.

Most results have been discussed in detail in the literature. Recently some summaries pertinent to the northern segment have been published by Hjelt (1991), Hjelt and Vanyan (1989) and Vaaraniemi (1989). The results of these investigations have been summarised as a map of the northern segment electromagnetic results (Map 11) and a table containing the numerical values on the key features of the conductivity structures. In the map all 2-D conductivity cross sections are shown with uniform depth and resistivity (=1/conductivity) scales. The location of the inductive current concentrations in the crust (determined by Pajunpää 1987, 1989) are shown as dots on the map, open ones when the current concentration indicates a change in average mid-crustal resistivity and black dots for anomalous crustal conductive structures. In addition the reverse side of the map shows the real part of the reversed induction arrows for the periods 300 s and 1000 s.

ON THE GEOELECTRICAL BLOCK STRUCTURE OF FINLAND

Based on the MV array data covering the Finnish part of the Baltic Shield, Pajunpää (1987, 1989) divided the middle and lower crust of southern and central Finland into five geoelectrically different blocks, surrounded by anomalous conductivity structures of the crust. In central Finland the blocks are surrounded by narrow, highly conducting band-like formations (small solid circles on Map 11). They are located in the middle crust, their upper surface being often in the region 6–10 km. The resistivities are typically 5–10 Ohm m. The greatest anomalous crustal regions have a conductance of 20 000 S and more. The lower crust is well-conducting in most parts of the Shield.

The question of the presence of a conducting asthenosphere (caused by partial melting of rock material) remains open for the northern segment region. In the northernmost parts of the northern segment source field problems do not allow information from greater depths to be obtained by EMS techniques.The apparent resistivity for the Baltic Shield coincides with the average global apparent resistivity (as is approximately the case for the resistive window in Kuhmo) (Hjelt and Vanyan 1989). The global (conductorless) average of resistivity is denoted as 'Standard' in the summary table.

The northern part of the magnetometer array region, including the basement gneisses of Pudasjärvi and Kuhmo-Ilomantsi and the central Lapland granite area, is more or less free of induction anomalies. The schist zones of Kuhmo, Kainuu as well the Karelian Peräpohja schists are slightly anomalous.The Kuhmo schist zone seems to divide electrically the Archean rocks on both sides of the zone.

The Bothnian area is seen by the array as a single conductive block, although it is geologically complex including both Svecofennidic schists and gabbro intrusions. The block is clearly distinct from the Oulu anomaly. A similar low resistivity block has been reported from EM studies in Sweden (Skellefte profile). The middle crust of the central Finland granite area is not electrically completely homogeneous, but the inhomogeneous regions are small in size. The area is surrounded by anomalies in the east, south and west. The SVEKA profile crosses this block. Southernmost Finland is probably better conducting than the northern areas being geologically complicated, including e.g. Svecofennidic schist areas.

According to magnetotelluric profiling (MTP) the well-conducting structures between the blocks may be up to several hundred kilometres long. They vary in width from 5 to 40 km, their upper surfaces lie at a depth of 6 –10 km and the resistivity is typically 5–10 Ohm m. The Southern Finland Conductivity Anomaly (SFCA) extends 500 km along the Svecofennian schists on the southern boundary of the granite. The width of the SFCA varies between 5 and 20 km, but the depth to its upper surface seems to be around 10 km both in the east and in its centre at the Tampere schist belt. The anomaly most probably continues out to the sea around the Jotnian Satakunta sandstone formation. According to Pajunpää (1987), a pure mineral content is not the most obvious explanation of the anomaly bands, probably additional fluids exist in the crust. Korja (1990) has discussed these anomalies.

Regional estimates using the HSG (Horizontal Spatial Gradient) technique have been reported for the Kiruna and Kevo areas (close to the EGT POLAR profile) by Jones (1982) and for some other areas in Finland by Pajunpää (1987) . The Kiruna and Kevo data requires a crustal conductive layer at the depth of 30 km and with a conductance of 400 Siemens. Jones (1982) interprets the sharp decrease in apparent resistivity at periods greater than 1 h as an indication of a good conductor in the upper mantle (asthenosphere). Osipova *et al.* (1989) have shown that, within limits of the experimental error, the decrease is more probably explained as the effect of the non-uniform source field.

MT PROFILES

The EGT POLAR Profile runs across the oldest crust of the Baltic Shield and the Granulite Arc of Lapland. The southernmost part of the profile has a low resistivity (<10 Ohm m) and it coincides with the Karasjok-Kittilä Greenstone formation. The 2-D electrical cross section on the map (from Korja *et al.* 1989), depicts rapid horizontal variations of the resistivity caused by granodioritic and granitic intrusions. The Granulite Arc is rather resistive (200–1000 Ohm m), but contains well-conducting layers inside its sheared part and on the bottom of the Arc. The conductive bottom layer rises close to the surface on the northern boundary of the Arc. Indications of a crustal conducting layer (at about 10 km) can also been seen in the boundary region. The main features of the geoelectric cross section are in agreement with the corresponding gravity and seismic models along the POLAR profile (Korja *et al.* 1989).

The special structures on both shores of the Bothnian Bay, around Oulu in Finland and in the Skellefteå area in Sweden have been discussed by Korja *et al.* (1986), Vaaraniemi (1989) and Rasmussen (1987) respectively. The resistivity of the Oulu anomaly seems to be as low as 0.5 Ohm m. The geometrical dimensions of the crustal conductor are large. In the northeast it extends to the Archaean basement. The anomalous electrical structure runs in the crust below the sediment of the Muhos formation, which consists of unfolded Jotnian silt and shale sediments (1300 Ma).

According to the data, the most conductive part is at least 10 to 15 km thick vertically. The conductance (resistivity x vertical thickness) of the structure is thus 20 000 S or more. The conductive graphite schists on the Baltic Shield often have resistivities of the order 0.01 Ohm m and less. If the Oulu anomaly is assumed to consist of layers of graphitic schists with such resistivities it would indicate that the total thickness of these layers is more than 100–200 m. Since the conductivity anomaly extends horizontally over rather large distances, this would mean the presence of huge amounts of graphite in the lower crust. The exceptional texture of the rock minerals of the lower crust and/or a combination of hydrothermal solutions and graphitic material should possibly be considered in order to explain the high conductance of the Oulu anomaly.

The resistivity of the Skellefteå anomaly is slightly higher, of the order 4 Ohm m, although geometrical features of the structure are very similar when compared to the Oulu anomaly. The lateral extent of the Skellefte structure along strike is not yet known. Fluids are a more probable explanation than a crust enriched in graphite or sulphides and it is proposed, that the structure is associated with an ancient subduction zone (Rasmussen 1987).

The SVEKA profile runs from the 2.6–2.8 old Archean Kuhmo area in NE across the 1.8–1.9 old Svecokarelidic formations, across the Central Finland Granite Area and the Southern Finland Conductivity Anomaly. The upper crust is mainly resistive (up to 10 000 Ohm m) and there is a conducting layer (conductance of 600–800 Siemens) in the lower crust. This layer coincides surprisingly well (depth to its upper surface about 45 km) with the Moho depth of the central part of SVEKA. The layer apparently rises into the middle crust towards South. The resistivity of the upper crust is from 10 000 to 30 000 Ohm m, typical values for granitic rocks of the Baltic Shield. Local resistivity distortions along the profile have horizontal dimensions of 20 km. Well-conducting crustal structures are connected with the Kainuu and the Tampere schist zones. For further details of the SVEKA electrical model see *e.g.*. Koivukoski *et al.* (1989) and Koivukosi (1990).

The Siljan impact structure in Central Sweden with its deep borehole has been the target

of much geoscientific interest during recent years. The geoelectric properties of the structure have been described by by Zhang *et al.* (1988) and Zhang (1989). Two perpendicular MT profiles exist across Siljan and one of the proposed geoelectric models is shown on the summary map.

The northern segment profile Uppsala-Oslo has been described in detail by Rasmussen (1988). The model, which has been fitted to the data differs considerably form the other 2-D structures presented for the Baltic Shield. The author proposes a model where the crust is layered and genuinely anisotropic. The author explains the anisotropy of the lower crust by using analogies with elastic anisotropy models. The data indicate a more conducting zone below 460 km depth, but shows no evidence for an asthenosphere channel within the uppermost 250 km.

The examples selected for this presentation visualize the geoelectric complexity of the crust of the Shield. The structures clearly are generally 2-D, in most cases even 3-D. Therefore the integration of the EM results on the northern segment into a single geotraverse (along the 'backbone' FENNOLORA) was not possible. Existing MTS data along FENNOLORA come from stations too far apart to justify even a reliable 1-D construction to be made (Rasmussen 1987, Rasmussen *et al.* 1987).

There are 30 MT stations along the profile covering six lithotectonic provinces (cf. Summary Table, below). The sounding curves vary rather strongly from site to site. According to Rasmussen (1987) the transfer functions show systematic features, when grouped according to area, allowing some qualitative statements to be made. The grouping shows reasonable coincidence with the geological subdivision. These result have been collected into the summary table of this short report.

The Norrbotten region has a resistive upper crust and some conductive layers in the middle crust. The model of an asthenospheric conductor suggested by Jones (1982) is not compatible with data for the most northern station. The Skellefte ore district with its highly conductive structure (cf. above) marks electrically the boundary between different crusts. The conductor does not directly correlate with the ore bodies in the district.

Central Norrland has also highly conductive structures in the upper crust at some sites. The Bergslagen region is characterised by near-surface inhomogeneities, and a highly complicated crust.There are no comments on the geoelectrics of the Småland–Värmland Belt and the southernmost unit, the Blekinge region shows minor features in the upper few kilometres. The upper crust is highly resistive. A model was tested to see if a conductive layer at 120 km in the upper mantle might exist. It must be well below 1500 S before it can be seen in MTS data.

The most recent EGT MT profile from the EUGENO-S area in Denmark has not yet been discussed in detail in the literature and the interpretation is still continuing (Rasmussen *et al.* in prep.). A preliminary 2-D interpretation (provided kindly by T. Rasmussen for this purpose) has been included on the map for completeness. The thick sedimentary cover in most parts of the profile limits the depth penetration of magnetotellurics. Additional data from other geophysical methods and boreholes have been used in constructing the model.

Summary Table

Profile/ region	Upper crust	Middle & lower crust	Upper mantle	Astheno-sphere
Profiles with 2-D models				
POLAR	hc + nsi	cl/var; 200–1000	nm	nm
Skellefteå	cl/ 4	hc; 1000–5000	-	nm
Oulu I	cl/ 6	hc	nm	nm
Oulu IV	cl/ 15–20	hc	nm	nm
Siljan (outside impact area)	10 000	1000 (possibly aa)	nm	nm
Uppsala/Oslo	10 000	aa	2000	cl/> 250 (if any)
Denmark (EUGENO-S)	1	-	nm	nm
SVEKA	10 000 + nsi	cl/ 5–12; 45	-	nm
FENNOLORA				
a. Norrbotten region	10 000	cc; 300	1000	nm
b. Skellefte ore district	cl/ 4	hc; 100–3000	-	nm
c. Central Norrland	300–3000	cc; 30–1000	-	nm
d. Bergslagen region	nsi	complicated	-	nm
e. Småland-Värmland Belt and	10 000	1000	S<1200 S	
f. Blekinge region				cl/ 120 possible
'Standard'	5–10x10^4	1–5x10^4	≈ 10^4	1–5x10^3

Abbreviations: aa = azimuthal anisotropy; cc = crustal conductors; cl/x = conducting layer starts at the depth x km; hc = highly conductive; hr = highly resitive; nsi = near-surface inhomogeneities; nm = not measurable; all other numbers are resistivities in Ohm m.

ACKNOWLEDGEMENTS

Data collection for the northern segment has been financed by the Academy of Finland. Planning and preparation of the summary map and its format were done by E. Vaaraniemi with much help from T. Korja and K. Koivukoski, all at the Department of Geophysics University of Oulu. Colleagues in Uppsala at the Department of Physics of the Solid Earth have been most helpful during all stages of the EGT project and provided summaries of their most recent models. Mr. Markku Pirttijärvi produced final versions of the maps.

Data sources

Information concerning the MT and GDS data for the northern segment, mentioned in this summary as well as possible new results can be obtained from following scientists:

Magnetometer array data (Finland and Sweden):

Dr. Kari Pajunpää, Nurmijärvi Geophysical Observatory, Nurmijävi, Finland

Magnetometer array data (Sweden):

Mrs. Birna Olafdottir, Swedish Geological Survey, Uppsala, Sweden

Magnetotelluric data (Finland):

Dr. Toivo Korja, Dept. Geophysics, University of Oulu, Oulu, Finland

Magnetotelluric data (Sweden and EUGENO-S):

Dr. Torkild Rasmussen, Dept. Solid Earth Geophysics, University of Uppsala, Uppsala, Sweden

11 Low electrical-resistivity anomalies (Central Europe)

ERCEUGT GROUP* (V. HAAK)

The map of geomagnetic induction arrows (Atlas Map 12) displays the lateral resistivity distribution of the crust in the central segment of the EGT. This complements electrical resistivity models as calculated from magnetotelluric measurements in the past 10 years compiled along the central segment of the EGT presented by the ERCEUGT group (1992). The almost 1000 km-long transect (see Figs. 11.1 and 11.2) shows low-resistivity structures in the middle and lower crust. These structures can be related to different tectonic units along the profile. Prominent features are the two-dimensional low-resistivity structures at the transition from the Moldanubian to the Saxothuringian and from the Saxothuringian to the Rhenohercynian unit of the Variscan Belt. Further obvious features are the depth correlation of the low-resistivity horizon in the Rhenish Massif with a seismic low-reflectivity band, the very high conductance of an upper to middle crustal layer in the North German Lowlands and its cessation at the river Elbe towards the Baltic Sea.

The question remains how representative these resistivity distributions along the transect may be for the Central European area of the Variscan belt. We can answer this question with respect to prominent lateral variation of low-resistivity anomalies. Such lateral resistivity changes within the crust and upper mantle can be mapped by geomagnetic induction vectors, which can be constructed almost directly from corresponding geomagnetic recordings. Since the construction and interpretation of geomagnetic inductions vectors is one of the earliest electromagnetic methods in geophysics, most of the central part of the EGT has been covered in the last 35 years with measurements of induction vectors. During this timespan the method and the instrumentation itself were developed, therefore the quality and reliability of individual results were inhomogeneous. Berktold (1991) critically collected all available vectors in the western part of Germany. With the political unification of Germany this collection of induction vectors was completed by Ritter (1990).

GEOMAGNETIC DEPTH SOUNDING OR MAGNETOVARIATIONAL METHOD

Although the basic framework of the magnetovariational method has been introduced in the previous chapter, our data handling and interpretation are slightly different. Risking repetition for the sake of clarity we give here the specific details of our method. We use the

*ERCEUGT=Electrical Resistivity along the Central segment of the EUropean GeoTraverse. ERCEUGT is: K. Bahr, A. Berktold, H. J. Brink, V. Haak, St. Hofer, H. Jödicke, A. Junge, K. Knödel, W. Losecke, E. Ritter, and R. Volbers.

three components of the time-varying geomagnetic field to derive a quantity called the 'induction arrow' or 'tipper' (Vozoff 1972). Graphical representations of the tipper in a map are often referred to as induction arrows.

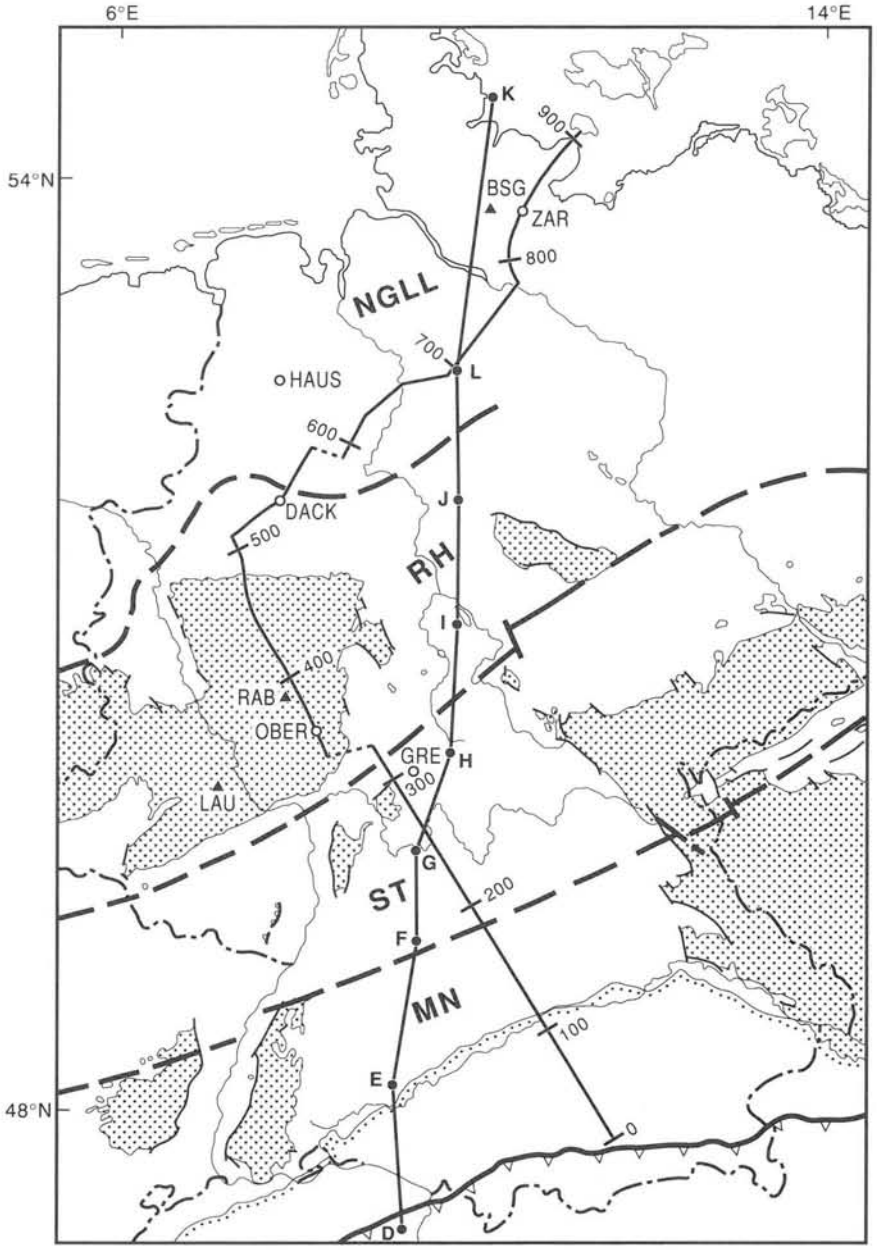

Fig. 11.1 The location of the electrical resistivity section. The map and the two boundaries between the three tectonic units Moldanubian region MN, Saxothuringian region ST and Rhenohercynian region RH were adapted from Franke et al. *(1990b). Northern boundary of the Variscan zone after Murawski* et al. *(1983). NGLL: North German Lowlands. D..K: shotpoints of the seismic EGT line (Aichroth and Prodehl 1990). Thin line (km 0-910): magnetotelluric profile. The numbers are distances from the most southernly sounding site. The profile is in the range 0-500 km identical with the profiles of DEKORP 2-S and DEKORP 2-N. Full circles with labels ZAR, HAUS, DACK, OBER, GRE refer to five sites for which the original data are discussed by ERCEUGT (1992). Triangles with labels BSG, RAB, LAU refer to three ultral-low-frequency MT sites for which a very deep (upper mantle) resistivity profile has been calculated (see ERCEUGT 1992).*

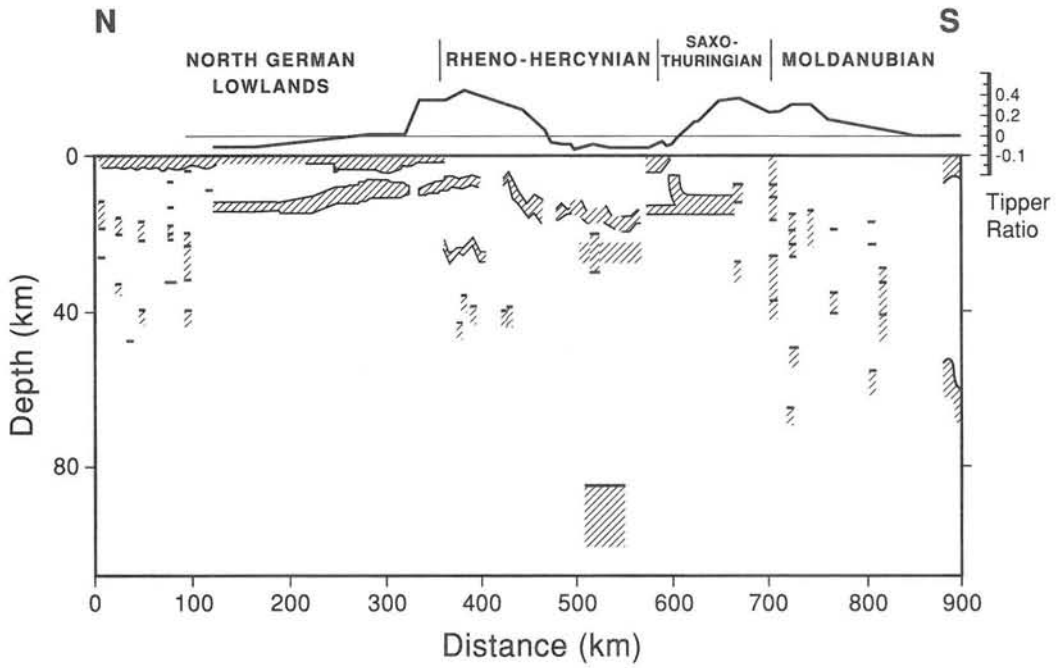

Fig. 11.2. The electrical resistivity section from the south (km 0) to the Baltic Sea (km 900).The tipper ratio (determined for 1000 s period) is associated with major variations of the electrical conductance of the low-resistivity layers in the crust. The conducting layer at 85 km depth which is shown at km 380 refers to the local determination of the asthenosphere at site RAB (see Fig. 6 in ERCEUGT 1992). No information on the conductivity of this depth range is available so far for other parts of the profile.

In the application of the tipper, a 2-D or 3-D earth and a homogenous source field is assumed. In an elongated very low-resistivity anomaly the increased currents produce a stronger inhomogeneous magnetic field at the surface. This increased magnetic field may immediately be recognised by the increased vertical to horizontal magnetic field ratio. This ratio may be positive or negative, the change of sign occurs over the centre of the elongated conductor.

THE GEOMAGNETIC INDUCTION ARROW

Induction arrows (Schmucker 1985) are derived from the linear relationship

(1) $B_{z,i}(T) = zH(T)\, B_{x,n}(T) + zD(T)\, B_{y,n}(T)$

where T = 2 π/*f* (*f* = frequency) the period

B_x, B_y, B_z = magnetic north (index *x*), east (index *y*) and vertical (index z) components

index n = normal, unaffected by an electrical conductivity anomaly

index i = in the electrical conductivity anomaly internally induced magnetic field

For data from a single station as they are presented here in the map equation (1) may be replaced by

(2) $B_z(T) = a(T)\, B_x(T) + b(T)\, B_y(T)$

where B_x, B_y, and B_z are the total field amplitude measured at the same site.

Here often the following approximations are valid (Jones 1981):

(3) $B_{z,\mathrm{i}} \approx B_z$, $B_{x,\mathrm{n}} \approx B_x$, $B_{y,\mathrm{n}} \approx B_y$
$z_H \approx a$ and $z_D \approx b$

with $a(T)$ and $b(T)$ as complex-valued functions of the period.

These two functions may be represented for a selected constant period graphically on a geographic map by arrows or vectors:

(4) $\mathbf{P} = -\mathbf{x}\, a_{\mathrm{r}} - \mathbf{y}\, b_{\mathrm{r}}$ the real arrow,
$\mathbf{Q} = \mathbf{x}\, a_{\mathrm{i}} + \mathbf{y}\, b_{\mathrm{i}}$ the imaginary arrow

where **x** and **y** are the unit vectors in north and south direction.

The Parkinson convention has been chosen here: the arrows point towards high-conductivity zones. Two other kinds of induction arrows are in use, see Jones (1981) and Gregori and Lanzerotti (1980) for their definition. The arrows supplied by Ritter (1990) in the eastern part of Germany are 'Wiese' arrows rotated by 180° to agree with the Parkinson convention.

GEOINFORMATION SUPPLIED BY INDUCTION ARROWS

Geomagnetic induction vectors are very useful to recognise the existence and outline of low-resistivity anomalies in the Earth's crust, see e.g. the reviews by Haak (1985) and Haak and Hutton (1986).

Induction vectors contain twofold information: (1) the direction of the vectors points (in the Parkinson convention) towards the low-resistivity structure, and (2) the length is proportional to the gradient from high to low resistivity. Furthermore, as with all electromagnetic quantities, induction vectors for the shorter period of 300 s are representative of the upper half of the Earth's crust, whilst for the longer period of 3000 s the induction vectors are representative of resistivity gradients for the whole crust and uppermost mantle.

Not all parameters of the electrical resistivity distribution can be equally well resolved by the geomagnetic depth-sounding method. The location of the axis of the low-resistivity anomaly can be determined to within 1–2 km. This parameter and also the intensity of the resistivity gradient and thus the significance of the anomaly can be best resolved. Therefore we concentrated on the horizontal location. The depth of a low-resistivity layer can be resolved to within 5% if additional magnetotelluric data are considered. Edwards *et al.* (1981) discuss estimation of depth in detail. However, usually thickness and absolute level of resisitivity within that layer can not be estimated. See appendix of ERCEUGT (1992) for further discussion of this subject.

INTERPRETATION OF THE MAP

The inference of low-resistivity anomalies from the distribution of the induction vectors from the map is performed by visual inspection. From south to north the following elongated anomalies can be recognised:

1. In the Alpine region and in southern Bavaria south of the river Danube the induction arrows are very small and therefore do not signify any major resistivity changes beneath the sedimentary cover.

2. In southern Germany, 80–90 km north of the river Danube, an elongated low-resistivity anomaly has been recognised by Berktold (1991). The existence of this structure is mainly deduced from magnetovariational studies (see variation of the tipper magnitude at km 200 in Fig. 2). The strike direction of its axis is about N 65° E.

In the west, north of Stuttgart, Winter (1973) has inferred an anomaly which seems to be part of this low-resistivity structure. The next indication further east of this low-resistivity structure coincides with the DEKORP 2-S crossover. In the east within Fränkische Schweiz the continuation of the anomaly may be seen. There is no indication from induction vectors that this low-resistivity structure continues across the Franconian Line and the KTB borehole.

This elongated low-resistivity structure coincides with the transition zone from the Moldanubian to the Saxothuringian unit. In general one might expect such low resistivities in tectonic suture zones are due to increased fluid or carbon content.

3. The border line between the Saxothuringian and the Rhenohercynian units turns out as the major low-resistivity elongated structure in central Europe. This may clearly be recognised by the reversion of the direction of most induction arrows. There are observation from the west around the Saar-Nahe-trough and all along the Kinzig valley and northern Franconia/eastern Hessen.

From magnetovariational and magnetotelluric data a 2-D low-resistivity anomaly was modeled in the crust between the Rhenish Massif and the area of the river Main (Hofer 1990, Berktold 1991, ERCEUGT 1992). The strike direction of this elongated structure is about N60°E. This low-resistivity anomaly was proved to exist over the whole range from the western to the eastern borders of Germany, thus of an extension of at least 300 km. By incorporating geological information Berktold (1991) supposed that the anomaly continues to the west into France. The 2-D low-resistivity anomaly coincides with the transition zone between the Saxothuringian and the Rhenohercynian unit of the Variscan belt.

The maximum conductance of the low-resistivity zone is 9000 Siemens exactly between the Northern Phyllite zone and the Mid-German Crystalline Rise. There the upper surface of the 2D low-resistivity structure is at 7 km depth, see ERCEUGT (1992).

The upper surface of this low-resistivity structure dips to the south to about 10 km depth and the conductance decreases continuously to 2000 S.

4. The whole Rhenish Massif is characterised by a low-resistivity layer in the middle crust with the tendency to dip from the north to the south (Jödicke *et al.* 1983, Volbers *et al.* 1990). Such an extended almost flat low-resistivity layer cannot produce any induction vectors. The observed induction arrows are changing their direction and length from site to site indicating thus lateral resistivity changes.

5. East of the Rhenish Massif a further low-resistivity structure as indicated by the rather heterogeneous directions of the induction arrows exists beneath the Hessen depression and the Leine Graben (Berktold 1991). These structures are, however, of much younger than Variscan age.

6. The North German–Polish conductivity anomaly (Schmucker 1959, Untiedt 1970, Haak 1985) is clearly indicated by the reversal of the induction arrow direction in North Germany. It is due to the rather broad and extreme low-resistivity anomaly of the German (Losecke *et al.* 1979, Jödicke 1990) and Polish Lowlands, see the corresponding part of the ERCEUGT (1992) transect.

ACKNOWLEDGEMENTS

We are grateful to the European Science Foundation for financial support and to R. Freeman for organising our contributions.

12 Heat-flow density

V. CÊRMÁK, N. BALLING, B. DELLA VEDOVA, F. LUCAZEAU, V. PASQUALE, G. PELLIS, R. SCHULZ AND M. VERDOYA

Atlas Map 13 shows the regional distribution of the heat-flow density along the EGT together with the distribution of individual heat-flow stations used to produce the isoline pattern. The isoline pattern is based on the measured and corrected values, which total approximately 140 for the northern for the EGT, 200 for the central and more than 1400 for the southern segments. This explanatory text briefly summarises the information on sources of original data, discusses correction of measured heat-flow values, and shows some examples of the use of heat-flow data for assessing the efect of deep temperature distribution on basic geothermal modelling.

Knowledge of the terrestrial heat flow, the outflow of thermal energy from the Earth's interior, is essential for any evaluation of the physics and energy budget of deep processes and for general evolution of the lithosphere with time. Surface heat-flow density as an upper boundary constraint is crucial for calculating temperature at depth.

For a valid determination of the heat-flow density value (Q), the equilibrium temperature gradient (grad T) in a borehole, deep mine, or a tunnel must be obtained and combined with the characteristic thermal conductivity (k) of the surrounding rocks: $Q = k \text{ grad } T$. To extrapolate the heat-flow value from the surface downwards, knowledge of heat production (A), i.e. the heat released by radioactive decay of natural radioelements of different rocks at depth, is required.

Regional variations in continental heat-flow density lie within a factor of two or three about the mean (which amounts to about 70 mWm^{-2}) while they could be far larger in the transitional or oceanic domains of the Mediterranean area. In both cases the magnitude of heat flow is closely related to age and tectonic setting. While the oldest blocks of the continental crust are characterised by low, and generally very stable, heat flow of about 40–50 mWm^{-2}, young and geologically active areas may reveal heat-flow values, which can exceed 100 mWm^{-2}. The EGT, which crosses the oldest structures of the European craton (Baltic Shield, older than 2000 Ma) in the north, the Variscan/Hercynian fold belt in its central part (230–400 Ma) and the active Alpine–Mediterranean deformational region in the south (the youngest products of the European geological history), is a good setting to investigate the existing heat-flow range and its corresponding lithospheric temperature distribution.

DATA

Even though the very first heat-flow observations in Europe were reported in late 1930s by Benfield (1939) for Great Britain, systematic investigations of terrestrial heat flow did not start before the mid-1960s. The first heat-flow map for the whole of Europe on a continental scale was constructed by Cermák and Hurtig (1979), followed by more detailed sets of subsurface temperatures and heat-flow maps of Western Europe compiled in two Atlases (Haenel 1980, Haenel and Staroste 1988). The most recent version of various geotemperature and heat-flow maps of Europe to the scale 1:2.5 million and 1:5 million have been recently prepared by a large group of authors (Hurtig *et al.* 1991).

A number of authors contributed to the general knowledge of the heat flow along the almost 4000 km long and about 600 km wide EGT strip, extending from northern Norway to southern Tunisia. Original data are scattered in numerous publications and here we can mention only several papers that compiled, discussed and interpreted heat-flow data for certain regions and which were used for the preparation of the EGT heat-flow map.

More than 300 values of heat flow have been collected to date in the Baltic Shield and its closest vicinity (Cermák *et al.* 1992), 140 of them fall into the EGT strip zone. Lubimova *et al.* (1972) and Arshavskaya *et al.* (1984) gave data for the westernmost part of the Kola peninsula in northern USSR, Järvimäki and Puranen (1979) and Kukkonen (1989a) provided data for Finland, Haenel *et al.* (1974, 1979), Swanberg *et al.* (1974) and Groenlie *et al.* (1977) reported data from Norway, Parasnis (1975, 1982) Eriksson and Malmqvist (1979), Landström *et al.* (1980) and Malmqvist *et al.* (1983) from Sweden, and Balling (1979, 1990) compiled data for Denmark.

For the construction of the heat-flow pattern along the central segment the most important data were reported for the territory of Federal Republic of Germany (Haenel 1971, 1983; Bram 1979, Hurtig and Oelsner 1979, Schulz 1990), Switzerland (Rybach and Finckh 1979, Finckh 1981, Bodmer and Rybach 1984), and Austria (Haenel and Zoth 1973) with additional information from the western part of Czechoslovakia (Cermák *et al.* 1991).

Heat-flow density data along the southern segment were compiled by Della Vedova *et al.* (1990, 1992) based on regional syntheses given for Italy (including Sardinia and Sicily) by Loddo and Mongelli (1979), Pasquale (1985) and Mongelli *et al.* (1991), for France and surrounding areas by Lucazeau and Vasseur (1989). More than 1400 heat-flow determinations have been compiled including the most recently published data for Sardinia (Loddo *et al.* 1982) for the Balearic and Tyrrhenian basins (Hutchison *et al.* 1985, Della Vedova *et al.* 1984, Della Vedova and Pellis 1986), for the Ligurian Sea (Jemsek 1988), for Algeria (Takherist and Lesquer 1988), for onshore and offshore Tunisia (Lucazeau and Ben Dhia 1989) and for the Pantelleria rift (Della Vedova *et al.* 1989). Recent heat-flow determinations for the Po Basin based on bottomhole temperatures (Pasquale and Verdoya 1990) have been also included.

CORRECTIONS

The subsurface temperature field may be disturbed by many surface, structural, and transient effects (Powell *et al.* 1988). Therefore heat-flow values based on shallow measured temperature gradients need not necessarily reflect the undisturbed outflow of heat from the depth. Evaluation of disturbances in borehole measurements that depend upon the method, such as correction for hole inclination, effect of drilling and borehole temperature

equilibrium, and effect of uneven surface topography, belongs to standard procedure and accordingly all borehole data have been routinely corrected for these factors.

Long-term variations of surface temperature, namely the global warming following the last ice age, may have left a signature on the present underground temperature distribution up to the 1–2 km depth range (Birch 1948) and thus heat-flow measurements in areas that were glaciated should be corrected. The corresponding correction is positive and, as the amplitude of the ground temperature increase since the retreat of the continental glacier decreases from south to north, the typical correction for the depth range of 200–500 m is up to 15 mWm^{-2} in southern Scandinavia and northern Central Europe, about 10 mWm^{-2} in central Scandinavia and 3–5 mWm^{-2} in the northernmost regions (Balling 1990).

However, the climate may have undergone significant changes in postglacial times and even in the last millenium (Zoth and Haenel 1988). Mongelli and Zito (1988) have shown that the palaeoclimatic effect on the underground temperature gradient is not limited only to areas that were covered by ice sheets in the last ice age.

While the temperature field in most of central and northern Europe is steadystate, underground temperatures may have been affected by recent geological history in areas that have undergone rapid sedimentation, erosion or uplift, i.e. in Alpine Europe. In the southern segment the measured values require careful evaluation; here application of the steadystate solution of the heat conductivity equation can be used only as a first approximation.

All conventional marine heat-flow observations have been corrected for the palaeoclimatic and sedimentation effects. For palaeoclimate the values of marine data were increased by about 8-10 mWm^{-2} following the model of Jemsek (1988) for bottom water temperature changes since the Late Pleistocene. Sedimentation correction is positive and amounts up to 30% for Tertiary deposits of the Balearic (since Oligocene) and Ligurian (since Miocene) Basins (Jemsek 1988); and up to 20% for the Plio-Quaternary deposition in the Tyrrhenian Sea (Della Vedova *et al.* 1984) and Sicily Channel (Della Vedova *et al.* 1989). Heat-flow estimates from BHT data in the Po Basin have also been corrected (from 6% to 30%) for the Plio-Quaternary sedimentation effect (Pasquale and Verdoya 1990).

CRUSTAL AND UPPER MANTLE TEMPERATURES, MOHO HEAT FLOW

To extrapolate surface heat-flow data to depth and to assess deep temperatures, knowledge of structure, vertical distribution of heat production, and of thermal conductivity is necessary. For the Atlas map, crustal temperatures were calculated separately for each of the three EGT segments using slightly different computation techniques according to local structures and tectonic conditions.

Northern segment

All observed heat-flow density values were palaeoclimatically corrected and the regional heat-flow pattern was assessed (Balling 1990), main emphasis being given to high quality data obtained in deep boreholes and in areas of known surface heat production. The pattern clearly outlines the lowest heat flow typical for the oldest part of the Baltic Shield and the increase of the heat-flow density from the northeast (40–50 mWm^{-2}) to the south and southwest (60–70 mWm^{-2}). Local short or intermediate wavelength anomalies (>100–200 km) of the order of ± 5–15 mWm^{-2}) superimpose the regional trend.

The heat equation was solved numerically for a steady-state model (Balling 1976, 1990). For the whole profile length (2200 km) 15 almost equispaced locations were selected and

respective 1-D models were derived. Heat production in the upper (crystalline) crust (seismic velocity v_p < 6.5 km/s) was assumed to be exponentially decreasing from the surface value A_0 ranging from 1.5 mWm^{-3} for the northern Shield areas (Kukkonen 1989b, Kremenetsky *et al.* 1989) to 2.5 mWm^{-3} in the Igneous Belt in southern Sweden (Gorbatschev 1984) with the logarithmic decrement D-value of 10 km. For deep crustal layers (generally over 20 km), a constant value of 0.2 mWm^{-3} was applied. For sedimentary units, a constant value of 1 mWm^{-3} was used. Thermal conductivity within the crust was treated as temperature dependent with a constant value of 4 $W(mK)^{-1}$ in the subcrustal lithosphere. Main results of the geothermal modelling along the EGT-N profile are summarised in Fig. 12.1.

Similar results (with slightly lower crustal temperatures) were also obtained by Baumann (1988) who applied a 2-D integrated finite-difference method on the FENNOLORA and EUGENO-S seismic data (Guggisberg 1986; Baumann and Rybach 1991). She also demonstrated that surface heat flow and heat production in the uppermost crust are the most

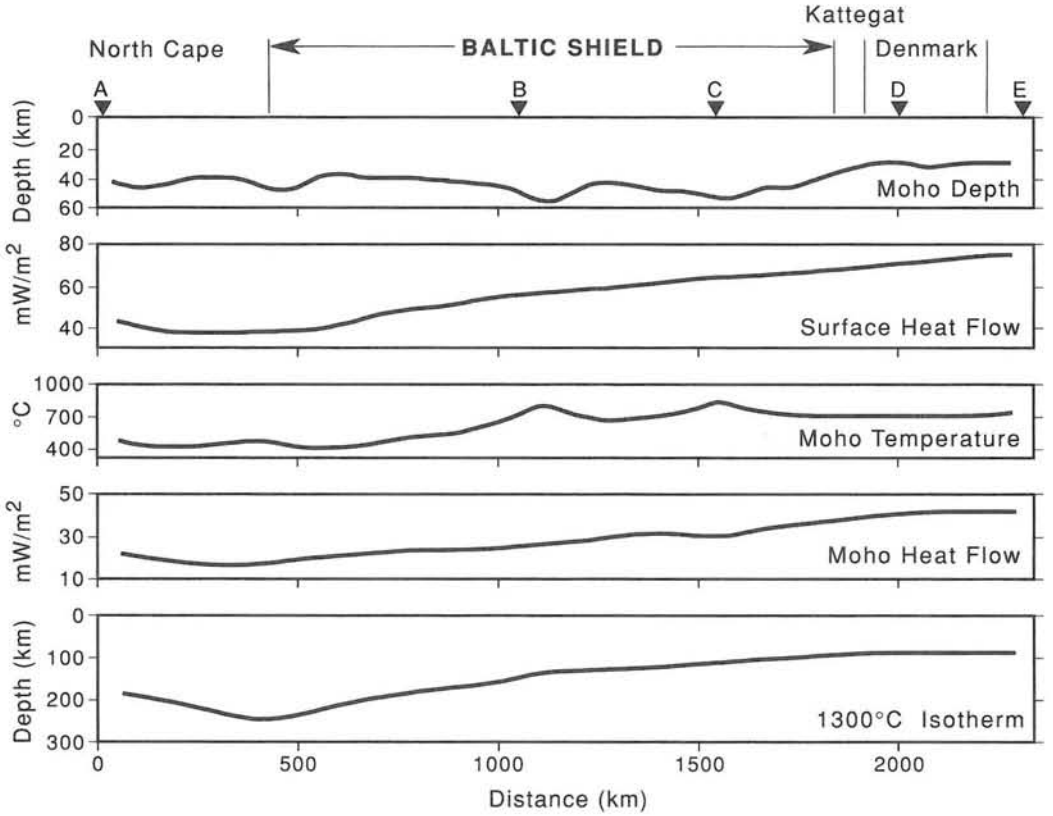

Fig. 12.1. Crustal thickness (Moho depth), observed surface heat flow, and the results of geothermal modelling along the northern segment of the EGT: temperature at the crust–upper mantle boundary, heat flow from the upper mantle, and assessed thickness of the thermal lithosphere (calculated depth of the 1300 °C isotherm), adopted after Balling (1990).

Moho temperature is generally low to very low, being about 450–500°C in the proper shield area and attains up to 700°C where the crust is thicker (50–55 km). Heat flow from the upper mantle (Moho heat flow) follows the same trend as the surface heat flow, but with a smaller amplitude. The typical Shield Moho heat flow amounts to 20–25 mWm^{-2} and increases to the south to about 30-40 mWm^{-2} in the transition zone between the Shield and Caledonian-Hercynian Europe. The depth to the 1300°C isotherm, indicating the approximate depth of the lithosphere–asthenosphere transition, varies from 200–250 km along the northernmost part of the profile to 80–100 km beneath the Danish and North German Basins.

sensitive parameters, and that differences between l-D and 2-D results are negligible when applied to upper crust regions such as stable shields. Small differences may be found for the lower crust where lateral temperature variations may be observed.

An analysis of the lithosphere thermal structure in the entire Baltic Shield (Pasquale *et al.* 1991) showed strong horizontal variations in lithosphere thickness, the maximum value of which was found to exceed 200 km in the Bothnian Gulf and northern Finland, confirming results inferred by surface wave data (Panza *et al.* 1980).

Central segment

To describe the deep temperature distribution along the more than 800 km long central segment Cermák *et al.* (1990) solved the 2-D steadystate heat equation in a non-homogeneous medium, the crustal heat production data being converted from the refraction seismic velocity distribution (Aichroth and Prodehl 1990) with the use of the v_p-A conversion formula proposed by Rybach and Buntebarth (1984).

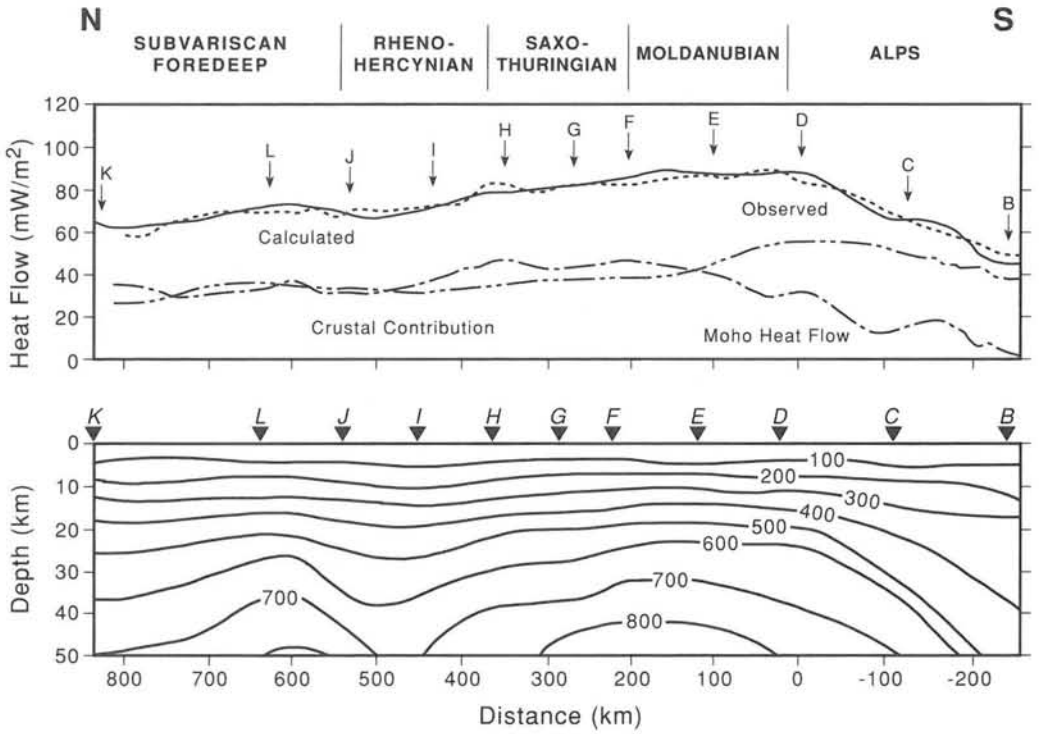

Fig. 12.2 Results of the temperature modelling along the central segment of the EGT. Top: comparison of the observed and calculated surface heat flow together with the assessed crustal contribution and the mantle (Moho) heat flow. Bottom: Calculated crustal temperatures (in °C). To compare the deep temperature below the Alps and below the Alpine foreland, the modelling was extended about 200 km farther to the south, encompassing the northernmost part of the southern segment. Adopted after Cermák et al. *(1990).*

Generally higher temperatures were found in the south where T calculated at 40 km depth attains 800–950 °C (surface heat flow Q_0~95 mWm^{-2}); in the north for comparison 650–700 °C (Q_0 ~65–70 mWm^{-2}) was calculated. As no error bars can be given, the comparison of several models with varying parameters helped estimate the uncertainty of the calculated temperatures at the crustal base to about 100–200 °C, this resolution characterises the possibilities of the present temperature modelling. The Moho heat flow along the central segment varies from about 30–35 in the north to over 40 mWm^{-2} in the south and the crustal contribution to the surface heat flow, due to the radiogenic heat sources, amounts to about 40 and 60 mWm^{-2} respectively.

To define the surface conditions, we took the heat-flow pattern (Schulz 1990) in a strip zone of 100 km wide along the EGT and smoothed it down by a sliding window technique (window size 25x100 km). The surface heat flow was assumed to be the sum of two components: $Q_0=Q_C+Q_M$ where Q_0 was the crustal contribution and Q_M was the Moho heat flow. Starting with an arbitrary value of Q_M and successively correcting the calculated Q_M value by the difference (Q_0-Q_B) and by repeatedly calculating the surface heat flow corresponding to the model, Q_B, we could set the conditions on the lower boundary of the model. Thermal conductivity was taken as temperature dependent $k=k_0(1+CT)^{-1}$, k_0 being the thermal conductivity at surface conditions and C the experimental parameter as shown by Cermák and Rybach (1982). Results of the temperature modelling (Fig. 12.2) revealed relatively flat crustal isotherms, which correspond to the surface heat-flow pattern.

Southern segment

Observed heat-flow data along the southern segment are more numerous, including a sizeable amount of conventional marine measurements in the Mediterranean Sea. Data were generally corrected for topography and palaeoclimate; lake and marine data and also heat-flow estimates from BHT data in the Po Basin were corrected for sedimentation. No corrections were applied to north African data, the majority of which are based on BHT temperatures in oil wells.

Contouring of the surface heat flow was set by an automatic procedure in a broad 500 km wide band along the EGT with 200 km overlapping in the north (Della Vedova *et al.* 1990, 1992). The data were sorted into different geological provinces to investigate their modal distribution by means of a statistical approach. The variogram technique has been applied to each province in order to assess the characteristic length scale of the regional variation of the heat-flow density field (Della Vedova *et al.* 1992). The universal kriging technique, based on the above variograms, has been used to produce the automatic contouring.

The southern segment is the most difficult of all Segments to modal geothermally due to the presence of non-steadystate conditions; surface heat flow, in addition to heat outflow from depth and crustal and/or lithosphere contributions may be in some places strongly controlled also by transient heat flow. Other than initial attempts to assess the crustal temperatures (Stegena and Meissner 1985) and the lithosphere thermal structure (Pasquale *et al.* 1990) along the whole EGT profile, only preliminary 2-D steadystate geothermal models have been solved so far (Della Vedova *et al.* 1990) . This preliominary 2-D model helped evaluate amplitude and wavelength of thermal transients by comparing surface heat flow calculated by foreword finite element methods with observed data (Fig. 12.3). Fixed temperature conditions were set on the lithosphere-asthenosphere boundary $T_L=(1100°C+3z)\cdot 0.85$, z being depth in km, the lithosphere base being independently deduced from the regional dispersion analysis of seismic surface waves (Panza *et al.* 1980). A standard lithospheric model of heat production and thermal conductivity was used, i.e. a simple exponential model with $A_0=2.5$ mWm^{-3} at the surface, $A_M=0.01$ mWm^{-3} at the Moho depth, and thermal conductivities corresponding to the assumed petrological model.

The Po Plain, northern Sardinia, and central Tunisia show fairly good agreement between calculated steadystate and measured heat flow, suggesting that the corresponding assessed Moho temperatures of about 500, 600, and again 600°C respectively, are reasonable. On the other hand the pronounced thermal transient anomalies corresponding to the Alpine Molasse (about 40 mWm^{-2} of excess heat flow), Ligurian Sea–northern Corsica (300 km wide and about 50 mWm^{-2} of excess heat flow) and Sardinia Channel–northern Tunisia (400km wide and about 80 mWm^{-2} of excess heat flow), are related to active tectonic deformation in those areas. Therefore steadystate temperature estimates for

these areas cannot be considered realistic. More advanced transient thermal modelling of these areas is underway. Preliminary results suggest Moho temperatures of about 700–800 °C under the Alpine Molasse, about 600–700 °C in the Ligurian Sea, and 700–800 °C under the Sardinia Channel and northern Tunisia.

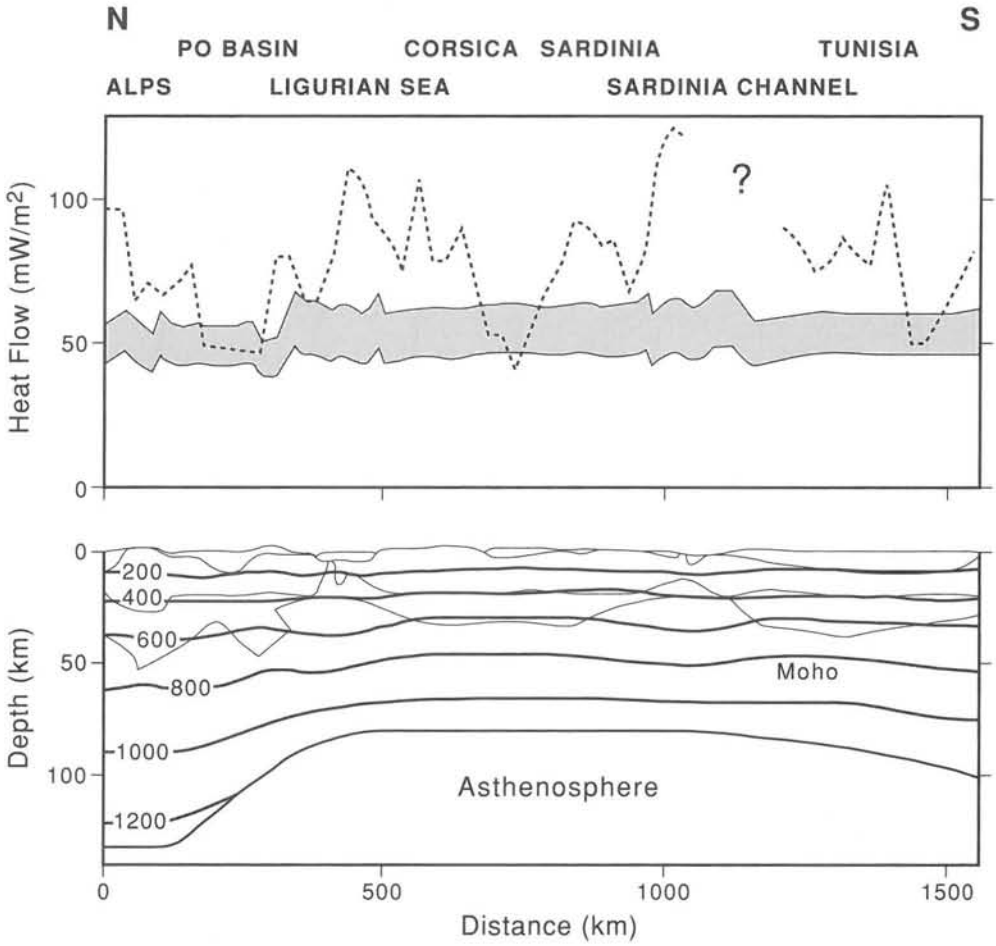

Fig. 12.3. Results of the temperature modelling along the southern segment. Top: computed surface heat flow (shaded band) compared with the observed data. Computed surface heat flow corresponds to model with lithospheric thickness varying by ± 20%, temperature at the lithospheric base by ± 5% and the radiogenic heat production at z=O by ± 20% with respect to the standard model. Bottom: Simplified structural model of the lithosphere along the EGTsouthern segment together with the computed steadystate isotherms (in °C), adopted after Della Vedova et al. *(1990).*

Heat flow is generally higher than 100 mWm^{-2} in the post-Eocene rifted areas, such as the Rhinegraben, the Pantelleria rift system and the younger part of the Sardinia rift. High heat-flow density values are also found in the Tyrrhenian, Ligurian, Provençal, and Balearic Basins, and in the central part of the Sardinia–Tunisia Channel. The Alps show values ranging between 50 and 80 mWm^{-2}, whereas the Alpine Molasse Basin exhibits significantly elevated heat flow (90 mWm^{-2}). The northern Apennines separate the low heat-flow foreland Po Basin region (40 mWm^{-2}) from the internal zone of the chain, which shows higher heat-flow values and a tensional stress regime. Values higher than 200 mWm^{-2} pertain to areas recently affected by magmatic and volcanic activity, such as the Tuscany-Latium geothermal area and the oceanic Tyrrhenian Basin.

The Hercynian crust of Sardinia and southern Corsica is characterised by a value of about 60 mWm^{-2}. The distribution of the heat-flow anomalies is not related in any simple way to the basic tectonic features, e.g. the high heat-flow anomaly of the Ligurian Sea and the Provençal Basin is assymetrically located with respect to basin geometry and low heat flow in southern Corsica and northern Sardinia does not correspond with tectonic boundaries.

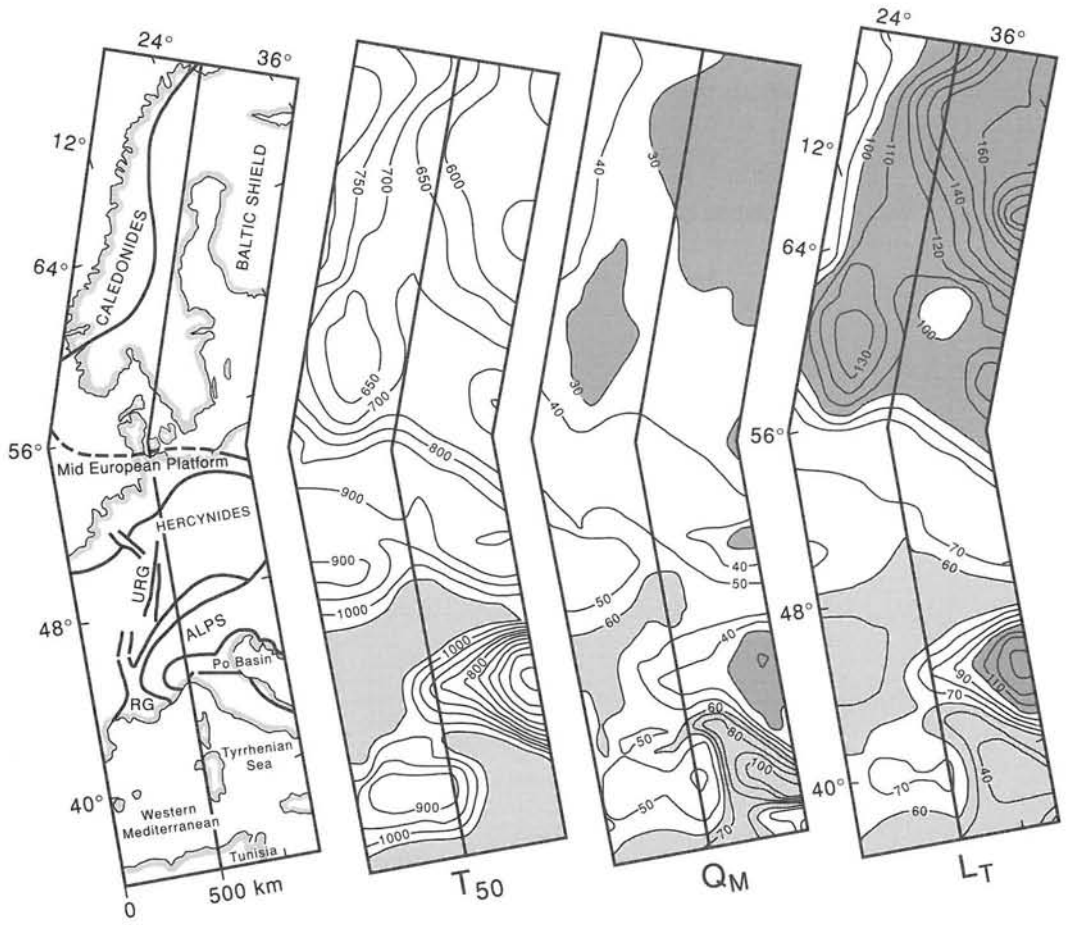

Fig. 12.4 Results of 3-D temperature modelling along the EGT: temperature at 50 km depth, Moho heat flow, and thickness of the thermal lithosphere, adopted after Cermák and Bodri (1992).

The calculated thickness of the thermal lithosphere varies from 150–170 km beneath the shield in the northernmost part of the EGT, to 70–120 km beneath the European Hercynides and to 50–70 km in the Alpine–Mediterranean region. The thinnest lithosphere exists beneath the extensional zones (Rhinegraben and the Ligurian Sea) and beneath the Tyrrhenian Sea (40–50 km).

A 3-D TEMPERATURE MODEL ALONG THE EGT

In order to link all the above models calculated for the individual Segments and to assess the crustal temperature field on a continental scale, Cermák and Bodri (1992) prepared a simplified 3-D model for the whole EGT. The following distributions of heat production $A(x, y, z)$ and thermal conductivity $k(x, y, z)$ were used:

$$A(x, y, z) = \begin{cases} 0.04\, Q_0 \exp(-z/10) & z \le 10 \text{ km} \\ 2.5 \exp(-z/10) & 10 < z \le M \\ 0.01 & z > M \end{cases}$$

$$k(x, y, z) = \begin{cases} 2.5 & z \le M \\ 3.5 & z > M \end{cases}$$

where M is the depth to the Mohorovicic discontinuity, heat flow (Q), heat production (A),

thermal conductivity (k) and depth (z) are given in mWm^{-2}, mWm^{-3}, $Wm^{-1}K^{-1}$, and km, respectively.

The crust is characterised as a simple two-layer exponential model, in which the distribution of radioactivity in the upper-ten kilometre layer satisfies (1) the Roy *et al.* (1968) and Lachenbruch (1968) linear relation between surface heat flow and near surface heat production, and (2) the 40–60% partition law between crustal and mantle heat-flow contributions (Pollack and Chapman 1977). The above thermal conductivities characterise the bulk volume of crustal and upper mantle rocks at the corresponding *in situ* temperature and pressure conditions, in general.

Figure 12.4 summarises the basic results of the modelling, i.e. the temperature distribution at 50 km depth, Moho heat flow, and calculated thickness of the thermal lithosphere. The thermal lithosphere is defined here as the crust and upper part of the mantle with temperatures below the melting relation, while deeper in the asthenosphere existing temperatures are close to or above the melting temperature of some minerals present in the rock material. Depth of the lithosphere–asthenosphere transition for this purpose was described by the melting temperature $T_L=(1100°C+3z)\cdot 0.85$; the lithosphere base defined by this relation is far from being isothermal and differences in existing temperatures may attain as much as 250–350°C.

13 Drift history of Fennoscandia

S.-Å. ELMING, M. LEINO, L. J. PESONEN, A. N. KHRAMOV, G. BYLUND, S. MERTANEN, A.F. KRASNOVA AND M. TERHO

The Precambrian (2.85–0.6 Ga) drift history of the Fennoscandian Shield depicted on Atlas Map 14 is based on a new database compiled by the Scandinavian Working Group of Palaeomagnetism (Elming *et al.* in prep.). The drift calculations are based on an apparent polar wander path defined by a spherical spline function described in Elming *et al.* (submitted) and the coloured figures of Fennoscandia shows the Shield positions at various times. Due to the axial symmetry of the Earth's magnetic field only the latitudinal drift and rotation of the Shield can be reconstructed. Motions along the latitudes are arbitrary and only made for visualising the drift. Major palaeoclimatological evidence for high (low) latitudes are also indicated, such as dropstones and tillite (cold climate), evaporites, red beds and weathering zones (warm climate) (Marmo and Ojakangas 1984) giving constraints to the palaeomagnetic interpretations of past latitudes. Also shown are the major orogenic events, rifting periods and large-scale magmatic intervals that took place in the Shield.

The map shows the gradual growth of Fennoscandia. The changing shape of Fennoscandia is due to the orthogonal projection used and the Shield is slightly enlarged to highlight the lateral growth during drift. The time of formation and extension of the different geological domains is indicated in black and pre-existing areas in red.

From the Archaean core, which today constitutes the northwestern part of the Shield, Fennoscandia grew southwestward (Gaal and Gorbatschev 1987). In Early Proterozoic, during the Svecofennian orogeny (2.0–1.75 Ga), the Archaean terrain was reworked and the Svecofennian domain accreted. A second major period of accretion was in the Late Proterozoic (*ca.* 1.6 Ga ago), when the southwest Scandinavian domain accreted.

14 The EGT CD-ROM

R. FREEMAN AND B. DOST

A CD-ROM is supplied with the Atlas. It contains data files that were used as sources for producing the maps. CD-ROMs are metal-and-plastic discs with read only memory. Information is stored digitally in the form of pits burned into the bottom surface with a laser beam. More than 550 megabytes of information can be stored on this120 mm diammeter disc in addition to a comprehensive error correction code. (Audio compact discs, or CDs, are essentially identical, lacking only the error correction codes.) The potential user must have a device to read the CD-ROM, a hardware connection to the host computer (most flexible is SCSI), and driver software to translate data and file structure into information understandable by the host computer system. On the host machine the CD-ROM will look like a hard disk ('disk' spelled with a 'k' usually denotes magnetic media), the only difference being that the user has no write permission. The necessary hardware and software are available for many computer systems from PCs to mainframes.

All data on the EGT CD-ROM is written in ASCII format. The filing system is the ISO 9660 (previously High Sierra) format similar to that used by the ORFEUS Data Centre (Utrecht) and the NEIC (National Earthquake Information Service, Golden, Colorado). This format can be accessed by all operating systems provided that the user has a device, a hardware connection, and driver software to read CD-ROMs.

We do not supply retrieval software with or on the disc because each type of data has a different character and different formats. In addition, the range of potential application is very large and we cannot foresee what the end use will be. All data files are small enough so that they can be copied as a complete file onto the host computer. The files are written in ASCII so that they can be easily edited to fit any application. The user must supply the input and output routines within his/her familiar operating system environment.

Any publication of results involving data on the CD-ROM should cite the sources given in the header to each file as well as the EGT CD-ROM (see example in the information sheet in CD-ROM jewel case).

FILING SYSTEM

General information and introductory notes are contained on the file README.TXT. The beginning of each data file contains the source reference (citation information) and an explanation of the format used. In addition, we list a FORTRAN algorithm a few basic plot

routines for transforming and plotting geographic into Lambert coordinates.

File hierarchy and naming system is purposely primitive and straightforward. Any revisions to the list given below are provided on the sleeve of the jewel case in which the CD-ROM is packaged or on the README.TXT file on the CD-ROM itself.

Contents of the CD-ROM

General information (text files; extension .txt)

README.TXT	general information on using the data files

Seismicity compilations (extension .sei)

FENNOS.SEI	the Ahjos and Uski (1992) catalogue 1375–1989
INPHIN.SEI	input file for historical seismicity, north sheet
FENSTA.SEI	Fennoscandia station locations
GERINS.SEI	German instrumental seismicity catalogue 1975–1989
GERSTA.SEI	German station locations
SWINST.SEI	Swiss instrumental seismicity catalogue1975–1989
SWISTA.SEI	Swiss earthquake station locations
GRENOB.SEI	Grenoble seismicity catalogue 1975–1989
GENOVA.SEI	Genova seismicity catalogue 1975–1989
ITALIA.SEI	Italy seismicity catalogue 1975–1989
ITASTA.SEI	Italian station locations
EMSCIN.SEI	EMSC catalogue 1965–1985

Focal-mechanism solutions (extension .fps)

ALLEGT.FPS	complete EGT file of focal plane solutions
INPEGT.FPS	input file for focal plane solution maps
REFERE.FPS	references for the focal plane solutions

Recent vertical crustal movement data (extension .rcm)

FENNOS.RCM	Fennoscandia tide gauge data
GERNOR.RCM	German uplift data, north
GERSOU.RCM	German uplift data, south
SWITZE.RCM	Swiss uplift data
ITALIA.RCM	Italian uplift data

Geoid and horizontal gravity disturbance components (extension .geo)

GNORTH.GEO	north
GSOUTH.GEO	south

Aeromagnetic data (extension .mag)

ANORTH.MAG	north
ACENTR.MAG	central
ASOUTH.MAG	south

Bouguer gravity anomaly data (extension .bou)

BNORTH.BOU	north
BCENTR.BOU	central
BSOUTH.BOU	south

Fennoscandia electromagnetic data (extension .emd)

MTFISI.EMD	MT sites in Finland, geographical coordinates
MVFISI.EMD	MV sites in Finland, geographical coordinates
MVSWSI.EMD	MV sites in Sweden, geographical coordinates
MV300S.EMD	reversed real induction arrows, 300 s period
MV1000.EMD	reversed real induction arrows, 1000 s period

German induction arrows (extension .wpf and .rpf)

300.WPF	'Wiese' induction arrows, 300 s period, western Germany
3000.WPF	'Wiese' induction arrows, 3000 s period, western Germany
300.RPF	real induction arrows, 300 s period, eastern Germany
3000.RPF	real induction arrows, 3000 s period, eastern Germany

Heat-flow data (extension .hfd)

AUSTRI.HFD	Austria
CZECHO.HFD	Czechoslovakia (east of 16°E only)
DENMAR.HFD	Denmark
FINLAN.HFD	Finland
FRANCE.HFD	France (east of 4°E)
GERMEAS.HFD	Germany (formerly GDR)
GERMWES.HFD	Germany (FRG)
ITALIA.HFD	Italy
NORWAY.HFD	Norway
MEDITE.HFD	Mediterranean Sea area
KOLKAR.HFD	Russia (Kola and Karelia only)
SWEDEN.HFD	Sweden
SWITZE.HFD	Switzerland
TUNISI.HFD	Tunisia

Programs (extensions .for, .par, .inp)

LAMBER.FOR	FORTRAN program to plot geographic data in Lambert conic conformal coordinates
LAMBER.PAR	example of parameter input file
LAMBER.inp	example of data input file

FINAL CONSIDERATIONS

The data have been written onto disc without error. However, even after repeated checking there may be errors of earlier origin stemming from transfer in collection, correction, and compilation. All those involved have done their utmost to eliminate errors, but experience shows that typing errors and unnoticed flaws invariably creep in.

Not all data sets are spatially or temporally complete nor is their quality homogeneous. Many modellers will need topography (height) and geography data that we were unfortunately not able to supply. Many catalogues that complement those listed here are available on magnetic tape from their respective compilers, e.g. topography, palaeomagnetic, and historical seismicity data.

No upgrades for the EGT CD-ROM are planned. However, comments, corrections, suggestions for improvement, and positive as well as negative experience with the data are welcome and should be addressed to the first author.

Finally, we wish to thank all those who have allowed us to publish their data and hope that these data continue to help reveal the European continent.

References

A.G.I.P. 1979. Rilievo aeromagnetico della Sardegna e del Mare Circostante. In: *Ente Minerario Sardo*, anno 7/73–4, Cagliari.

Ahjos, T. and Korhonen, H. 1984. *On a Catalogue of Historical Earthquakes in Fennoscandian Area*. Inst. Seismol., Univ. Helsinki, Rep. S–10.

Ahjos, T. and Uski, M. 1992. Earthquakes in northern Europe in 1375–1989. *Tectonophysics* **207** (in press).

Ahorner, L. and Schneider, G. 1974. Herdmechanismen von Erdbeben im Oberrheingraben und seinen Randgebirgen. In: *Approaches to Taphrogenesis*, pp. 103–17. E. Schweizerbart'sche Verlagsbuchhandlung, Stuttgart.

Aichroth, B. and Prodehl, C. 1990. EGT Central segment refraction seismic. In: R. Freeman and St. Mueller (eds), *Sixth EGT Workshop: Data Compilation and Integrated Interpretation*, pp. 105–25. European Science Foundation, Strasbourg.

Aichroth, B., Prodehl, C. and Thybo, H. 1992. Crustal structure along the Central Segment of the EGT from seismic refraction studies. *Tectonophysics* **207** (in press).

Aki, K. and Richards, P. 1980. *Methods of Quantitative Seismology*. Freeman, San Francisco.

Alpine Explosion Seismology Group 1976. A lithospheric seismic profile along the areas of the Alps, 1975; I: First results. *Pure App. Geophys.* **114:** 1109–130.

Andersen, O. B. and Engsager, K. 1977. Surface-ship gravity measurements in Danish waters. *Geodædstk instituts Skrifter*, 3. Række, Bind XLIII.

Andersen, O. B. 1978. Bouguer anomaly map of Denmark and surrounding waters, *Geodædstk instituts Skrifter*, 3. Række, Bind XLIV.

Anderson, H. and Jackson, J. 1987. Active tectonics of the Adriatic region. *Geophys. J. Roy. Astr. Soc.* **91:** 937–83.

Angenheister, G., Bogel, H., Gebrande, H., Giese, P., Schmidt-Thome, P. and Zeil, W. 1972. Recent investigations of surficial and deeper crustal structure of the eastern and Southern Alps. *Geol. Rundschau* , **61:** 304–26.

Arca S. and Beretta G. P. 1985. Prima sintesi geodetico-geologica sui movimenti verticali del suolo nell'Italia Settentrionale (1897–1957). *Bolletino di geodesia e scienze affini*, **1985/2:** 125–56.

Arisi Rota, F. and Fichera R. 1987. Magnetic interpretation related to aeromagnetic provinces: the Italian case history. *Tectonophysics* **138:** 170–96.

Arshavskaya, N. I., Galdin, N. E., Karus, E. V., Kuznetsov, O. L., Lubimova, E. A., Milanovski, S. Y. Nartikoev, V. D., Semashko, S. A. and Smirnova, E. V. 1984. Geothermic investigations. In: Ye. A. Kozlovsky (ed.), *The Superdeep Well of the Kola Peninsula*, pp. 378–93. Springer Verlag, Berlin, Heidelberg, New York.

Arvidsson, R. 1991. Seismodynamics of Sweden deduced from earthquake-source and seismic-wave characteristics. *Acta Univ. Ups., Comprehensive Sumaries of Uppsala Dissertations from the Faculty of Science* **354**, Uppsala.

Arvidsson, R. and Kulhanek, O. (Submitted). Seismodynamics of Sweden deduced from earthquake focal mechanisms, (submitted to *Geophys. J. Int.).*

Assinovskaya, B.A. 1986. Focal Mechanisms for Earthquakes in the Northeastern Part of the Baltic Shield. *Izvestiya, Earth Physics*, **22/1.**

Augath, W. 1986. The determination of recent crustal movements in Western Europe-present state, problems and future activities. In: H. Pelzer and W. Niemeier (eds), *Determination of Heights and Height Changes*, pp. 475–86. Bonn.

BABEL Working Group 1990. Evidence for early Proterozoic plate tectonics from seismic reflection profiles in the Baltic shield. *Nature*, **348:** 34–8.

Bachmann, G. H. and Grosse, S. 1989. Struktur und

Entstehung des Norddeutschen Beckens–geologische und geophysikalische Interpretation einer verbesserten Bouguer-Schwerekarte. *Nds. Akad. Geowiss. Veröffl.* **2:** 23–48.

Ballerin, S., Palla, B. and Trombetti, C. 1972. The construction of the gravimetric map of Italy. *Publ. Comm. Geodet. Ital.* 3a Ser. 19.

Balling, N. 1976. Geothermal models of the crust and uppermost mantle of the Fennoscandian shield in South Norway and Danish Embayment. *J. Geophys.* **42:** 237–56.

Balling, N. 1979. Subsurface temperatures and heat flow estimates in Denmark. In: V. Cermak and L. Rybach (eds), *Terrestrial Heat Flow in Europe*, pp. 53–68. Springer Verlag, Berlin.

Balling, N. 1990. Heat flow and lithospheric temperature along the Northern Segment of the European Geotraverse. In: R. Freeman and St.Mueller (eds), *Sixth EGT Workshop: Data Compilations and Synoptic Interpretation* , pp. 405–16. European Science Foundation, Strasbourg.

Banda, E., Egger, A., Demartin, M., Maistrello, M. and Ansorge, J. 1985. Crustal structure under Sardinia. In: D. A. Galson and St. Mueller (eds), *Second EGT Workshop: the Southern Segment*, pp. 201–6. European Science Foundation, Strasbourg.

Bartelsen, H., Lüschen, E., Krey, Th., Meissner, R., Schmoll, H., Walter, Ch. 1982. The combined seismic-reflection-refraction investigation of the Urach geothermal anomaly. In: R. Haenel, (ed.), *The Urach Geothermal Project*, pp. 231-45. Schweizerbart, Stuttgart.

Baumann, M and Rybach, L. 1991. Temperature field modelling along the Northern Segment of the European Geotraverse and the Danish Transition Zone, *Tectonophysics* **194:** 387–407.

Baumann, M. 1988. Geothermische Aspekte der europäischen Geotraverse (EGT Nordsegment: FENNOLORA, EUGENO-S). Diplomarbeit, Institut für Geophysik, ETH Zürich.

Bayer, M. and Lesquer, A. 1976. *Carte Gravimétrique de la Corse*, Centre Géologique et Géophysique (CNRS, Montpellier).

Bayer, M. and Lesquer, A. 1977. Étude gravimétrique de las Corse. *Bulletin B.R.G.M.* (2me série) Section II, no 1: 1–12.

Bayer, R., Le Mouël, J. L. and Le Pichon X. 1973. Magnetic anomaly pattern in the Western Mediterranean. *Earth Planet. Sci. Lett.* **19:** 168–76.

Båth, M. 1956. *An Earthquake Catalogue for Fennoscandia for the Years 1891–1950*. Sveriges Geol. Unders., Ser. C 545.

Båth, M., Kulhanek, O., van Eck, T. and Wahlström, R. 1976. *Engineering analysis of ground motion in Sweden*. Seismol. Inst. Univ. Uppsala, Rep. 5–76.

Behrens, K., Goldflam, S., Heikkinen, P., Hirschleber, H., Lindquist, C. and Lund, C.-E. 1989. Reflection seismic measurements across the Granulite Belt of the POLAR Profile in the northern Baltic Shield, Northern Finland. *Tectonophysics* **162:** 101–11.

Behrens, K., Hansen, J., Flueh, E. R., Goldflam, S. and Hirschleber, H. 1986. Seismic investigations in the Skagerrak and Kattegat. *Tectonophysics* **128:** 209–28.

Benfield, A. E. 1939. The terrestrial heat flow in Great Britain. *Proc. Roy. Soc. A*, London **1973:** 428–50.

Berdichevsky, M. N. and Dmitriev, V. I. 1976. Basic principles of interpretation of magnetotelluric sounding curves. In: A. Adam (ed.), *Geolectrical and Geothermal Studies*, pp. 165–221. Akad. Kiado, Budapest.

Berdichevsky, M. N. and Zhdanov, M. S. 1984. *Advanced Theory of Deep Electromagnetic sounding*, pp. 408. Elsevier, Amsterdam.

Berktold, A. 1991. Electrical conductive structures of regional extension in the earth crust beneath central Europe. *Münchner Geophysikalische Mitteilungen*, no. 6, in preparation.

Bialas, J., Flueh, E. R. and Jokat, W. 1990. Seismic of the Ringkoebing-Fyn High on Langeland, Denmark. *Tectonophysics* **176:** 25–41.

Birch, F. 1948. The effect of Pleistocene climatic variations upon geothermal gradients. *Am. J. Sci.* **246:** 729–60.

Blundell, D., Freeman, R. and Mueller, St. 1992. *A Continent Revealed: The European Geotraverse*. Cambridge University Press, Cambridge.

Bodmer, Ph. and Rybach, L. 1984. *Geothermal Map of Switzerland. Materaux pour la Geologie de la Suisse*. Geophysique No. 22, Comm. Suisse Geophysique.

Bolliger, J. 1967. *Die Projektion der Schweizerischen Plan-und Kartenwerke*. Winterthur.

Bonjer, K. P., Gelbke, C., Gilg, B., Rouland, D., Mayer-Rosa, D. and Massinon, B. 1984. Seismicity and dynamics of the Upper Rhinegraben. *J. Geophys.* **55:**1–12.

Bormann, P., Bankwitz, P., Conrad, W. and Oelsner, Ch. 1989. Crustal structure and development in Central Europe. *Gerlands Beiträge Geophysik* **98(5):** 353–67.

Bormann, P., Bankwitz, P., Schulze A., Apitz, E., Conrad, W., Neunhofer, H., Porstendorfer, G., Rugenstein, B. and Wolter, J. 1987. Methodical contributions to complex geophysical and geological investigations of the Earth's crust in the GDR, Part I: Geophysical methods and results: *Gerlands Beiträge Geophysik* **96(3/4):** 291–310.

Bortfeld, R. K., Gowin, J., Stiller, M., Baier, B., Behr, H.-J., Heinrichs, T., Durbaum, H. J., Hahn, A., Reichert, C., Schmoll, J., Dohr, G., Meissner, R., Bittner, R., Milkereit, B. and Gebrande, H. 1985. First results and preliminary interpretation of deep reflection seismic recordings along profile DEKORP-2-South. *J. Geophys.* **57:** 137–63.

Bortfeld, R. K., Keller, F., Sieron, B., Söllner, W., Stiller, M., Thomas, R., Franke, W., Weber, K., Vollbrecht, A., Heinrichs, T., Dürbaum, H. J.,

Reichert, C., Schmoll, J., Dohr, G., Meissner, R., Bittner, R., Gebrande, H., Bopp, M., Neurieder, P. and Schmidt, T. 1988. Results of the DEKORP4/ KTB Oberpfalz deep seismic reflection investigations-DEKORP Research Group. *J. Geophys.* **62:** 69–101.

Bram, K. 1979. Heat flow measurements in the Federal republic of Germany. In: V.Cêrmák and L. Rybach (eds), *Terrestrial Heat Flow in Europe*, pp. 191–6. Springer Verlag, Berlin.

Brennecke, J., Lelgemann, D., Reinhart, E., Torge, W., Weber, G. and Wenzel, H.-G. 1983. *A European Astro-Gravimetric Geoid.* Deutsche Geodätische Kommision (DGK), München, Reihe B, Nr. 269.

Briggs, I. C. 1974. Machine contouring using minimum curvature. *Geophys.* **35 (1):** 39–48.

Buness, H. and Giese, P. 1990. A crustal section through the northwestern Adriatic plate. In: R. Freeman, P. Giese, and St. Mueller (eds), *The European Geotraverse: Integrative Studies*, pp. 297–304. European Science Foundation, Strasbourg.

Bungum , H. and Fyen, J. 1980. Hypocentral distribution, focal mechanism, and tectonic implications of Fennoscandian earthquakes, 1954–1978. *Geol. Fören. Stockh. Förh.* **101/4:** 261–71. Stockholm.

Bungum, H., Hokland, B.K., Husebye, E.S. and Ringdal, F. 1979. An exceptional intraplate earthquake sequence in Meløy, northern Norway. *Nature* **280:** 32–5.

Campbell, J., Schuh, H., Pradler, E. and Vierbuchen, J. 1989. Horizontal and vertical station displacements observed by VLBI. Paper presented at the IAG General Meeting, Edinburgh, 1989.

Carter, W.E., Aubrey, D.G., Baker, T., Boucher, C., Leprovost, C., Pugh, D., Peltier W.R., Zumberge, M., Rapp, R.H., Schutz, R.E., Emery, K.O. and Enfield, D.B. 1989. *Geodetic Fixing of Tide Gauge Bench Marks.* Woods Hole Oceanographic Institute Technical Report, WHOI-89–31.

Cassano, E., Marcello, A., Nannini, R., Pretti, S., Ranieri, G., Salvaderi, R., Salvadaori, I. 1979. Rilievo aeromagnetico della Sardegna e del Mare Circostante. *Boll. Serv. Geol. Ital.* **C:** 199–234.

Cassell, B R., Mykkeltveit, S., Kanestrom, R. and Husebye, E. S. 1983. A North Sea-southern Norway seismic crustal profile. *Geophys. J. Roy. Astr. Soc.* **72:** 733–53.

Cérmák J V., Bodri, L. and Tanner, B. 1990. Deep crustal temperature along the Central Segment of the EGT. In: R.Freeman and St.Mueller (eds), *Sixth EGT Workshop: Data Compilations and Synoptic Interpretation*, pp. 423–9. European Science Foundation, Strasbourg.

Cêrmák, V. and Bodri, L. 1992. Three-dimensional deep temperature modelling along the European Geotraverse. *Tectonophysics* (in press).

Cêrmák, V. and Hurtig, E. (eds) 1979. Heat Flow Map of Europe 1:5,000,000. In: V. Cêrmák and L. Rybach (eds), *Terrestrial Heat Flow in Europe*, Springer Verlag, Berlin, colour enclosure.

Cèrmák, V. and Rybach, L. 1982. Thermal conductivity and specific heat of minerals and rocks. In: G. Angenheister (ed.), *Physical Properties of Rocks.* Landolt-Börnstein New Series Vol. V1a, pp. 305–43. Springer Verlag, Berlin.

Cêrmák, V., Balling, N., Kukkonen, I. and Zui, V.I 1992. Heat flow in the Baltic shield: Results of the lithospheric geothermal modelling. *Precamb. Geol.* (in press).

Cêrmák, V., Kral, M., Kresl, M., Kubik, J. and Safanda, J. 1991. Heat flow, regional geophysics and lithosphere structure in Czechoslovakia and adjacent part of Central Europe. In: V. Cèrmák and L. Rybach (eds), *Terrestrial Heat Flow and the Lithosphere Structure*, pp. 133–65. Springer Verlag, Berlin.

Closs, H. and Hahn, A. 1957. Bemerkungen zur Karte der Schwerestörungen des deutschen Alpenvorlandes (mit Beiträgen von Alfred Schleusener). *Geol. Jb.* **72:** 503–28.

Closs, H. and Labrouste, Y. 1963. *Seismologie. Recherches Seismologiques dans les Atpes Occidentales au moyen de grande explosions en 1956,1958, and 1960.* Mémoire Collectif de Groupe d'Etudes des Explosions Alpines. CNRS.

Clowes, R. H., Gens-Lenartowitcz, E., Demartin, M. and Saxov, S. 1987. Lithospheric structure in Southern Sweden–results from FENNOLORA. *Tectonophysics* **142:** 1–14.

Cordell, L. and Grauch, V. J. S. 1985. Mapping basement magnetization zones from aeromagnetic data in the San Juan basin, New Mexico. In: Hinze, W.J. (ed.), *The Utility of Regional Gravity and Magnetic Anomaly Maps*, pp. 181–97. Society of Exploration Geophysicists, Tulsa.

Dahl-Jensen, T., Dyrelius, D. and Palm, H. 1991. Deep crustal seismic reflection profiling across two major tectonic zones in southern Sweden. *Tectonophysics* **195:** 209–40.

Deichmann, N. 1987. *Seismizität der Nordschweiz, 1983–1986.* Technischer Bericht 87–05 der Nationalen Genossenschaft für die Lagerung radioaktiver Abfälle, Baden.

Deichmann, N. 1990. *Seismizität der Nordschweiz, 1987–1989, und Auswertung der Erdbebenserien von Günsberg, Läufelingen und Zeglingen.* Technischer Bericht 90–46 der Nationalen Genossenschaft für die Lagerung radioaktiver Abfälle, Baden.

Deichmann, N. and Baer, M. 1990. Earthquake focal depths below the Alps and northern Alpine foreland of Swtizerland. In: R. Freeman, P. Giese, and St. Mueller (eds), *The European Geotraverse: Integrative Studies*, pp. 277–88. European Science Foundation, Strasbourg.

Deichmann, N., Ansorge, A., Mueller, St. 1986. Crustal structure of the southern Alps beneath the intersection with the European Geotraverse. *Tectonophysics* **126:** 57–83.

DEKORP Research Group 1985. First results and

preliminary interpretation of deep-reflection seismic recordings along profile DEKORP 2-South. *J. Geophys.* **57:** 137–63.

DEKORP Research Group 1988. Results of the DEKORP 41KTB Oberpfalz deep seismic reflection investigations. *J. Geophys.* **62:** 69–101.

DEKORP Research Group, Anderle, H.-J., R. Bittner, R., Bortfeld, R., Bouckaert, J., Büchel, G., Dohr, G., Dürbaum, H.-J., Durst, H., Fielitz, W., Flüh, E., Gundlach T., Hance, L., Henk, A., Jordan, F., Kläschen, D., Klöckner, D., Meissner, R., Meyer, W., Oncken, O., Reichert, Ch., Ribbert, K-H., Sadowiak, P., Schmincke, H.-U., Schmoll, J., Walter, R., Weber, K., Weihrauch, U. and Wever, Th. 1991. Results of the DEKORP 1 (BELCORP-DEKORP) deep seismic reflection studies in the western part of the Rhenish Massif. *Geophys. J. Int.* **106:** 203–27.

Della Vedova, B. and Pellis, G. 1986. Realizzazione della mappa di flusso di calore per i mari italiani. *Rapporto Finale del P.F. Oceanografia e Fondi Marini, S. P. Risorse Minerale*, pp. 295–340. CNR, Roma.

Della Vedova, B., Lucazeau, F., Pasquale, V., Pellis, G. and Verdoya, M. (Submitted). Heat flow density map along the EGT Southern Segment and adjacent zones. Submitted for publication to *Tectonophysics*.

Della Vedova, B., Lucazeau, F., Pellis, G. and Pasquale, V. 1990. Heat flow and tectonics along the southern segment of the EGT. In: R. Freeman and St. Mueller (eds), *Sixth EGT Workshop: Data Compilations and Synoptic Interpretation*, pp. 431–40. European Science Foundation, Strasbourg.

Della Vedova, B., Pellis, G. and Corubolo, P. 1989. Evidenze termiche del rifting continentale nel canale di Sicilia. *Atti VI Conv. Gruppo Nazionale de Geofisica del la Terra Solida*, pp. 687–98. CNR, Roma.

Della Vedova, B., Pellis, G., Foucher, J.-P. and Reheault, J. P. 1984. Geothermal structure of the Tyrrhenian Sea. *Marine Geol.* **55:** 271–89.

Denker, H. (1989). *A New Gravimetric Quasigeoid for the Federal Republic of Germany*. Deutsche Geodätische Kommision (DGK), Munich, Reihe B, Nr. 291.

Edwards, R. N., Bailey, R. C. Garland, G. D. 1981. Conductivity anomalies: lower crust or asthenosphere? *Phys. Earth and Planet. Int.* **25:** 263–72.

Egger, A. 1992. The Lithospheric Structure along a Transect from the Northern Apennines to Tunisia from Seismic Refraction Data. Ph.D Thesis ETH Zürich, Dissertation Nr. 9675.

Egger, A., Demartin, M., Ansorge, J., Banda, E., Maistrello, M. 1988. The gross structure under Corsica and Sardinia. *Tectonophysics* **150:** 363–89.

Ekman, M. 1989. Impacts of geodynamic phenomena on systems for height and gravity. *Bull. Geod.* **63:** 281–96.

Elming, S. Å., Pesonen, L. J., Leino, M., Khramov, A. N., Mikhailova, N.P., Krasnova, A. F., Mertanen, S., Bylund, G. and Terho, M. (Submitted). The continental drift of Fennoscandia and Ukraina during the Precambrian, submitted to *Tectonophysics*.

Elming, S. Å., Torsvik, T. H., Mertanen, S., Krasnova, A. F., Bylund, G., Khramov, A. N., Leino, M., Pesonen, L. J., Smethurst, M. and Terho, M. (in prep.). *Catalogue of Palaeomagnetic Directions and Poles from Fennoscandia: Archean to Tertiary*, second issue (in preparation).

ERCEUGT group 1992. An electrical resistivity crustal section from the Alps to the Baltic Sea (Central Segment of the European Geotraverse). *Tectonophysics* **207** (in press).

Erdbebenrisikokarten der Schweiz (1977). Bericht erarbeitet durch den Schweiz. Erdbebendienst/ Institut für Geophysik, ETH Zürich und durch Basler & Hofmann, Ingeniuere und Planer, Zürich.

Eriksson, K.G. and Malmqvist, D. 1979. A review of the past and present investigations of heat flow in Sweden. In: V. Cermák and L. Rybach (eds), *Terrestrial Heat Flow in Europe*, pp. 267–77. Springer Verlag, Berlin, Heidelberg, New York.

EUGEMI Working Group 1990. The European Geotraverse seismic refraction experiment of 1986 from Genova, Italy to Kiel, Germany. *Tectonophysics* **176:** 43–57.

EUGENO-S Working Group 1988. Crustal structure and tectonic evolution of the transition between the Baltic Shield and the North German Caledonides (the EUGENO-S Project). *Tectonophysics* **150:** 253–384.

Eva, C. Augliera, P. Cattaneo, M. and Giglia, G. 1990. Some considerations on seismotectonics of northwestern Italy. In: R. Freeman, P. Giese, and St. Mueller (eds), *The European Geotraverse: Integrative Studies*, pp. 289–96. European Science Foundation, Strasbourg.

Eva, C. 1989. Dipartimento di Scienze della Terra, Univ. Genova, computer file.

Finckh, P. 1981. Heat flow measurements in 17 perialpine lakes. *Bull. Geol. Soc. Am.*, **92/2:** 452–514.

Finetti, I. and Morelli, C. 1973. Geophysical Exploration of the Mediterranean Sea. *Boll. Geof. Teor. Appl.* **15/60:** 263–340.

Fischer, G., Schnegg, P.-A. and Sesiano, J. 1979. A new geomagnetic survey of Switzerland. *Géologie Suisse-Série Géophysique* **19**.

Franke, W., Bortfeld, R. K., Brix, M., Drozdzewksi, G., Dürbaum, H. J., Giese, P., Janoth, W., Jödicke, H., Reichert, Ch., Scherp, A., Schmoll, J., Thomas, R., Thünker, M., Weber, K., Wiesner, M. G. and Wong, H. K. 1990a. Crustal structure of the Rhenish Massif: results of deep seismic reflection lines DEKORP 2-North and 2-North-Q. *Geol. Rundschau* **79/3:** 523–66.

Franke, W., Giese, P., Grosse, S., Haak, V., Kern, H., Mengel, K. and Oncken, O. 1990b. Geophysical imagery of geological structures along the central

segment of the EGT. In: R. Freeman, P. Giese, and St. Mueller (eds), *The European Geotraverse: Integrative Studies*, pp. 177–86. European Science Foundation, Strasbourg.

Gaal, G. and Gorbatschev, R.,1987. An outline of the Precambrian evolution of the Baltic shield. *Precamb. Res.* **35:** 15–52.

Gajewski, D. and Prodehl, C. 1985. Crustal structure beneath the Swabian Jura, SW Germany, from seismic refraction investigations. *J. Geophys.* **56:** 69–80.

Gajewski, D. and Prodehl, C. 1987. Seismic refraction investigation of the Black Forest. *Tectonophysics* **142:** 27–48.

Gajewski, D., Holbrook, W.S. and Prodehl, C. 1987. A three-dimensional crustal model of Southwest Germany derived from seismic refraction data. *Tectonophysics* **142:** 49–70.

Galdéano, A. and Rossignol, J. C. 1977. Assemblage à altitude constante des cartes d'anomalies magnétiques couvrant l'ensembre du Bassin occidental de la Méditerranée. *Bull. Soc. Géol. France* **19/3:** 461–8.

Galdéano, A. and Rossignol, J.C. 1977. Contribution de l'aéromagnétisme à l'étude du Golfe de Valence. *Earth Planet. Sci. Lett.* **34:** 85–99.

Gasparini, C., Iannaccone, G. and Scarpa, R. 1985. Fault-plane solutions and seismicity of the Italian peninsula. *Tectonophysics* **117:** 59–78.

Gebrande, H., Bopp, M., Neurieder, P. and Schmidt, T. 1989. Crustal structure in the surroundings of the KTB drill site as derived from refraction and wide-angle seismic observations. In: R. Emmermann and J. Wohlenberg (eds), *The Continental Deep Drilling Program (KTB)*, pp. 151–76. Springer Verlag, Berlin, Heidelberg, New York.

Geiger, A., Kahle, H.-G. and Gubler, E. 1986. Recent crustal movements in the Alpine-Mediterranean region analyzed in the Swiss Alps. *Tectonophysics* **130:** 289–98.

Geod. Inst. and Geol. Surv. Finland, Norway and Sweden (Nordkallote Project) 1986. *Gravity anomaly map, Northern Fennoscandia. Scale 1:1,000,000*. Geod. Inst. and Geol. Surv. Finl., Norway and Sweden.

German Research Group for Explosion Seismology, 1964. Crustal Structure in Western Germany. *Z. Geophys.* **30:** 209–34.

Gibert, D. and Galdéano, A. 1985. A Computer Program to Perform Transformations of Gravimetric and Magnetic Surveys. *Computers and Geosciences* **11:** 553–88.

Giese, P. 1990. Crustal Thickness in Central Europe. In: R. Freeman, P. Giese, and St. Mueller (eds), *The European Geotraverse: Integrative Studies*, pp. 115–19. European Science Foundation, Strasbourg.

Giese, P. and Prodehl, C. 1976. Main features of crustal structure of the Alps. In: P. Giese, C. Prodehl, A. Stein (eds), *Explosion Seismology in Central Europe-Data and Results*, pp. 347–76. Springer Verlag, Berlin, Heidelberg, New York.

Giese, P., Buness, H., Roeder, D. 1991. The fragmented lithosphere of the northwestern Adriatic microplate as revealed by deep seismic sounding. In: P. Giese, D. Roeder and R. Nicolich (eds), *Joint Interpretation of Geophysical and Geological Data Applied to Lithospheric Studies*, pp. 217-45. NATO ASI Series C 338.

Giese, P., Prodehl, C., Stein, A. (eds) 1976. *Explosion Seismology in Central Europe–Data and Results*. Springer, Berlin, Heidelberg, New York.

Ginzburg, A., Makris, J., Nicolich, R. 1985. A seismic refraction profile across the Ligurian Sea. In: D A. Galso and St. Mueller (eds), *Second EGT Workshop: the Southern Segment*, pp. 201–6. European Science Foundation, Strasbourg.

Goldschmidt-Rokita, A., Sellevoll, M. A., Hirschleber, H B. and Avedik, F. 1988. In: Y. Kristoffersen (ed.), *Progress in Studies of the Lithosphere in Norway, Proceedings of a Meeting Reporting Progress in Norwegian Research in the International Lithosphere Programme, held at Sundvollern, Norway, 12-13 November 1987*, pp. 49–57. Norges Geologiske Undersokelse, Special publication no. 3.

Golovkov, V.P., Rolomijtzeva, G.I., Ronyashchenko, L.P. and Semyonova, G.M. 1983. *The Summary of the Annual Mean Values of Magnetic Elements at the World Magnetic Observatories (XVI)*. Academy of Sciences of the USSR, Moscow.

Gorbatschev, R. 1984. The significance of suture/ductile shear belts in southern Sweden. In: D. Galson, St. Mueller and B. Munsch (eds), *First EGT Workshop: the Northern Segment*, pp. 99–100. European Science Foundation, Strasbourg.

Grad, M. and Luosto. U. 1987. Seismic models of the crust of the Baltic shield along the Sveka profile in Finland. *Ann. Geophys.* **5B:** 639–49.

Graf, C. K. 1988. *Verwendung geodätischer Abbildungen bei der Geocodierung von Satelliten-Bilder*. Remote Sensing Series Nr. 13, Dept. of Geography, Univ. Zürich.

Green, C.M., Stuart, G.W., Lund, C.-E. and Roberts, R.G. 1988. P-wave crustal structure of the Lake Vänern area, Sweden: EUGENO-S Profile 6. *Tectonophysics* **150:** 349–61.

Gregori, G.P. and Lanzerotti, L. J. 1980. Geomagnetic depth sounding by induction arrow representation: A review. *Rev. Geophys. Space Phys.* **18:** 203–32.

Groenlie, G., Heier, K.S. and Swanberg, C. A. 1977. Terrestrial heat flow determinations from Norway. *Nor. Geol. Tidsskr.* **57:** 153–7.

Grosse, S., Conrad, W., Behr, H. J. and Heinrichs,T. 1990. Major gravity axis and anomalies in central Europe. In: R. Freeman, P. Giese, and St. Mueller (eds): *The European Geotraverse: Integrative Studies*, pp. 135–46. European Science Foundation, Strasbourg.

Grossmann, W. 1964. *Geodätische Rechnungen und*

Abbildungen in der Landesvermessung. Stuttgart.

Gubler, E., Kahle, H.-G., Klingelé E., Mueller, St. and Olivier, R. 1981. Recent crustal movements in Switzerland and their geophysical interpretation. *Tectonophysics* **71:** 125–52.

Gubler, E., Schneider, D. and Kellerhals, P. 1984. *Bestimmung von rezenten Bewegungen der Erdkruste mit geodätischen Methoden*. Technischer Bericht 84–17 der Nationalen Genossenschaft für die Lagerung radioaktiver Abfälle, Baden.

Guggisberg, B. 1986. Eine zweidimensionale refraktions-seismische Interpretation der Geschwindigkeits-Tiefen-Struktur des oberen Erdmantels unter dem Fennoskanddischen Schild (Projekt FENNOLORA). Ph.D. Thesis Nr. 7945 ETH Zürich.

Haak, V. 1985. *Anomalies of the Electrical Conductivity in the Earth's Crust and Upper Mantle*. Landolt-Börnstein V/2b, pp. 397–436. Springer Verlag, Heidelberg, New York, Tokyo.

Haak, V. and Hutton, V. R. S. 1986. Electrical resistivity in continental lower crust. In Dawson, J.B., Carswell, D.A., Hall, J. and Wedepohl, K.H. (eds), *The Nature of the Lower Crust*. Geol. Soc. Special Publication, Blackwell, Oxford, **24:** 35–49.

Haenel, R (ed.) 1980. *Atlas of Subsurface Temperatures in the European Community*. Th. Schäfer, Hannover.

Haenel, R. 1971. Heat flow measurements and first heat flow map of Germany. *Z. Geophys.* **37:** 975–92.

Haenel, R. 1983. Geothermal investigation in the Rhenish Massif In: K. Fuchs, K. von Gehlen, H. Mälzer, H. Murawski and A. Semmel (eds), *Plateau Uplift, the Rhenish Shield - a Case History*, pp. 228–46. Springer Verlag, Berlin, Heidelberg, New York.

Haenel, R. and Staroste, E. (eds) 1988. *Atlas of Geothermal Resources in the European Community, Austria and Switzerland*. Th. Schäfer, Hannover.

Haenel, R. and Zoth, G. 1973. Heat flow measurements in Austria and heat flow maps of Central Europe. *Z. Geophys.* **38:** 425–39.

Haenel, R., Groenlie, G. and Heier, K. S. 1974. Terrestrial heat flow determinations from lakes in southern Norway. *Nor. Geol. Tidsskr.* **54:** 423–8.

Haenel, R., Groenlie, G. and Heier, K. S. 1979. Terrestrial heat flow determinations in Norway and an attempted interpretation. In: V. Cermák and L. Rybach (eds), *Terrestrial Heat Flow in Europe*, pp. 232–39. Springer Verlag, Berlin, Heidelberg, New York.

Hahn, A. 1986. Magnetic Anomalies. In: R. Freeman, St. Mueller, and P. Giese (eds), *Third EGT Workshop: the Central Segment*, pp. 113–6. European Science Foundation, Strasbourg.

Havskov, J. and Bunum, H. 1987. Source parameters for earthquakes in the northern North Sea. *NORSAR Contributions* No. 338.

Hayford, J. F. 1909. *The Figure of the Earth and Isostasy from Measurements in the United States*. U.S. Coast and Geodetic Survey. Washington, D.C., U.S.A.

Hjelt, S.-E. 1991. Geoelectric studies and conductivity structures of the Eastern and Northern parts of the Baltic Shield. *Tectonophysics* **189:** 249–60.

Hjelt, S.-E. and Vanyan, L. L. (eds.) 1989. *The Geoelectric Model of the Baltic Shield. Final Report, Project 13 Between the Academy of Finland and the Academy of Sciences of the USSR*. Department of Geophysics, Univ. Oulu, Report No 15.

Hofer, St. 1990. Ableitung der Leitfähigkeitsverteilung in der Erdkruste im Bereich der grosstektonischen Grenze Rhenoherzynikum-Saxothuringikum östlich des Rheingrabens, aus einer gemeinsamen Interpretation flächenhafter Messungen der Magnetotellurik und der Erdmagnetischen Tiefensondierung, Ph.D. Thesis, Faculty of Geosciences, Ludwig Maximillian Univ. Munich.

Hurtig, E. and Oelsner, Chr. 1979. The heat flow field on the territory of the German Democratic Republic. In: V. Cermák and L. Rybach (eds), *Terrestrial Heat Flow in Europe*, pp. 186-90. Springer Verlag, Berlin, Heidelberg, New York.

Hurtig, E., Cermák, V., Haenel, R. and Zui, V. I. 1991. *Geothermal Atlas of Europe*. Hermann Haack Verlagsanstalt GmbH., Gotha.

Hutchison, I., Von Herzen, R. P., Louden, K.E., Sclater, J. G. and Jemsek, J. 1985. Heat flow in the Balearic and Tyrrhenian basins, western Mediterranean. *J. Geophys. Res.*, **90:** 685–701.

IAGA Division I Working Group 1 1986. International Geomagnetic Reference Field revision 1985. *Geophys. J. Roy. Astr. Soc.* **85:** 217–20.

IGC-CGMW-STMW (International Geological Commission, Commission for the Geologic Map of the World, Subcommission for the Tectonic Map of the World) 1973. *International Tectonic Map of Europe and Adjacent Areas*, Academy of Sciences of the USSR/Unesco, Unesco, Paris.

Italian Explosion Seismology Group 1978. Prelimenary Interpretation of the Profile HD across the eastern Alps. *Boll. Teor. Appl.*, **20/79:** 287–301.

Italian Explosion Seismology Group and Institute of Geophysics and ETH Zürich 1981. Crust and upper mantle structures in the Southern Alps from deep seismic soundings (1977–8) and surface wave dispersion analysis. *Boll. Teor. Appl.* **3/92:** 297–330.

Järvimäki, P. and Puranen, M. 1979. Heat flow measurements in Finland. In: V. Cermák and L. Rybach (eds), *Terrestrial Heat Flow in Europe*, pp. 172–8. Springer Verlag, Berlin, Heidelberg, New York.

Jemsek, J.P. 1988. Heat flow and tectonics of the Ligurian Basin and margins. Ph. D. Thesis, MIT/WHOI, WHOI-25.

Jimenez-Garcia, M. J. and Pavoni, N. (1984). Focal mechanisms of recent earthquakes 1976–82 and seismotectonics in Switzerland. In: Stiller, H. & Ritsema, A. (eds.), *Proc. Sess. 12, IASPEI XVIII. Gen. Ass. Hamburg 1983*, 77–84. Veröff. Zentralinst. Phys. Erde, Potsdam.

Jones, A. 1981. Comment on 'Geomagnetic depth sounding by induction arrow representation: A review' by G. P. Gregori and L. J. Lanzerotti. *Rev. Geophys. Space Phys.* **19:** 687.

Jones, A.G. 1982. Observations of the electrical asthenosphere beneath Scandinavia. *Tectonophysics* **90:** 37–55.

Jouanne, V., Grandis, H., Menvielle, M. and Pajunpää, K. 1991. Bayesian inversion using thin sheet models: application to geomagnetic data from Finland. Paper presented at the XX General Assembly of IUGG, Wien, 12.-23. 8. 1991.

Jödicke, H. 1990. Zonen hoher elektrischer Krustenleitfähigkeit im Rhenoherzynikum und seinem nördlichen Vorland. PhD Thesis, Univ. Münster.

Jödicke, H., Untiedt, J., Olgemann, W. Schulte, L. and Wagenitz, V. 1983. Electrical conductivity structure of the crust and upper mantle beneath the Rhenish Massif. In: K. Fuchs, K. von Gehlen, H. Mälzer, H. Murawski and A. Semmel (eds), *Plateau Uplift, the Rhenish Shield - a Case History*, pp. 288–302. Springer Verlag, Berlin, Heidelberg, New York.

Kakkuri J. 1985. Die Landhebung in Fennoskandien im Lichte der heutigen Wissenschaft. *Z. Vermessungswesen*, **2/1985:** 51–9.

Kakkuri J. 1986. Newest results obtained in studying the Fennoscandian land uplift phenomenon. *Tectonophysics* **130:** 327–31.

Kaneström, R. and Haugland, K. 1971. The Trans-Scandinavian seismic profile of 1969: profile section 34. In: A. Vogel (ed.), *Progress of the Colloquium on Deep Seismic Sounding in Northern Europe, held in Uppsala on December 1 and 2,1969*: 76–91.

Kim, W.Y., Wahlström, R. and Ahjos, T. 1988. Source parameters of earthquakes in the Baltic Shield. recent seismological investigations in Europe. *Proc. 19. Gen. Assembly Eur. Seismol. Comm., Moscow, Oct. 1-6, 1984*, pp. 252–9. Nauka, Moscow.

Kim, W.Y., Wahlström, R. and Uski, M. 1989. Regional spectral scaling relations of source parameters for earthquakes in the Baltic Shield. *Tectonophysics* **166:** 151–61.

Klingelé, E. 1976. ISOVAG Programmbeschreibung. Schweiz. Geophys. Komm., internal report.

Klingelé E. and Olivier, R. 1979. *Schwere-Karte der Schwiez (Bouguer-Anomalien), Karte 4 der Geophysikalischen Landeskarten 1:500 000.* Bundesamt für Landestopographie, Wabern/Bern.

Klingelé E. and Olivier, R. 1980. La nouvelle carte gravimétrique de la Suisse. *Beitr. z. Geologie der Schweiz, Serie Geophysik* **20:** 54.

Klingelé, E., Lahmeyer, B., Marson, I., Schwarz, G. 1990. A 2-D gravity model of the seismic refraction profile of the EGT Southern Segment. In: R. Freeman and St. Mueller (eds), *Sixth EGT Workshop: Data Compilations and Synoptic Interpretation*, pp. 271–8. European Science Foundation, Strasbourg.

Koivukoski, K., 1990. Magnetotelluric soundings along the SVEKA profile. M.Sc. Thesis, Dept. of Geophysics, Univ. Oulu (in Finnish).

Koivukoski, K., Vaaraniemi, E. and Korja, T. 1989. On the geoelectric structure of the Fennoscandian (Baltic) Shield in Central Finland. [In Finnish]. In J. Forsius (ed.), *XIV Nat. Conf. on Geophysics, Helsinki 3-4 May,1989*. pp. 45–52.

Korja, T. 1990. Electrical conductivity of the lithosphere. Magnetotelluric studies in the Fennoscandian Shield, Finland. PhD. Thesis. *Acta Univ. Oulu* A 215.

Korja, T., Hjelt, S.-E., Kaikkonen. P., Koivukoski, K., Rasmussen, T.M. and Roberts, R.G. 1989. The geoelectric model of the POLAR profile, Northern Finland. *Tectonophysics* **162:** 113–33.

Korja, T., Zhang, P. and Pajunpää, K. 1986. Magnetovariational and magnetotelluric studies of the Oulu anomaly on the Baltic Shield in Finland. *J. Geophys.* **59:** 32–41.

Kozlovsky, Ye. (ed.)1987. *The Kola Superdeep Drillhole*. Springer Verlag, Berlin, Heidelberg, New York.

Kremenetsky A. A., Milanovski, S. Yu. and Ovchinikov, L. N. 1989. A heat generation model for continental crust based on deep drilling in the Baltic shield. *Tectonophysics* **159:** 231–46.

Kukkonen, I. 1989a. Terrestrial heat flow in Finland, central Fennoscandian shield. Ph.D. Thesis, Univ. Helsinki.

Kukkonen, I. 1989b. Terrestrial heat flow and radiogenic heat production in Finland, the central Baltic shield. *Tectonophysics* **164:** 219–30.

Kunze, T. 1982. Seismotektonische Bewegung in Alpenbereich. Ph.D. Thesis, Univ. Stuttgart.

Lachenbruch, A. H. 1968. Preliminary geothermal model of the Sierra Nevada. *J. Geophys. Res.* **73:** 6977–89.

Landström, 0., Larson, S.A., Lind, G. and Malmqvist, D. 1980 Geothermal investigations in the Bohus granite area in southwestern Sweden. *Tectonophysics* **64:** 131–62.

Le Borgne, E., Bayer, R. and Le Mouël, J. L. 1972. La cartographie magnétique de la partie sud du bassin algéro-provençal. Comptes Rendu de la Academie Science Paris (Ser. D) **274:** 1291–4.

Le Borgne, E., Le Mouël, J. L and Le Pichon, X. 1971. Aeromagnetic survey of Southeastern Europe. *Earth Planet. Sci. Lett.* **12/3:** 287–793.

Le Douran, S., Burrus, J., Avedik, F. 1984. Deep structure of the north-western Mediterranean Basin: Results of a two ship survey. *Marine Geol.* **55:** 325–45.

Le Mouël, J. L. and Le Borgne, E. 1970. Les anoma-

lies magnétiques du Sud-Est de la France et de la Méditerranée Occidentale. *C. R. Acad. Sci. Paris* **(Sér. D) 271:** 1348–50.

Lee, M. J. and Green, C. A. 1990. Shaded-relief images of the European Geotraverse (EGT) gravity data. In: R. Freeman and St. Mueller (Editors), *Sixth EGT Workshop: Data Compilations and Synoptic Interpretation*, pp. 255–69. European Science Foundation, Strasbourg.

Legros, Y. and Bonnin, J. 1990. Seismic activity in the vicinity of 'Geotraverse' Southern Segment. In: R. Freeman and St. Mueller (eds), *Sixth EGT Workshop: Data Compilations and Synoptic Interpretation*, pp. 363–70. European Science Foundation, Strasbourg.

Leonhard, T. 1988. *Zur Berechnung von Höhenänderungen in Norddeutschland: Modelldiskussion, Lösbarkeitsanalyse und numerische Ergebnisse*. Wiss. Arbeit der Fachrichtung Vermessungswesen der Universität Hannover, Heft Nr.152.

Leydecker, G. 1986. Erdbebenkatalog für die Bundesrepublik Deutschland mit Randgebieten für die Jahre 1000–1981. *Geol. Jahrbuch* **E36:** 3–83.

Loddo, M. and Mongelli F. 1979. Heat flow in Italy. In V. Cermák and L. Rybach (eds), *Terrestrial Heat Flow in Europe*, pp. 221–31. Springer Verlag, Berlin, Heidelberg, New York.

Loddo, M., Mongelli, F., Pecorini, G. and Tramacere, A. 1982. *Prime Misure di Flusso di Calore in Sardegna*. CNR-RFE-RP 10, Pisa, pp. 181–210.

Losecke, W., Knödel, K. and Müller, W. 1979. The conductivity distribution in the North German sedimentary basin derived from widely spaced areal magnetotelluric measurements. *Geophys. J. Roy. Astro. Soc.* **58:** 169–79.

Lubimova, E. A., Karus, E. V., Firsov, F. V., Starikova, G. N., Vlasov, V. K., Lyusova, L. N. and Koperbakh, K. 1972. Terrestrial heat flow on Precambrian shields in the USSR. *Geothermics* **1**: 81–9.

Lucazeau, F. and Ben Dhia, H. 1989. Preliminary heat flow density data from Tunisia and the Pelagian Sea. *Can. J. Earth. Sci.* **26:** 993–1000.

Lucazeau, F. and Vasseur, G. 1989. Heat flow density data from France and surrounding margins. *Tectonophysics* **164:** 251–58.

Lund, C.-E. 1979. Crustal structure along the Blue Road Profile in northern Scandinavia. *Geol. Fören. Stockh. Förhan.* **101:** 191–204.

Luosto, U. 1991. *Structure and Dynamics of the Fennoscandian Lithosphere. Proceedings of the Second Workshop on Investigation of the Lithosphere in the Fennoskandian Shield by Seismological Methods, Helsinki, May 14-18, 1990.* Institute of Seismology, Univ. Helsinki, report S-25.

Luosto, U., Tiira, T., Korhonen, H., Azbel, I., Burmin, V., Buyanov, A., Kominskaya, I., Ionkis, V. and Sharov, N. 1990. Crust and upper mantle structure along the DSS Baltic profile in SE Fmland. *Geophys. J. Int.* **101:** 89–110.

Luosto, U., Flueh, E. R., Lund, C.-E. and Working Group 1989. The crustal structure along the Polar Profile from seismic refraction investigations. *Tectonophysics* **162:** 51–85.

Lüschen, E., Wenzel, F., Sandmeier, K.-J., Menges, D., Ruhl, Th., Stilker, M., Janoth, W., Keller, F., Sollner, W., Thomas, R., Krohe, A., Stenger, R., Fuchs, K, Wilhelm, H. and Eisbacher, G. 1987. Near-vertical and wide-angle seismic surveys in the Black Forest, SW Germany. *J. Geophys.* **62:** 1–30.

Lüschen, E., Wenzel, F., Sandmeier, K.-J., Menges, D., Ruhl, Th., Stiller, M., Janoth, W., Keller, F., Sollner, W, Thomas, R., Krohe, A., Stenger, R., Fuchs, K., Wilhelm, H. and Eisbacher, G. 1989. Near-vertical and wide-angle seismic surveys in the Schwarzwald. In: R. Emmermann and J. Wohlenberg (eds), *The Continental Deep Drilling Program (KTB)*, pp. 297–362. Springer Verlag, Berlin, Heidelberg, New York.

Malmqvist, D., Larson, S.A., Landström, 0. and Lind, G. 1983. Heat flow and heat production from the Malinsbo granite, central Sweden. *Bull. Geol. Inst., Univ. Uppsala* **9:**137–52.

Marmo, J. S. and Ojakangas, R. W. 1984. Lower Proterozoic glaciogenic deposits, eastern Finland. *Geol. Soc. Am. Bull.* **95:** 1055–62.

Mälzer, H. 1979. On the 'Map of Height Changes in the Federal Republic of Germany- Status 1979' 1:1 000 000. *Allgemeine Vermessungs-Nachrichten* **10:** 362–4.

Mälzer, H. 1990. *DGK-Arbeitskreis für Rezente Krustenbewegungen-Berechnung von Höhenänderungen im Bayerischen Haupthöhennetz unter Verwendung unterschiedlicher Modelle.* Deutsche Geodätische Kommission, München, Reihe B, Heft Nr.293.

McKenzie, D. 1972. Active tectonics of the Mediterranean region. *Geophys. J. Roy. Astr. Soc.* **30:** 109–85.

Mechie, J., Prodehl, C. and Fuchs, K. 1983. The long range seismic refraction experiment in the Rhenish Massif. In: K. Fuchs, K. Von Gehlen, H. Malzer, H. Murawski and A. Semmel (eds), *Plateau Uplift, the Rhenish Massif - a Case History*, pp. 260–75. Springer Verlag, Berlin, Heidelberg, New York.

Meissner, R. and Bortfel, R. K. (eds) 1990. *DEKORP-Atlas. Results of Deutsches Kontinentales Reflexionsseismisches Tiefbohrprogramm.* Springer Verlag, Berlin, Heidelberg, New York.

Meissner, R., Bartelsen, H. and Murawski, H. 1980. Seismic reflection and refraction studies for investigating fault zones along the Geotraverse Rhenoherzynikum. *Tectonophysics* **64:** 59–84.

Midassi, M. S. 1982. Regional Gravity of Tunisia. M.Sc. Thesis, Univ. Southern California.

Mikkola, L. 1983. Mean Height Map of Finland. *Publications of the Finnish Geodetic Institute*, **98**, Helsinki.

Miller, H., Mueller, St., Perrier, G. 1982. Structure and Dynamics of the Alps: A Geophysical Inventory. In: H. Berckhemer and K. Hsü (eds), Alpine-Mediterranean Geodynamics. *Am. Geophys. Union, Geodynamics series* **7:** 175–204.

Mongelli, F. and Zito, G. 1988. Effect of recent temperature change on shallow geothermal measurements. *Geothermics* **17:** 765–76.

Mongelli, F., Zito, G., Della Vedova, B., Pellis, G., Squarci, P and Taffi, L. 1991. Geothermal regime of Italy and surrounding seas. In: V. Cermák and L. Rybach (eds), *Terrestrial Heat Flow and the Lithosphere Structure*, pp. 381–94. Springer Verlag, Berlin, Heidelberg, New York.

Mooney, W. D. and Prodehl, C. 1978. Crustal structure of the Rhenish Massif and adjacent areas; a reinterpretation of existing seismic-refraction data. *J. Geophys.* **44:** 573–601.

Morelli, C. 1975. The gravity map of Italy. In: Ogniben, L., Parotto, M. and Praturlon, A. (eds), Structural Model of Italy. *Quarderni de 'La Ricerca Scientifica' (CNR)* **90:** 427–47.

Morelli, C., Giese, P., Carrozzo, M.T., Colombi, B., Guera, I., Hirn, A., Letz, H., Nicolich, R., Prodehl, C., Reichert, C., Rower, P., Sapin, M., Scarascia, S. and Wigger, P. 1977. Crustal and upper mantle structure of the northern Apennines, the Ligurian Sea and Corsica, derived from seismic and gravimetric data. *Boll. Geof. Teor. Appl.* **75–76:** 199–260.

Morelli, C., Giese, P., Cassinis, R., Colombi, B., Guera, I., Luongo, G., Scarascia, S. and Schutte, K-J. 1975. Crustal structure of southem Italy. A seismic refraction profile between Puglia-Calabria-Sicily. *Boll. Geof. Teor. Appl.* **17/67:** 183–210.

Moritz, H. 1980. Geodetic Reference System 1980. *Bulletin Geodesique, (The Geodesist's Handbook)* **54/3:** 395–402.

Mostaanpour, M. 1984. Einheitliche Auswertung krustenseismischer Daten in Westeuropa. Darstellung von Krustenparametem und Laufzeitanomalien. *Berliner Geowiss. Abh. B* **10:** 1-96.

Mouge, P. and Galdéano, A. 1991. Magnetic mapping of the western Alps: compilation and geological implications. *Tectonophysics* **190:** 155–72.

Murawski, H., Albers, H.J., Bender, P., Berners, H.P., Dürr, St., Huckriede, R., Kauffmann, G., Kowalczyk, G., Meiburg, P., Müller, R., Muller, A., Ritzkowski, S., Schwab, K., Semmel, A., Stapf, K., Walter, R., Winter, K.-P. and Zankl, H. 1983. Regional tectonic setting and geological structure of the Rhenisch Massif. In: K. Fuchs, K. von Gehlen, H. Mälzer, H. Murawski and A. Semmel (eds), *Plateau Uplift, the Rhenish Shield - a Case History*, pp. 9-38. Springer Verlag, Berlin, Heidelberg, New York.

Nadir, S. 1988. Structure de la croute continentale entre les Alpes Occidentales et les Alpes Ligures. These de doctorat de l'Université Paris VII.

Nicolich, R. 1987. Crustal structures from seismic studies in the frame of the European Geotraverse and CROP Projects. In: A. Boriani et al. (eds), *The Lithosphere in Italy*. Ac. Naz. Lincei, Roma.

Olafsdottir, B., Thomsen, I.D., Pajunpää, K. and Rasmussen, T. 1991. Magnetometer array studies in Northern Sweden. Paper presented at the XX General Assembly of IUGG, Wien, 12.–23. 8. 1991.

Olsen, K. H. and Lund, C.-E. 1986. Precambrian crustal structure of the northern Baltic Shield from the Fennolora Profile: evidence for upper crustal anisotropic laminations. In: M. Barazangi and L. Brown (eds), Reflection seismology: the continental Crust. *Am. Geophys. Union Geodynamic series* **14:** 121–26.

Osipova, I. L., Hjelt, S.-E. and Vanyan, L. L. 1989. Source field problems in northern parts of the Baltic Shield. *Phys. Earth Planet. Int.* **53:** 337–42.

Pajunpää, K. 1987. Conductivity anomalies in the Baltic Shield in Finland. *Geophys. J. Roy. Astro. Soc.* **91:** 657–66.

Pajunpää, K. 1989. Magnetometer array studies in Finland. PhD Thesis, *Acta Univ. Oul.*, **A 205**.

Panasenko, G.D. 1977. *Fennoscandian Earthquakes in 1951–70* (catalogue). Soviet Geophys. Comm., Acad. Sci. USSR, Moscow (in Russian).

Panasenko, G.D. 1979. *Fennoscandian earthquakes in 1971–75* (catalogue). Soviet Geophys. Comm. Acad. Sci. USSR, Moscow (in Russian).

Panza, G.F., Mueller, St. and Calcagnile, G. 1980. The gross features of the lithosphere-asthenosphere system in Europe from seismic surface waves and body waves. *Pure appl.Geophys.* **118:** 1209–13.

Parasnis, D.S. 1975. Temperature phenomena and heat flow estimates in two Precambrian ore-bearing areas in Sweden. *Geophys. J. Roy Astr. Soc.* **43:** 531–54.

Parasnis, D.S. 1982. Geothermal flow and phenomena in two Swedish localities north of the Arctic circle. *Geophys. J. Roy. Astr. Soc.* **71:** 545–54.

Pasquale, V. 1985. A review of heat flow density values in northern Italy. *Collana Studi e Ric., Accad. Lig. Sci. lett.* **6:** 77–90.

Pasquale, V. and Verdoya, M. 1990. Geothermal regime of the Po basin, Italy. In: F. Roure, P. Heitzmann and R. Polino (eds), *Deep Structure of the Alps*, pp. 135–43. Mem. Soc. Geol. Fr., Paris **156**; Mem. Soc. Geol. Suisse, Zürich,**1**, Vol. Spec. Bull. Geol. It., Roma **1**.

Pasquale, V., Cabella, C. and Verdoya, M. 1990. Deep temperatures and lithosphere thickness along the European Geotraverse. *Tectonophysics* **176:** 1–11.

Pasquale, V., Verdoya, M. and Chiozzi, P. 1991. Lithospheric thermal structure in the Baltic shield. *Geophys. J. Int.* **107:** 107–17.

Pavoni, N. (1987): Zur Seismotektonik der

Nordschweiz. *Eclogae geol. Helv.* **80:** 461–72.

Pavoni, N. and Roth, Ph. 1990. Seismicity and seismotectonics of the Swiss Alps. Results of microearthquake investigations 1983–1988. *Mém. Soc. géol. Fr.*, **156**, *Mém. Soc. géol. suisse*, **1**, *Vol. spec. Soc. Geol. It.* **1**: 129–34.

Plaumann, S. 1987. *Karte der Bouguer-Anomalien in der Bundesrepublik Deutschland 1:1 500 000.* Geol. Jahrb., Reihe E, Heft 40, pp. 7.

Pollack, H. N. and Chapman, D. S. 1977. On the regional variation of heat flow, geotherms, and lithosphere thickness. *Tectonophysics* **8:** 279–96.

Posch, E. and Wallach, G. 1989. *Bestimmung des Bougerschwerefeldes in Vorarlberg.* Mitt. Österr. Geol. Ges., Wien.

Postpischl, D. 1985. Catalogo dei terremoti italiani dall'anno 1000 al 1980. In: D. Postpischl (ed.), *CNR Progetto Finallizzato Geodinamica*, Graficoop, Bologna.

Powell, W. G., Chapman, D.S., Balling, N. and Beck, A. E. 1988. Continental heat flow density. In: R. Haenel, L. Rybach and L. Stegena (eds), *Handbook of Terrestrial Heat Flow Density Determination*, pp. 167–222. Kluwer Acad.Publ., Dordrecht.

Prodehl C. and Giese, P. 1990. Seismic Investigations around the EGT in Central Europe. In: R. Freeman, P. Giese, and St. Mueller (eds), *The European Geotraverse: Integrative Studies*, pp. 77–97. European Science Foundation, Strasbourg.

Prodehl, C. and Kaminski, W. 1984. Crustal structure under the Fennolora Profile. In: D. A. Galson and St. Mueller (eds), *The First EGT Workshop: the Northern Segment*, 43–8. European Science Foundation, Strasbourg.

Rasmussen, T.M. 1987. Magnetotelluric investigations of the Baltic Shield in Sweden: techniques and geophysical implications. Ph. D. Thesis, Univ. Uppsala.

Rasmussen, T.M. 1988. Magnetotellurics in Southwestern Sweden: Evidence for electrical anisotropy in the lower crust? *J. Geophys. Res.* **93/B7:** 7,897–907.

Rasmussen, T.M., Roberts, R.G. and Pedersen. L.B. 1987. Magnetotellurics along the Fennoscandian Long Range Profile. *Geophys. J. Roy. Astr. Soc.* **89:** 799–820.

Reigber, Ch., Ellmer, W., Müller, H., Geiss, E. and Schwintzer, P. 1989. Plate motions derived from the DGFI-L04 solution. Paper presented at the IAG General Meeting, Edinburgh 1989.

Reilly, J. W. and Gubler, E. 1990. Crustal strain in Switzerland 1870–1970. *Geophys. J. Int.* **103:** 251–6.

Research Group for Lithospheric Studies in Tunisia 1990. EGT'85 seismic experiment in Tunisia: a reconnaissance of the deep structures. In: R. Freeman and St. Mueller (eds), *Sixth EGT Workshop: Data Compilation and Synoptic Interpretation*, pp. 197–210. European Science Foundation, Strasbourg.

Research Group for Lithospheric Studies in Tunisia 1992. EGT'85 seismic experiment in Tunisia: a reconnaissance of the deep structures. *Tectonophysics* **207** (in press).

Ritter, E. 1990. Geomagnetische Tiefensondierungen am Adolf-Schmidt-Observatorium in Niemegk. In: V. Haak (ed.), *Protokoll Kolloquium Elektromagnetische Tiefenforschung in Hornburg University of Frankfurt a.M. und J. Homilius, Niedersächsisches Landesamt für Bodenforschung, Hannover*, pp. 3–12. Hornburg.

Roure, F., Heitzmann, P. and Polino, R. (eds) 1990. *Deep Structure of the Alps*, Mém. Soc. géol. France, Paris, **156**; Mém. Soc. géol. suisse, Zürich, **1**; Vol. spec. Soc, Geol, It., Roma, **1**.

Roy, R. F., Blackwell, D. D. and Birch, F. 1968. Heat generation of plutonic rocks and continental heat flow provinces. *Earth Planet.Sci. Lett.* **5:** 1–12.

Rybach, L. and Buntebarth, G. 1984. The variation of heat generation, density and seismic velocity with rock type in the continental lithosphere. *Tectonophysics* **103:** 335–44.

Rybach, L. and Finckh, P. 1979. Heat flow data in Switzerland. In: V. Cermak and L. Rybach (eds), *Terrestrial Heat Flow in Europe*, pp. 278–82. Springer Verlag, Berlin, Heidelberg, New York.

Salvioni, G. 1957. I movimenti del suolo nell'Italia centro-settentrionale. *Boll. Geodes. Sci. Aff.* **1957/3:** 325–44.

Scarascia, S. 1980. *Struttura Crostale della Sardegna dagli Esperimenti di Sismica Attiva Condotti nel 1979.* CNR Int. Report, Milano.

Scarascia, S. and Maistrello, M. 1990. Refraction results from the eastern fans and profiles in the Alps-Po Plain-northern Apennines area. In: R. Freeman and St. Mueller (eds), *Sixth EGT Workshop: Data Compilation and Synoptic Interpretation*, pp. 169–77. European Science Foundation, Strasbourg.

Schleusener, A. 1959. *Karte der mittleren Höhen von Zentraleuropa.* Angewandte Geodäsie B 60, Frankfurt.

Schmoll, J., Bittner, R., Durbaum, H.J., Heinrichs, T., Meissner, R., Reichert, C., Ruhl, Th. and Wiederhold, 1989. Oberpfalz deep seismic reflection survey and velocity studies. In: R. Emmermann and J. Wohlenberg (eds), *The Continental Deep Drilling Program (KTB)*, pp. 99–149. Springer Verlag, Berlin, Heidelberg, New York.

Schmucker, U. 1959. *Erdmagnetische Tiefensondierung in Deutschland 1957/59. Magnetogramme und erste Auswertung.* Abhandlung der Akademie der Wissenschaften, Göttingen, Mathematisch-Physikalische Klasse, Beiträge zum International Geophysikalischen Jahr, Heft 5.

Schmucker, U. 1985. Magnetic and electric fields due to electromagnetic induction by external sources. In: K. Fuchs and H. Soffel (eds), *Landolt-Börnstein, Numerical data and functional relationships in science and technology, New series,*

Group V: Geophysics and Space Research, Subvolume IIb, pp. 100–24. Springer Verlag, Berlin, Heidelberg, New York.

Schulz, R. 1990. Subsurface temperature and heat flow density maps for the Central Segment of the EGT. In: R.Freeman and St. Mueller (eds), *Sixth EGT Workshop: Data Compilations and Synoptic Interpretation*, pp. 417–22. European Science Foundation, Strasbourg.

Sjöberg L.E. 1982. *Studies on the land uplift and its implications on the geoid in Fennoscandia.* Department of Geodesy, Rep. No.14, Univ. Uppsala.

Sjöberg, L. E. 1983. Land uplift and its implications on the geoid in Fennoscandia. *Tectonophysics* **97**: 87–101.

Slunga, R. and Ahjos, T. 1986. Fault mechanisms of Finnish earthquakes, crustal stresses and faults. *Geophysica*, **22/1-2:** 1–13.

Slunga, R. 1981a. Earthquake source mechanism determination by use of body wave-amplitudes, an application to earthquakes in Sweden. *Bull. Seis. Soc. Am.* **71:** 25–35.

Slunga, R. 1981b. Fault mechanisms of Fennoscandian earthquakes and regional crustal stresses. *Geol. Fören. Stockh. Förhan.* **103/1:** 27–31.

Slunga, R. 1982. *Research on Swedish earthquakes 1980–1981.* Swedish Nat. Defence Res. Inst., Rep. C20477-T1.

Slunga, R. 1985. *The Seismicity of Southern Sweden 1979–1984, Final Report.* Swedish Nat. Defence Res. Inst., Rep. C20572-T1.

Slunga, R. 1989a. *Earthquake Mechanisms in Northern Sweden Oct 1987 - Apr 1988.* Swedish Nat. Defence Res. Inst., SKB Tech. Rep. 89(28).

Slunga, R. 1989b. Focal mechanisms and crustal stresses in the Baltic shield. In: . Gregersen and P. Basham (eds), *Earthquakes at North-Atlantic Passive Margins: Neotectonics and Postglacial Rebound*, 261–276. NATO ASI Ser. C, 266.

Slunga, R., Norrman, P. and Glans, A. 1984. *Seismicity of Southern Sweden.* Swedish Nat. Defence Res. Inst., Rep. C20543-T1

Stegena, L. and Meissner, R. 1985. Velocity structure and geothermics of the earth's crust along the European Geotraverse. *Tectonophysics* **121:** 87–96.

Steinmetz, L., Ferucci, F., Hirn, A., Morelli, C. and Nicolich, R. 1983. A 550 km long Moho traverse in the Tyrrhenian Sea from O.B.S recorded Pn waves. *Geophys. Res. Lett.* **10/6**: 428–31.

Suhadolc, P. 1990 Fault-plane solutions and seismicity around the EGT Southern Segment. In: R. Freeman and St. Mueller (eds), *Sixth EGT Workshop: Data Compilations and Synoptic Interpretation*, pp. 371–82. European Science Foundation, Strasbourg.

Swain, C. J. 1975. A FORTRAN IV program for interpolation of irregularly spaced data using the difference equations for minimum curvature. *Computer and Geosciences* **1:** 231–40.

Swanberg, C. A., Chessman, M.D., Simmons, G., Smithson, S., Groenli, G. and Heier, K. S. 1974. Heat flow-heat generation studies in Norway. *Tectonophysics* **23:** 31–48.

Takherist, D. and Lesquer, A. 1988. Mise en evidence d'importantes variations regionales de flux de chaleur en Algerie. *Can. J. Earth Sci.* **26:** 615–26.

Tardy, M., Deville, E., Fudral, S., Guellec, S., Ménard, G., Thouvenot, F. and Vialon, P. 1990. Interprétation structurale des données du profil de sismique réflexion profonde Ecors-Crop Alpes entre le front Pennique et la ligne du Canavese (Alpes occidentales). In: F. Roure, P. Heitzmann, R. Polino (eds.), *Deep Structure of the Alps*, pp. 217–226. Mém. Soc. géol. Fr., Paris, **156**; Mém. Soc. géol. suisse, Zürich, **1**; Vol. spec. Soc. Geol. It., Roma, **1**.

Thouvenot, F., Ansorge, J., Eva, C. 1985. Deep structure of the westem Alps: New constraints from the EGT-S 1983 seismic experiment. In: D. A. Galson and St. Mueller (eds), *Second EGT Workshop: the Southern Segmen*t, pp. 109–14. European Science Foundation, Strasbourg.

Thouvenot, F., Frechet, J., Guyoton, F., Guiget, R. and Jenatton, L. 1990. Sismalp: an automatic phone-interrogated seismic network for the Western Alps. In: Seismic Networks and rapid digital transmission and exchange. *Cahiers de Centre Européan de Géodynamique et Sismologie* **1:** 1–10.

Thybo, H. 1990. A seismic velocity model along the EGT profile-from the North German Basin into the Baltic shield. In: R. Freeman, P. Giese, and St. Mueller (eds), *The European Geotraverse: Integrative Studies*, pp. 99–108. European Science Foundation, Strasbourg.

Torge, W., Basic, T., Denker, H., Doliff, J. and Wenzel, H.-G. 1989. *Long Range Geoid Control through the European GPS Traverse.* Deutsche Geodätische Kommision (DGK), Munich, Reihe B, Nr. 290.

Trudu, R. 1962. Rilevamento gravimetrico della Sardegna. *Boll. Geof. Tero. e Appl.* **4/15:** 299–339.

Tscherning, C.C. and Forsberg, R. 1986. Geoid Determination in the Nordic Countries A Status Report. *Proceedings 10th General Meeting of the Nordic Geodetic Commission*, pp. 279–90. Helsinki.

Untiedt, J. 1970. Conductivity anomalies in Central and Southern Europe. *J. Geomag. Geoelect.* **22:** 131–50.

USGS/NEIC 1991. *Global Hypocentre Data Base, version 1.0.* (CD-ROM and retrieval software 'EPIC'). USGS/NEIC, Denver.

Vaaraniemi, E. 1989. Electromagnetic studies of the lithosphere on the Northern Segment of the EGT. (In Finnish). M.Sc. Thesis, Deptartment of Geophysics, Univ. Oulu.

Valasek, P., Mueller, St., Frei, W. and Holliger, K. 1991. Results of NFP20 seismic reflection profil-

ing along the Alpine section of the European Geotraverse (EGT). *Geophys. J. Int.* **105:** 85–102.

Van Gils, J. M. and Leydecker, G. 1991. *Catalogue of European Earthquakes with Intensities Higher than 4*. Commission for the European Communities, Nuclear Science and Technology Series EUR 13406 en. Office for Official Publications of the European Communities, Luxumbourg.

Vanícek, P. and Krakiwsky, E. 1986. *Geodesy: The Concepts, 2nd Ed.* North-Holland, Amsterdam, New York, Oxford, Tokyo.

Vanyan, L. L. (ed.) 1967. *Electromagnetic Depth Soundings*. Consultants Bureau, New York.

Velikhov Ye. P., Zhamaletdinov, A. A., Belkov, I. P., Gorbunov, G. I., Hjelt, S.-E., Lisin, A. S., Vanyan, L. L., Zhdanov, M. S., Demidova, T. A., Korja, T., Kirillov, S. K., Kuksa, Yu. I., Poltanov, A. Ye., Tokarev, A. D. and Yevstingeyev, V. V. 1987. Electromagnetic studies on the Kola Peninsula and in Northern Finland by means of a powerful controlled source. *J. Geody.* **5:** 237–56.

Volbers, R. 1990. Magnetotellurik und erdmagnetische Tiefensondierung entlang des reflexionsseismischen Profils DEKORP 2-N. PhD Thesis, Faculty of Mathematical and Natural Sciences, Univ. Münster.

Volbers, R., Jödicke, H. and Untiedt, J. 1990. Magnetotelluric study of the Earth's crust along the deep seismic reflection profile DEKORP 2-N, *Geolog. Rundschau* **79/3:** 581–601.

Voppel, D. and Wienert, R. 1974. *Die geomagnetische Vermessung der Bundesrepublik Deutschland, Epoche 1965.0*. Deutsches hydrographisches Zeitschrift **27/2**, Hamburg.

Vozoff, K. 1972. The magnetotelluric method in the exploration of sedimentary basins. *Geophys.* **37:** 98–141.

Wahlström, R. and Ahjos, T. 1982. *Determination of Local Magnitude and Calibration of Magnitude Scales for Earthquakes in the Baltic Shield*. Inst. Seismol., Univ. Helsinki, Publ. 185.

Warrick, R. A. and Oerlemans, J. 1990. *Sea level Rise in Scientific Assessment of Climate Change*, pp. 261–85. Intergovernmental Panel on Climate Change.

Wenzel, F., Brun, J. B. and the ECORS-DEKORP working group 1991. A deep reflection seismic line across the Northern Rhine Graben. *Earth Planet. Sci. Lett.* **104:** 140–50.

Wever, Th., Meissner, R., Sadowiak, P. and the DEKORP Group 1990. Deep reflection seismic data along the central part of the European Geotraverse in Germany: a review. *Tectonophysics* **176:** 87–101.

Wigger, P. 1984. *Die Krustenstruktur des Nordapennins und angrenzender Gebiete mit besonderer Berücksichtigung der geothermischen Anomalie der Toskana*. Berliner Geowiss. Abhandl., Reihe B, Heft 9.

Winter, R. 1973. Der Oberrheingraben als Anomalie der elektrischen Leitfähigkeit, untersucht mit Methoden der Erdmagnetischen Tiefensondierung. Ph.D. Thesis, Mathematical-Natural Sciences Faculty, Univ. Göttingen.

Wolf, D. 1982. Comment on 'Geomagnetic depth sounding by induction arrow representation: A review' by G. P. Gregori and L. J. Lanzerotti. *Rev. Geophys. Space Phys.* **20:** 519.

Yan, Q. and Mechie, J. 1989. A fine structural section through the crust and lower lithosphere along the axial region of the Alps. *Geophys. J. Int.* **98:** 465–88.

Ye, S. and Ansorge, J. 1990. A crustal section through the Alps derived from the EGT seismic refraction data. In: R. Freeman, P. Giese and St. Mueller (eds), *The European Geotraverse: Integrative Studies*, pp. 237–44. European Science Foundation, Strasbourg.

Zeis, St., Gajewski, D. and Prodehl, C. 1990. Crustal structure of Southern Germany from seismic-refraction data. *Tectonophysics* **176:** 59–86.

Zhang, P. 1989. Magnetotelluric studies of the Siljan impact region: techniques and results. Ph.D. Thesis, Univ. Uppsala.

Zhang, P., Rasmussen, T. and Pedersen. L. B. 1988. Electrical resistivity structure of the Siljan impact region. *J. Geophys. Res.* **93/B6:** 6,485–502.

Zippelt, K. 1988. *Modellbildung, Berechnungsstrategie und Beurteilung von Vertikalbewegungen unter Verwendung von Präzisionsnivellements*. Deutsche Geodätische Kommission, München, Reihe C, Heft 343.

Zoth, G. and Haenel, R. 1988. Density Determination. (Appendix). In: R. Haenel, L. Rybach and L. Stegena (eds), *Handbook of Terrestrial Heat Flow*, pp. 449–66. Kluwer Acad. Publ., Dordrecht.

The atlas and CD-ROM form the most comprehensive database of geological and geophysical information that has been produced on a continental scale. The maps, at a scale of 1:2.5 million, give a comprehensive picture of the data for comparison of large-scale features. The CD-ROM contains the actual data for researchers to take the analysis further. This unique compilation has been geared to the analysis of large wavelength features (>500km), which are the key to the understanding of Europe's lithosphere–asthenosphere system.

Critical in the interpretation of the data is a knowledge of how the data were acquired, the quality of the data and the inherent errors. The information is provided here in this accompanying text. Each chapter looks at a particular type of data and provides background information on the data, on its sources and on the availability of further data. Any data reduction or processing is explained. The choice of formats and parameters are detailed, although data formats have been standardised wherever possible.

The European Geotraverse has been a scientific undertaking on an unprecedented scale in the earth sciences. The 5000 km long, 250 km wide traverse crosses each of the major tectonic provinces of Europe, from the oldest Precambrian in northern Scandinavia to the modern, active region of the Mediterranean, and looks at the deep interior of Europe to a depth of 500 km. Supported by the European Science Foundation, the ethos of the EGT project has been founded on the idea that the understanding of the workings of a continent and its evolution through geological time demands a well defined programme of linked experiments involving international collaboration and a large number of earth scientists with the widest possible experience and knowledge. The experiments, the network of study centres and the workshops held throughout the European Geotraverse have brought scientists together for a common purpose, and have broadened the vision of many, leading to new scientific liaisons and new collaborative experiments.

CAMBRIDGE
UNIVERSITY PRESS